MAJOR ELEMENT AND ISOTOPIC STUDIES ON THE JAMES RUN/PORT DEPOSIT ASSOCIATION, MARYLAND: TECTONIC ANALOGUES AND TACONIC DEFORMATION

by

Richard Peter Lesser

Thesis submitted to the Graduate Faculty of the
Virginia Polytechnic Institute and State University
in partial fulfillment of the requirements for the degree of
MASTER OF SCIENCE
in
Geology

APPROVED:

A. K. Sinha, Chairman

D. R. Wones

D. R. Gray

D. A. Hewitt

J. F. Read

December, 1982
Blacksburg, Virginia

ACKNOWLEDGEMENTS

The author thanks Dr. A. K. Sinha, whose advice and support, particularly towards the conclusion of this thesis, proved invaluable. The author's parents provided understanding and support. Special thanks are expressed to Dr. Wones and Dr. Gilbert for their insight into particular geologic phenomena. Dr. Read, Dr. Gray, and Dr. Hewitt gave constructive criticisms of the manuscript. J. D. Meyers gave pertinent suggestions for reorganization. Prepublication data were made available by Dr. M. Higgins and Dr. L. Pavlides. Laboratory direction and philosophy were provided by Hal Pendrak. K. Affholter and B. Chakamoukas performed the XRD analyses. R. Guy allowed stimulating discussion on low-K_2O granitoids. Drafts of figures were drawn by I. Whaley under the guidance of S. Chiang. L. Sharpe assisted in the photography. M. Strickler typed the manuscript. The Anne Arundel Sand and Gravel Company, A. Hopkins, J. Buck and innumerable others allowed access to and collection from outcrops in the field area. "M" provided discount advice, at considerable risk.

This thesis is dedicated to A. Andrew, without whom it would not have seen completion.

Field and analytical studies were supported by National Science Foundation grant No. EAR-8206822 to A. K. Sinha.

TABLE OF CONTENTS

TABLE OF CONTENTS (continued)

LIST OF FIGURES

LIST OF FIGURES (continued)

LIST OF PLATES

LIST OF TABLES

INTRODUCTION

The meta-sedimentary and meta-igneous rocks of the eastern Maryland Piedmont have been the focus of classic studies which address the nature of Paleozoic continental margin tectonics. Considerable discussion is concerned with the tectonic origins and relations between the Baltimore Mafic Complex, the meta-igneous James Run Formation/Port Deposit pluton and their correlatives, and the wildflysch diamictites of the Wissahickon terrane (Hopson, 1964; Southwick, 1969; Higgins, 1970; Higgins et al., 1971; Higgins, 1972; Crowley, 1976; Southwick, 1979; Fisher et al., 1979; Sinha et al., 1980; Hanan, 1980; Drake and Lyttle, 1981; Drake and Morgan, 1981; Pavlides, 1981; Pavlides et al., 1982b; Higgins, 1982). The lack of fossil remains and infrequent bedrock exposures has allowed isotopic dating methods to play a pivotal role in the correlation and interpretation of these rocks both along and across strike. Unfortunately, the significance of data from several different isotopic systems (i.e., U-Pb zircon, Rb-Sr whole rock, and Rb-Sr mineral) in polymetamorphosed terranes is subject to multiple interpretation (Stern et al., 1965; Pidgeon et al., 1970; Gulson and Krogh, 1973; Higgins et al., 1977; Zartman, 1978; Mose and Nagel, 1982).

Sinha et al. (1980) sketched the thermal history of the Maryland Piedmont by dating magmatic episodes at 520, 420 and 300 Ma. The 520 Ma event produced bimodal tholeiite-dacite volcanics (the James Run Formation, Baltimore Paragneiss, Relay Quartz Diorite) and hypabyssal trondhjemitic plutons (Port Deposit Gneiss, Kensington Quartz Diorite). The 420 Ma event produced granodioritic plutons (Ellicott City,

Woodstock, Guilford) and the 300 Ma event produced the two-mica Gunpowder Granite.

Hopson (1964), Southwick (1969), Higgins (1972), and Pavlides (1981) considered the trondhjemitic affinities of the 520 Ma rocks to be the product of subsolidus alteration of island arc igneous rocks. Detailed sampling and petrographic/geochemical studies, combined with the application of U-Pb zircon, Rb-Sr whole rock, and Rb-Sr mineral data for the James Run and Port Deposit volcanic/plutonic association has allowed a reevaluation of the geochronologic and geochemical information for these rocks and correlative units in the Central Appalachian Piedmont.

REGIONAL GEOLOGY

Figure 1 shows the geology of the northeastern Maryland Piedmont. The felsic rocks along this corridor may be divided, from northwest to southeast, into three distinct units (Southwick, 1969; Higgins, 1982):

I. Conowingo Diamictite

II. Port Deposit Complex

   A. Sheared Port Deposit Gneiss

   B. Port Deposit Gneiss

III. James Run Formation

The Conowingo Diamictite is an elongate body 23 x 5.5 km maximum dimensions with an outcrop area of approximately 100 km^2. The Port Deposit measures 32 x 5 km maximum dimensions with an approximate outcrop area of 140 km^2. The James Run Formation is discontinuously exposed from the northeastern corner of Maryland to 35 km southwest of the Susquehanna and has an approximate outcrop area of 350 km^2.

Hopson (1960) suggested the Conowingo diamictite was the product of a deepwater submarine slide. Crowley (1976) and Fisher et al. (1979) interpret the Sykesville and Laurel diamictites (not shown on map) which crop out west and south of Baltimore City, Maryland, as tectonic markers which were shed from the allochthonous Baltimore Mafic Complex and James Run Formation during their emplacement onto the continental shelf. Higgins (1970) suggested the meta-igneous Port Deposit Complex was a hypabyssal, plutonic equivalent of the felsic volcanics in the James Run Formation. Higgins (1972) addressed the extent of this volcanic/plutonic belt and concluded they represent an early Paleozoic(?) island arc which

Figure 1. Generalized geology of the northeastern Maryland Piedmont. Data from Southwick and Owens (1968), Fisher et al. (1979), Hanan (1980), and Higgins (1982).

(○) Field stop

(●) Field stop, textural analysis and numerical data

L I T H O L O G Y K E Y

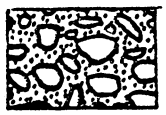

"Mixed Zone:

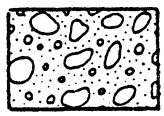

Conowingo Diamictite, Wissahickon Formation

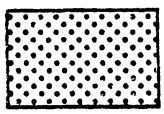

Metagreywacke and amphibolite, Wissahickon Formation

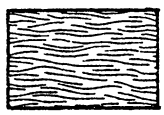

Sheared Port Deposit Gneiss

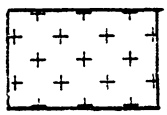

Port Deposit Gneiss

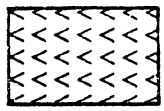

James Run Formation


GEOLOGY OF NORTHEASTERN MARYLAND PIEDMONT
BALTIMORE
GABBRO
CONOWINGO DAM
SUSQUEHANNA RIVER
Aberdeen
COASTAL
PLAIN
0 1 2 3 4 5 km
85
86
84
88
87
89
79

extended from Georgia to New York. Crowley (1976), Hanan (1980), and Higgins (1982) considered the James Run/Port Deposit association as a discrete thrust block in fault contact with the Susquehanna Block of the Baltimore Gabbro and the Aberdeen mafic rocks. Crowley (1976) considered the Aberdeen to be unrelated to the Baltimore Gabbro, whereas Hanan (1980) regarded the Aberdeen as the easternmost equivalent.

Figure 2 shows the sample locations for the field studies on the James Run/Port Deposit and Conowingo rocks with detailed sampling being possible along the Susquehanna River cliffs. Reconnaissance sampling in other areas provided all the samples used in this study. Lesser (this study), Appendix I, presents sample location information in written directives. The significance of the Port Deposit Complex with its sheared and gneissic fabrics and its possible relations with the Maryland diamictites is the focus of this report.

Conowingo Diamictite

The Conowingo diamictite is an arkosic conglomerate containing scattered clasts of amphibolite and felsic material. Southwick (1969) and Hanan (1980) mapped the Conowingo Diamictite/Baltimore Gabbro contact as a thrust fault. Southwick (1969) described the contact as an extensively sheared mixed zone of diamictite, quartz gabbro, and fragments of Baltimore Gabbro. Relict sedimentary textures can be observed in the diamictite in the outcrops below Conowingo Dam. Shearing produced gneissic textures not unlike the sheared textures of the metaigneous Port Deposit. These foliations strike northeast-southwest and

Figure 2. Sample locations for rocks analyzed in this study.

(○) Field stop

(◐) Field stop, textural analysis

(●) Field stop, textural analysis and numerical data

L I T H O L O G Y K E Y

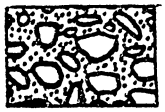

"Mixed Zone:

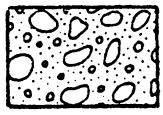

Conowingo Diamictite, Wissahickon Formation

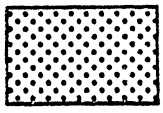

Metagreywacke and amphibolite, Wissahickon Formation

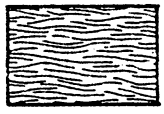

Sheared Port Deposit Gneiss

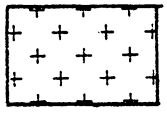

Port Deposit Gneiss

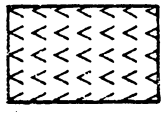

James Run Formation

SAMPLE TRAVERSE

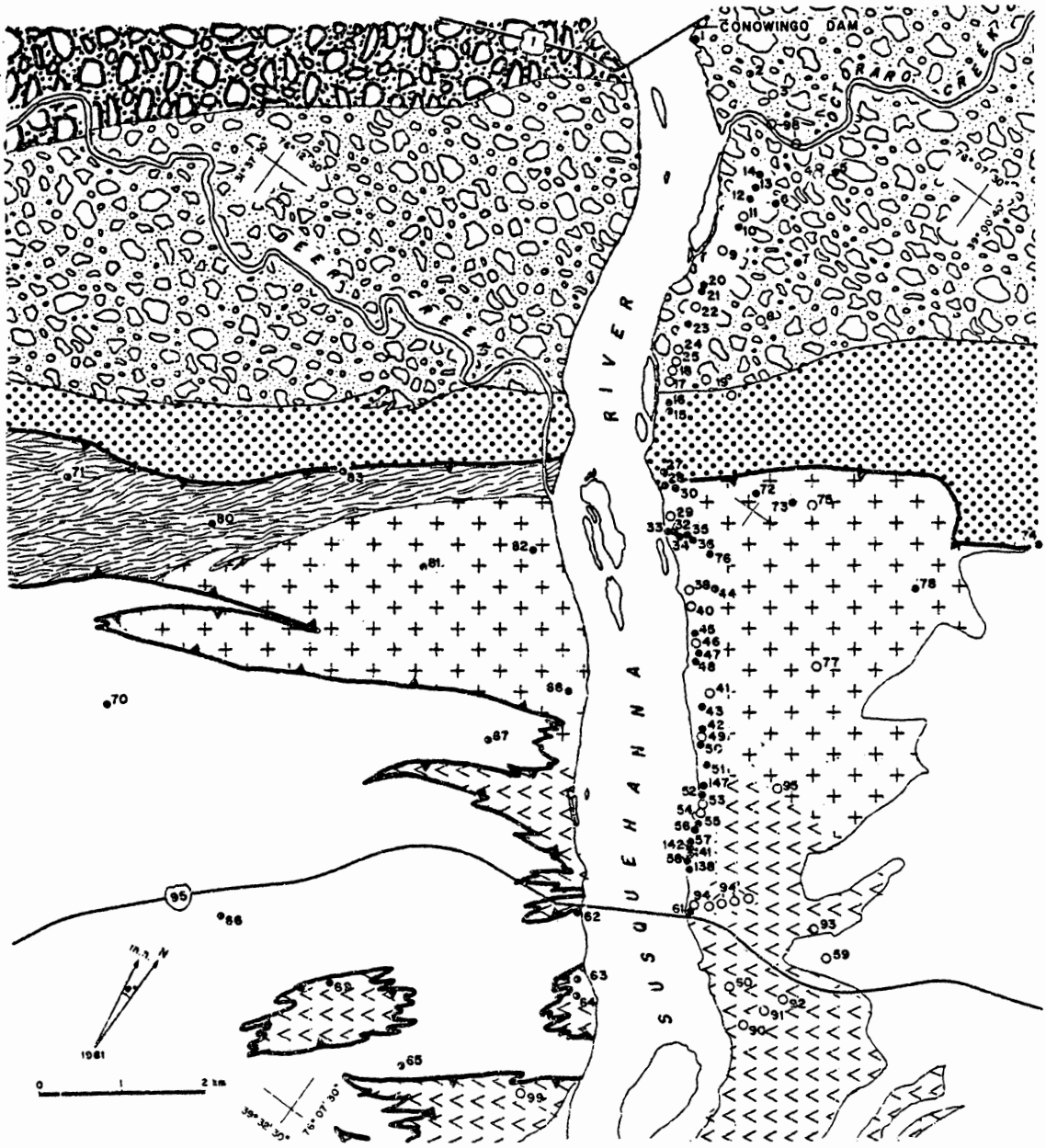

dip steeply to the southeast (Hershey, 1937). The diamictite is interbedded with metagreywacke to the southeast.

Port Deposit Complex

Sheared Port Deposit Gneiss

Southwick (1969) mapped a sheared Port Deposit gneiss which separates the Port Deposit Gneiss from the Wissahickon terrane and Baltimore Gabbro. These rocks are texturally similar to the sheared rocks northeast of the Susquehanna which separate the Port Deposit gneiss from the Wissahickon. The Wissahickon-Port Deposit Complex contact is mapped as a fault by Higgins (1982) and Lesser (this study). At or near this contact, inclusions of amphibolite and gneiss lie in a finer grained blastomylonitic matrix. This contact is knife-sharp and subparallel to the regional foliations described in Hershey (1937). The amphibolite inclusions are similar to those exposed in the Wissahickon terrane immediately to the northwest, and the gneiss inclusions are similar to the Port Deposit gneiss (described below). These rocks are considered to represent a fault breccia formed at the time of deformation (Plate 1).

Rocks texturally similar to the sheared Port Deposit Gneiss are not confined to the northwest margin of the Port Deposit Complex. The contact between these two Port Deposit members is gradational. A shear zone 1.5 meters in width is exposed as far southeast as the Port Deposit Quarry with blastomylonitic fabrics nearly identical to the sheared Port Deposit Gneiss.

Plate 1. The knife-sharp Port Deposit Complex - Wissahickon Contact. Inclusions of mafic material are present in a Sheared Port Deposit Gneiss matrix. Scale in centimeters. Field stop #30.

Port Deposit Gneiss

The Port Deposit Gneiss is a relatively homogeneous, fine grained leucocratic tonalite gneiss with occasional inclusions of amphibole quartz diorite. The felsite/amphibolite ratio estimated in the field exceeds 20/1. The foliations strike northeast-southwest and dip steeply towards the southeast (Hershey, 1937). Dykes show remnant chilled contact margins. Relict hypidiomorphic granular fabrics are found, but are most common near the gradational James Run/Port Deposit contact on the southeast where the metavolcanic rocks of the James Run Formation are weakly and variably sheared. These relict plutonic fabrics led Hershey (1937) and Southwick (1969) to conclude that the Port Deposit Gneiss protolith was a pluton. The gradational James Run/ Port Deposit contact led Higgins (1970) to conclude the Port Deposit was a hypabyssal, plutonic equivalent of the felsic James Run metavolcanics: protoclastic granulation immediately after igneous consolidation obscured the volcanic/plutonic contact.

James Run Formation

The James Run Formation is a bimodal volcanic sequence of amphibolites and felsic rocks. The estimated felsite/amphibolite outcrop ratio for the James Run is at least 5/1. The James Run bears a gradational contact with the Port Deposit and is weakly and variably sheared near this contact. The metavolcanics are interpreted to be in thrust contact with the Aberdeen Metagabbro (Crowley, 1976; Hanan, 1980). Intrusive felsic rocks can display remnant quench textures. Intrusive mafic

rocks have been completely recrystallized to amphibolite, but may show relict chilled border textures. Pillow lavas with relict amygdules led Higgins (1971) to conclude that these rocks were erupted at shallow depths. Arkosic metasediments crop out near the southeastern margins of the James Run.

PETROGRAPHY

Additional photographs of pertinent microtextures are presented in Lesser (this study), Appendix III. Point counts were performed on stained thin sections 4 x 2 cm in area and on stained slabs 8 x 5 cm in area. 1000 points were counted, and representative modal compositions are presented in Table I. Point count data for all samples analyzed for this study are presented in Lesser (this study), Appendix IV.

Conowingo Diamictite

Following McBryde's classification (1963), the Conowingo Diamictite is characterized as an arkose or lithic arkose (Figure 3).

Quartz is present as semi-spherical relict detrital grains (10 x 6 mm), elongated schlieren with length/width ratios of 5/1 (S_1), and as interstitial grains 0.05 mm*. Albitic plagioclase (10 x 6 mm) is present as detrital grains and interstitial to quartz and detrital albite. Potassium feldspar is detrital, but more commonly is interstitial to quartz and plagioclase. Anti-rapakivi and perthitic textures can be found in a single thin section that contains potassium feldspar and plagioclase grains that lack such exsolution textures, implying the diamictite was derived from different sources with different cooling histories and compositions.

Biotite defines a weak anastomosing fabric and is also present as rare books poikilitically enclosing quartz and plagioclase (S_2,S_3?). Muscovite is present as sericite after feldspar, as small books, and

---

*Measurements refer to maximum grain sizes.

Table I. Representative modal mineralogy for the Conowingo Diamictite (CD), Port Deposit Gneiss (PD), Sheared Port Deposit (PD-s) and James Run Formation (JR). 1000 counts were performed on stained thin sections 4 x 2 cm^2 and stained slabs 8 x 5 cm^2 according to the grain sizes of the sample. Sample RL-80-57 is blastoporphyritic and so both thin section and slab point counts were performed. All data from Lesser (this study).

Sample No.	RL-80-6	RL-80-7	RL-80-39	RL-80-49	MJ 8151	RL-81-44	RL-80-57
Unit	CD	CD	PD	PD	PD	PD-s	JR
Phase			Stained thin sections				
Plagioclase	X	X	42.6	19.6	52.8	33.5	57.8
Quartz	X	X	44.4	2.3	36.5	45.8	33.6
K-feldspar	X	X	1.0	-	0.1	1.2	-
Hornblende	-	-	-	53.6	-	-	-
Biotite	X	X	5.5	-	4.6	5.6	4.0
Epidote	X	X	3.3	11.4	3.9	4.7	1.1
Piemontite	X	X	0.1	-	-	-	tr.
Zoisite	-	-	-	8.7	-	-	-
Zircon	-	X	tr.	-	-	tr.	-
Muscovite	X	X	2.9	2.6	2.1	7.9	2.9
Magnetite	X	X	tr.	0.8	tr.	0.6	0.4
Rutile	-	X	-	-	-	-	-
Apatite	-	X	tr.	tr.	-	0.1	-
Titanite	X	X	tr.	-	-	0.1	-
Allanite	-	-	tr.	-	tr.	-	-
Garnet	-	-	0.2	-	-	tr.	-
Chlorite	X	X	tr.	1.0	tr.	0.5	0.2

Table I (continued).

Sample No.	RL-80-6	RL-80-7	RL-80-39	RL-80-49	MJ 8151	RL-81-44	RL-80-57
Unit	CD	CD	PD	PD	PD	PD-s	JR
Phase			Stained slabs				
							Phenocrysts
Plagioclase	29	52					22
Quartz	39	39					12
K-feldspar	11	0					1
Mafics	21	9					1
							Groundmass
							63

Figure 3. McBryde's (1963) sandstone classification for the Conowingo Diamictite. Data from Hopson (1964) and Lesser (this study).

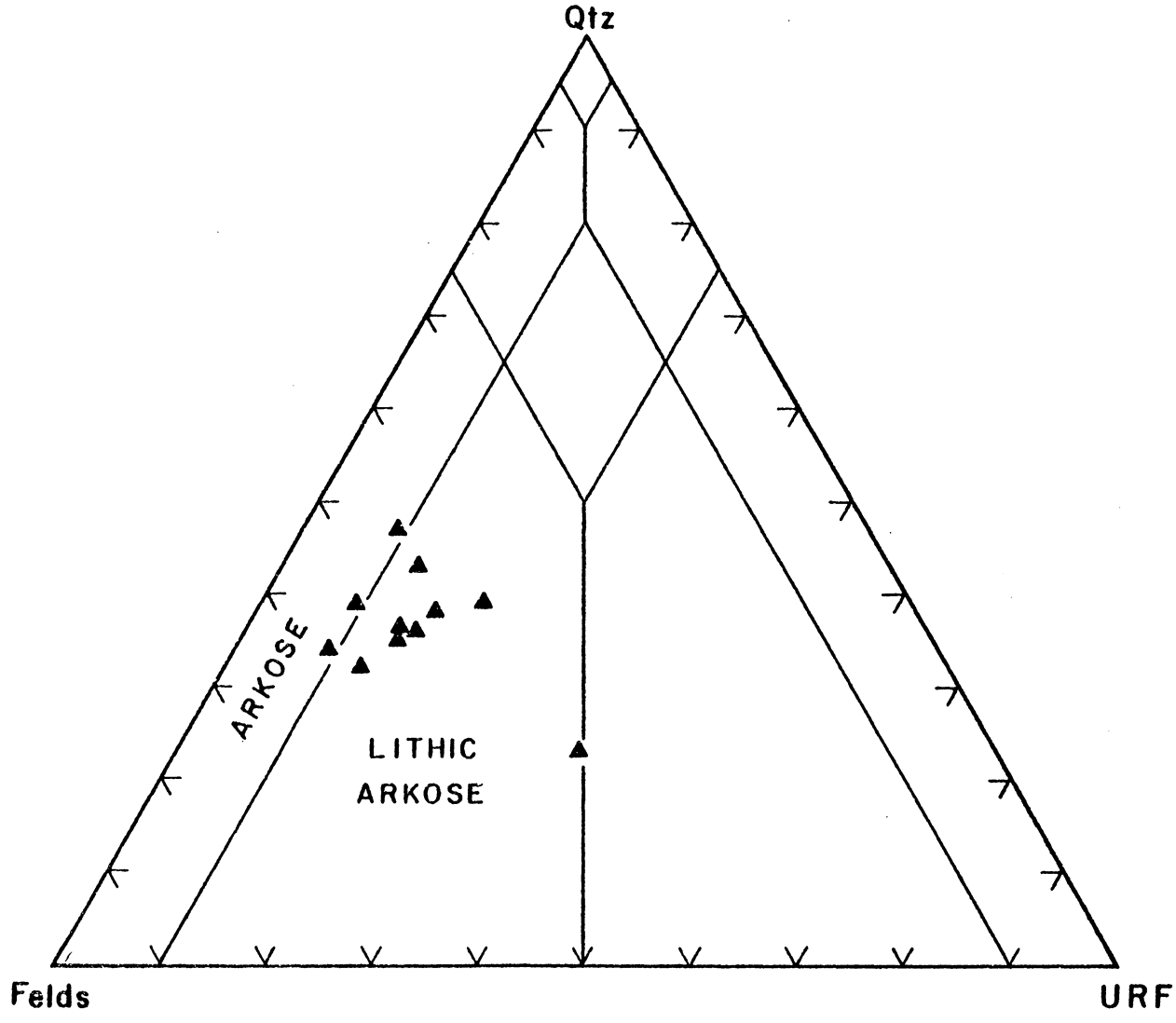
Qtz
ARKOSE
LITHIC
ARKOSE
Felds
URF

defining a very weak late-stage disjunctive cleavage (S_3?,S_4?). This sequence of microtexture development mimics the sequence of the gneissic Port Deposit and James Run rocks (Table II, further discussion below).

Unzoned epidote is replacing plagioclase, and zoned epidote is associated with cleavages defined by biotite. Garnet is rare and displays good crystal form. Allanite is zoned, metamict, and rimmed with epidote. Piemontite is present but very rare. Magnetite is the only opaque phase found in reflected light studies.

Port Deposit Complex

Sheared Port Deposit Gneiss

The sheared Port Deposit Gneiss consists of meta-granodiorite and meta-tonalite gneisses with blastomylonitic fabrics (Figure 4; Southwick, 1969).

Quartz and plagioclase are segregated into discrete domains which have length/width ratios of 30/1. The quartz has been recrystallized and shows polygonal textures. Occasional potassium feldspar is associated with the plagioclase domains. Plagioclase porphyroblasts are very rare.

Biotite disjunctive cleavages are subparallel to the gneissosity and show decussate textures. The biotite may be heavily chloritized. The quartz and feldspar domains are truncated by these cleavages. Sericitic muscovite is present and is subparallel to the overall foliation. Allanite shows overgrowths of zoned zoisite and epidote. Garnets are similar to garnets of the Port Deposit Gneiss. Magnetite was the

Table II. Interpretative sequence of mineral development based on microtextural overprint relations. This sequence is based on felsic rocks only. The relative infrequency of amphibolitic rocks with polydeformational features precludes their use in a microtextural comparison. See text for discussion.

	James Run	Port Deposit		Conowingo Diamictite
Primary	magnetite apatite plagioclase quartz potassium feldspar	magnetite apatite plagioclase quartz potassium feldspar	Detrital	plagioclase quartz potassium feldspar
Pre-tectonic	epidote, unzoned sericite garnet allanite	epidote, unzoned sericite garnet allanite	Pretectonic	epidote, unzoned sericite garnet allanite
S_1	quartz-albite stringers epidote, unzoned & zoned sericite	quartz-albite stringers epidote, unzoned & zoned sericite		quartz-albite stringers epidote, unzoned & zoned sericite
S_2 and S_3	biotite epidote, zoned & unzoned magnetite	biotite epidote, zoned & unzoned magnetite piemontite		biotite epidote, zoned & unzoned magnetite piemontite
S_4	sericitic muscovite	sericitic muscovite		sericitic muscovite

Figure 4. Modal and normative quartz-plagioclase-potassium-feldspar plots with the classification fields of Streckeisen (1973, 1979) for the Port Deposit Complex and James Run Formation. Data from Higgins (1972), Southwick (1969), and Lesser (this study).

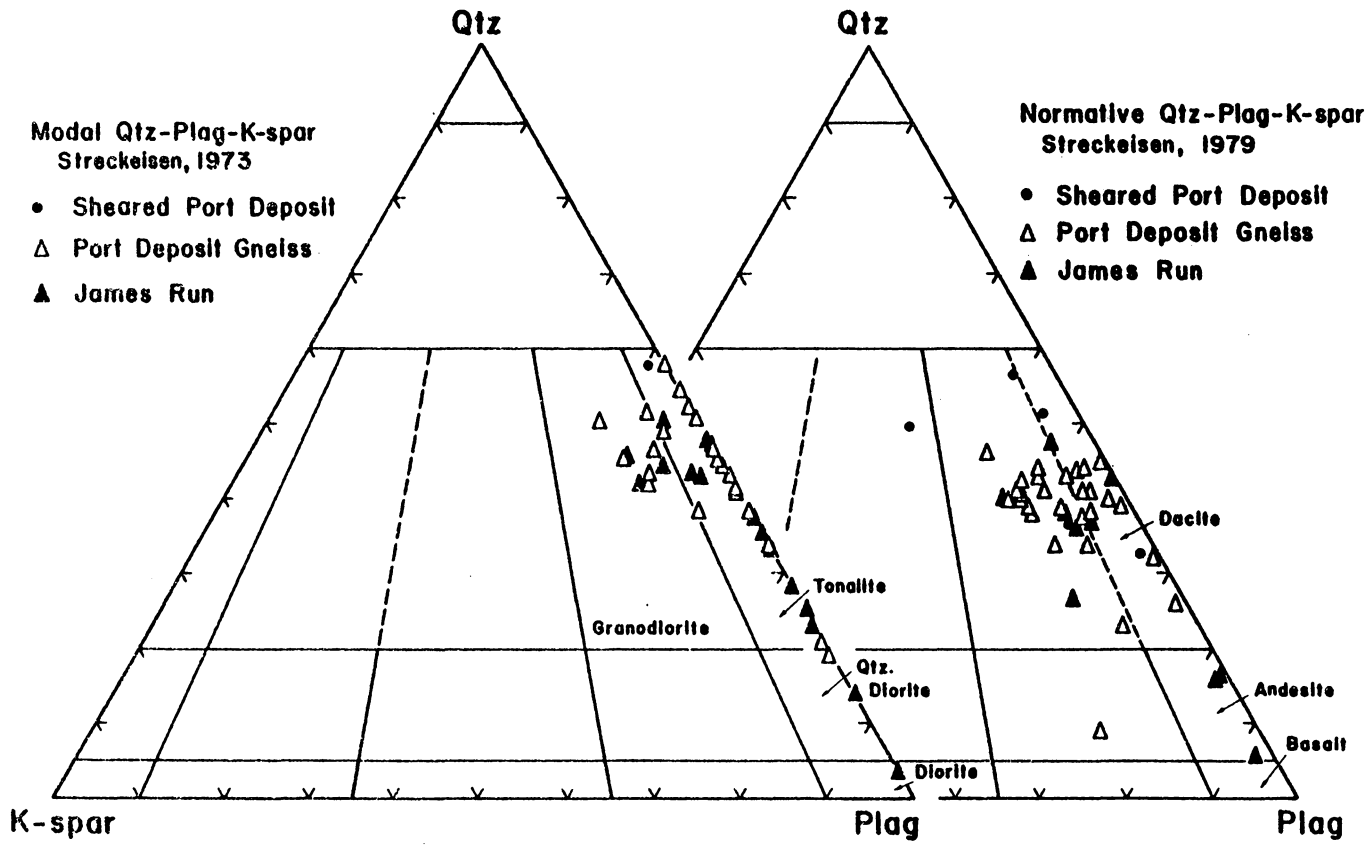
Qtz
Qtz
Modal Qtz-Plag-K-spar
Streckeisen, 1973
• Sheared Port Deposit
△ Port Deposit Gneiss
▲ James Run
Normative Qtz-Plag-K-spar
Streckeisen, 1979
• Sheared Port Deposit
△ Port Deposit Gneiss
▲ James Run
Granodiorite
Tonalite
Qtz.
Diorite
Diorite
Dacite
Andesite
Basalt
K-spar
Plag
Plag

only opaque phase identified in reflected light. The sequence of secondary mineral development is similar to that of the Conwingo Diamictite, Port Deposit Gneiss and James Run felsites (Table II, discussion above and below).

Port Deposit Gneiss

In normative and modal quartz-plagioclase-potassium-feldspar diagrams, the Port Deposit gneiss falls into the meta-quartz diorite, meta-tonalite, and meta-granodiorite fields of Streckeisen (1973) (Figure 4), and shows gneissic and relict plutonic fabrics (Plates 2 and 3).

Quartz defines anastomosing stringers 1 mm long with length/width ratios of 20/1 on the northwest and 10/1 on the southeast (S_1). Less sheared samples may show quartz interstitial to plagioclase porphyroblasts. Rare ribbon textures and deformation bands are present, but more commonly the quartz has been recrystallized and displays polygonal textures. These stringers are truncated by later anastomosing biotite (S_2,S_3) (Plates 2 and 3) and muscovite (S_4) disjunctive cleavages. Quartz augen 5 x 2 mm in size consist of several quartz stringers of smaller size that are separated by thin cleavages of biotite.

Albitic plagioclase is slightly zoned and contains epidote and sericite concentrations in the cores. The plagioclase is found as subhedral porphyroblasts (0.9 x 0.8 mm) with mortared margins, untwinned anhedral subgrains (0.05 mm), and anhedral grains with pronounced mechanical twins. In the gneissic rocks, feldspars are segregated into domains (1 x 0.3 mm) of feldspar subgrains (0.05 mm) (S_1).

Plate 2. Port Deposit Gneiss with biotite dysjunctive cleavages. Scale in centimeters. Sample RL-81-21, Field Stop #76.


0 1 2 3 cm

Plate 3. Port Deposit Gneiss without clear S_2 and S_3 biotite dysjunctive cleavage development. RL-81-25, Field Stop #79.


0 1 2 3 cm

The subhedral porphyroblasts and subgrains can be almost entirely sericitized. Symplectitic intergrowths of quartz and plagioclase are found near the James Run contact. Orthoclase is present as anhedral subgrains 0.05 mm, and contains rare inclusions of quartz and epidote.

Biotite is present as books (0.3 x 0.05 mm), defining an anastomosing fabric with decussate texture (S_2), and as a weak crenulation cleavage (S_3). It is rarely in the feldspar or quartz domains, but is rather subparallel and cross-cuts the gneissosity. Some chloritization has occurred, but more often the biotite is associated with muscovite.

Muscovite has three associations: sericite after plagioclase (pre-S_1?,S_4?), sericite in a disjunctive cleavage (S_4), and as minute books with straight margins associated with biotite having irregular margins. This sericite is subparallel to biotite cleavages, and thus overprinting relations are not diagnostic indicators of its sequence of development.

Epidote has two associations: with biotite in the disjunctive cleavages (S_2 and S_3), and in plagioclase as an alteration product with sericite. The epidote associated with biotite displays zoned rims and unzoned cores, whereas the epidote that replaces plagioclase has no such zoning. Magnetite was the only opaque phase observed in reflected light and is associated with epidote and biotite in the disjunctive cleavages. X-ray diffraction analyses were performed on opaque mineral separates: no evidence for ilmenite was found.

Idioblastic and anhedral garnets do not have helcitic textures and have biotite in pressure shadows. The rims are inclusion free, whereas the cores contain quartz and feldspar inclusions. The anhedral garnets display both straight crystallographic faces and irregular,

curved margins. The idioblastic and anhedral garnets display no systematic mineralogic relationships or associations: they exist in disjunctive phyllosilicate cleavages as well as in feldspar and quartz domains. These garnets are interpreted as fragments of mechanically fractured grains and imply pre-S_1 development.

S_1 is defined by elongated quartz-feldspar domains. S_2 and S_3 are defined by biotite-epidote disjunctive cleavages (Plates 2 and 3), and S_4 is defined by sericitic muscovite (Plate 4, Table II).

Quartz diorite amphibolite float is common over the Port Deposit terrain. These rocks display blocky hornblende grains with minor quartz and plagioclase. Epidote, magnetite, and apatite are accessory phases. Zoisite and muscovite are post-deformation alteration products. The textures are similar to amphibolites of the James Run.

James Run Formation

The James Run is a bimodal meta-volcanic sequence with relict primary and superposed tectonic fabrics. In normative and modal quartz-plagioclase-potassium-feldspar diagrams (Figure 4), the rocks fall into the meta-basalt, meta-andesite, and meta-dacite fields of Streckeisen (1979).

Metadacites

Quartz is present as bipyramidal blastophenocrysts (2.5 x 2.5 mm) and as mesostasis crystals (0.05 mm) that display varying degrees of ribbon and mortar textures, undulatory extinction, and/or polygonal texture. Length/width ratios on quartz schlieren approach 5/1 (S_1).

Sericitization of zoned plagioclase phenocrysts (3.5 x 3.5 mm) is absent to minor, but increases in intensity towards the northwest. Albite, Carlsbad, Baveno, and mechanical twins are present. Granophyric intergrowths of quartz and plagioclase are observed as jackets about plagioclase, as phenocrysts, and in the groundmass.

Small biotite books are present, but more commonly biotite defines a weak disjunctive cleavage in association with zoned epidote and magnetite (S_2 and S_3). Muscovite is more abundant at the southern end of the Port Deposit town near the James Run/Port Deposit contact: as sericite with unzoned epidote in plagioclase (pre-S_1?) and defining a weak disjunctive cleavage (S_4). Epidote generally has cores with zoned rims when in association with biotite, and piemontite is ubiquitous. Allanite is zoned, metamict, rimmed with epidote, and confined to areas near the Port Deposit contact. Garnet is idioblastic and contains quartz and feldspar inclusions; the garnet rims are inclusion free. Titanite is present in association with chloritized biotite. Apatite needles are found enclosed by plagioclase blastophenocrysts. Magnetite is the only opaque phase observed in reflected light and occurs as euhedral inclusions (0.05 mm) in plagioclase blastophenocrysts and as anhedral grains (0.03 mm) in association with biotite.

Four foliations are observed: elongation of quartz phenocrysts to stringers with length/width ratios of 5/1 (S_1); as anastomosing cleavages of biotite and zoned epidote (S_2 and S_3); and a very weak disjunctive cleavage of sericitic muscovite (S_4) (Table II). The intensity of cleavage development increases towards the northwest.

Meta-andesites and Meta-basalts

Andesine-albite plagioclase is present as blastophenocrysts (3.5 x 3.0 mm) and in the mesostasis as subgrains (0.05 mm). Plagioclase blastophenocrysts show blastotrachytic textures.

Three amphiboles are present: grunerite(?), pale green brown hornblende, and dark green hornblende. The grunerite is rimmed by hornblende. All three amphiboles are not necessarily present in each sample. In the meta-andesites, amphiboles measure 5 x 1 mm, in the meta-basalts subhedral to anhedral blocks of amphibole are 2.5 x 2.5 mm in size. Two foliations are defined.

Quartz shows foam texture and rare deformation bands. Amygdaloidal infillings consist of albite, epidote, zoisite, and magnetite. Magnetite is also present as blastomicrophenocrysts 2 x 2 mm. Pyrite and pyrrhotite 2.5 x 2.0 mm are accessory opaques.

Discussion

The Port Deposit, James Run, and Conowingo felsic rocks are similar in mineralogy and textures. A comparative analysis reveals these features:

(1) Decrease in the maximum size of plagioclase porphyroblasts or blastophenocrysts, from 3.5 x 3.5 mm (James Run) to 0.9 x 0.8 mm (Port Deposit Gneiss). This is associated with the development of mortar textures.

(2) Decrease in the maximum size of quartz blastophenocrysts or porphyroblasts, from 2.5 x 2.5 mm (James Run) to 1.0 x 0.4 mm

(Port Deposit Gneiss). Composite domains of quartz constitute augen which reach 5 x 2 mm; however, the individual quartz domains are considerably smaller. The decrease is associated with a concomitant increase in quartz length/width ratios, from 1/1 to 30/1.

(3) Garnet has been mechanically fractured in the Port Deposit.

(4) The James Run, Port Deposit, and Conowingo diamictite felsic rocks exhibit an identical sequence of secondary mineral and microtextural development (Table II, discussions above).

Segregation of quartz and feldspar into discrete domains of large length/width ratios with concomitant grain size reduction, and the presence of fractured garnets, is characteristic of shear zones operative at upper greenschist P-T conditions or higher (Hobbs et al., 1976; Sibson, 1977; Mitra, 1978; Beach, 1979). This metamorphic grade is consistent with the epidote-amphibolite mineralogies of the meta-basalts and meta-andesites of the James Run. The placement of a thrust fault at the Wissahickon-Port Deposit contact is consistent with the observation that these felsites show the highest length/width ratios when compared with less sheared material of similar mineralogy to the southeast and northwest. In addition, it is consistent with Higgins' (1982) observation that cross-cutting amphibolite dikes are present in the James Run and Port Deposit association, but are absent from stratigraphically lower Wissahickon metasediments to the northwest.

GEOCHEMISTRY

Analytical Methods

Samples weighing 2-10 kg were crushed, split by the cone and quartering method to 1 kg, powdered in a tungsten carbide mill, and then resplit to 0.25 kg for regrinding to an average grainsize of 5.0 microns prior to chemical and isotopic analyses. Major element determinations were performed with a Phillips Sequential X-ray Analysis System Model 1450 using techniques outlined by Norrish and Hutton (1969), Harvey et al. (1973), and Norrish and Chappell (1977). Rb, Sr, and Na_2O concentrations were determined on pressed powder pellets (Norrish and Chappell, 1977). Sr isotopic compositions were measured on a 35 cm solid source mass spectrometer interfaced to an LSI/1 minicomputer. Mineral separates and selected powders were spiked with mixed Rb-Sr spike to measure Rb and Sr concentrations. Strontium blanks averaged 465 picograms (eight analyses) and Rb blanks averaged 70 picograms (two analyses).

Instrumentation modifications during Sr-data collection caused a change in the measured values of the Eimer and Amend $SrCO_3$ standard. Prior to modification, the measured values averaged 0.70831 ± 3 ($n = 19$), and subsequent to modification, the measured values averaged 0.70861 ± 3 ($n = 21$). The decay constant of ^{87}Rb was taken as $\lambda = 1.42 \times 10^{-11} yr^{-1}$ (Steiger and Jager, 1977). Regressions were calculated according to the method of York (1966) as presented by Faure (1977); ages and MSRS values are quoted from regression Model II. All standard errors of the mean are quoted at the two sigma confidence level. Symbols for data

plots in this study meet or exceed the two sigma uncertainty range, except if noted for the individual diagram.

Major Element Chemistries

Table III presents representative chemical data for all rocks analyzed in this study. Comprehensive chemical data, values for accepted USGS rock standards, and data tables of replicate analyses are presented in Lesser (this study), Appendix V.

Conowingo Diamictite

The Conowingo rocks range from 62-73% SiO_2 (n = 5) with an average of approximately 70% silica. Higgins (1972) used chemical data from the Conowingo unit to evaluate its sedimentary nature, whereas Southwick (1979) pointed out such data is not necessarily applicable. The diamictite is chemically similar to the meta-igneous Port Deposit and James Run felsites (discussion below), but petrographic distinctions discussed above establish its metasedimentary nature.

Port Deposit Complex

A silica histogram (Figure 5-A) for the sheared Port Deposit Gneiss and Port Deposit Gneiss units show a bimodal distribution with the felsic component (average SiO_2 = 74%, n = 35) dominant over the mafic and intermediate components (average SiO_2 = 58%, n = 11).

The sheared Port Deposit Gneiss is dominantly trondhjemitic by the refined chemical classification of Barker (1979b) (Figure 5-B). Bulk chemical and AFM diagrams (Figures 5-C and 5-D) do not present a range

Table III. Representative major element chemistries for the Conowingo Diamictite (CD), Port Deposit Gneiss (PD), Sheared Port Deposit (PD-s), and James Run Formation (JR). All data from Lesser (this study).

Sample No.	RL-80-3 CD	RL-80-39 PD	RL-80-49 PD	MJ 8151 PD	RL-81-44 PD-s	RL-80-57 JR	RL-80-66 JR
Oxide			Major Element Chemistries				
SiO_2	62.03	74.82	53.91	73.40	72.48	74.04	67.45
TiO_2	1.08	0.23	0.79	0.24	0.28	0.22	0.72
Al_2O_3	15.25	12.08	14.84	13.33	13.81	13.27	14.67
Fe_2O_3	7.28	2.43	11.46	2.74	3.08	2.45	5.26
MnO	0.15	0.06	0.20	0.08	0.10	0.04	0.09
MgO	1.86	0.60	4.76	0.55	0.66	0.59	1.79
CaO	6.52	1.53	10.63	2.85	2.72	2.01	3.54
Na_2O	2.03	5.45	0.15	3.65	4.52	7.12	5.38
K_2O	0.65	0.64	0.19	1.94	1.34	1.30	0.20
P_2O_5	0.24	0.06	0.05	0.05	0.08	0.04	0.24
LOI	2.58	0.70	1.95	0.77	0.68	0.63	0.69
Total	99.67	99.62	98.91	99.60	99.82	101.80	99.93

Table III (continued).

Sample No.	RL-80-3 CD	RL-80-39 PD	RL-80-49 PD	MJ 8151 PD	RL-81-44 PD-s	RL-80-57 JR	RL-80-66 JR
Phase	C.I.P.W. Normative Minerals						
Q	32.66	40.34	26.47	38.41	34.80	52.88	26.02
C	0.00	0.50	0.00	0.17	0.17	4.78	0.00
Or	3.96	10.99	1.16	11.60	7.99	8.47	1.19
Ab	17.69	33.35	0.87	31.25	38.61	19.34	45.07
An	31.50	11.47	40.73	13.98	13.09	10.09	15.41
Wo	0.00	0.00	4.72	0.00	0.00	0.00	0.00
En	4.77	0.48	12.23	1.39	1.66	1.52	4.49
Hm	7.50	2.51	11.82	2.77	3.11	2.55	5.30
Il	0.33	0.11	0.44	0.17	0.22	0.09	0.19
Tn	0.14	0.00	1.43	0.00	0.00	0.00	0.97
Ru	0.88	0.17	0.00	0.15	0.17	0.18	0.23
Ap	0.59	0.10	0.12	0.12	0.19	0.10	0.33

Figure 5-A. Silica histograms for the Port Deposit Complex and James Run Formation. Data from meta-igneous rocks only are plotted. Data from Southwick (1969), Hanan (1980), Higgins (1982), and Lesser (this study).

Silica Histograms

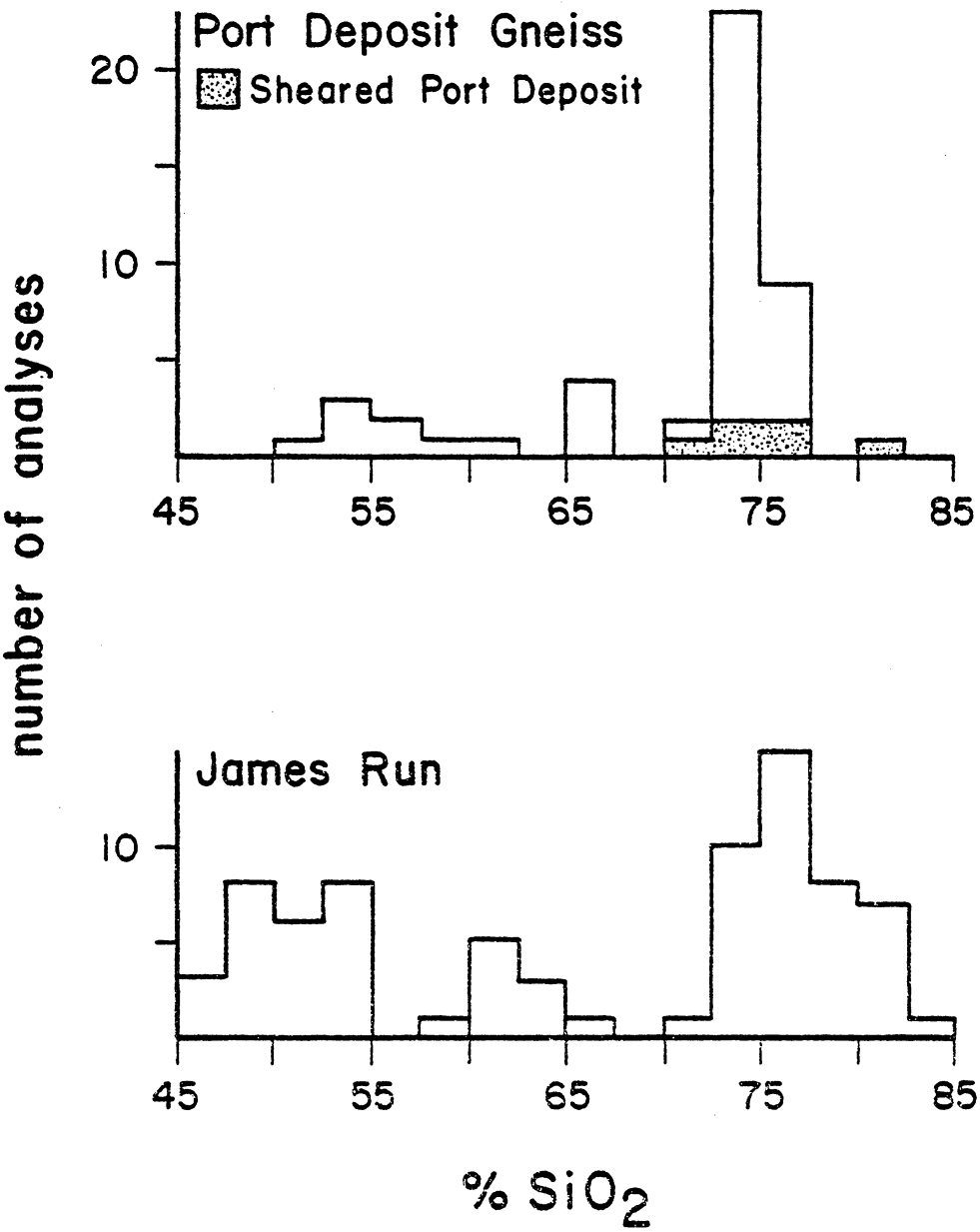

Figure 5-B. Normative orthoclase-albite-anorthite plot of O'Connor (1965) as modified by Barker (1979). Sheared Port Deposit Gneiss (●), Port Deposit Gneiss (△), and James Run Formation (▲). Data from meta-igneous rocks only are plotted. Data from Southwick (1969), Hanan (1980), Higgins (1982), and Lesser (this study).

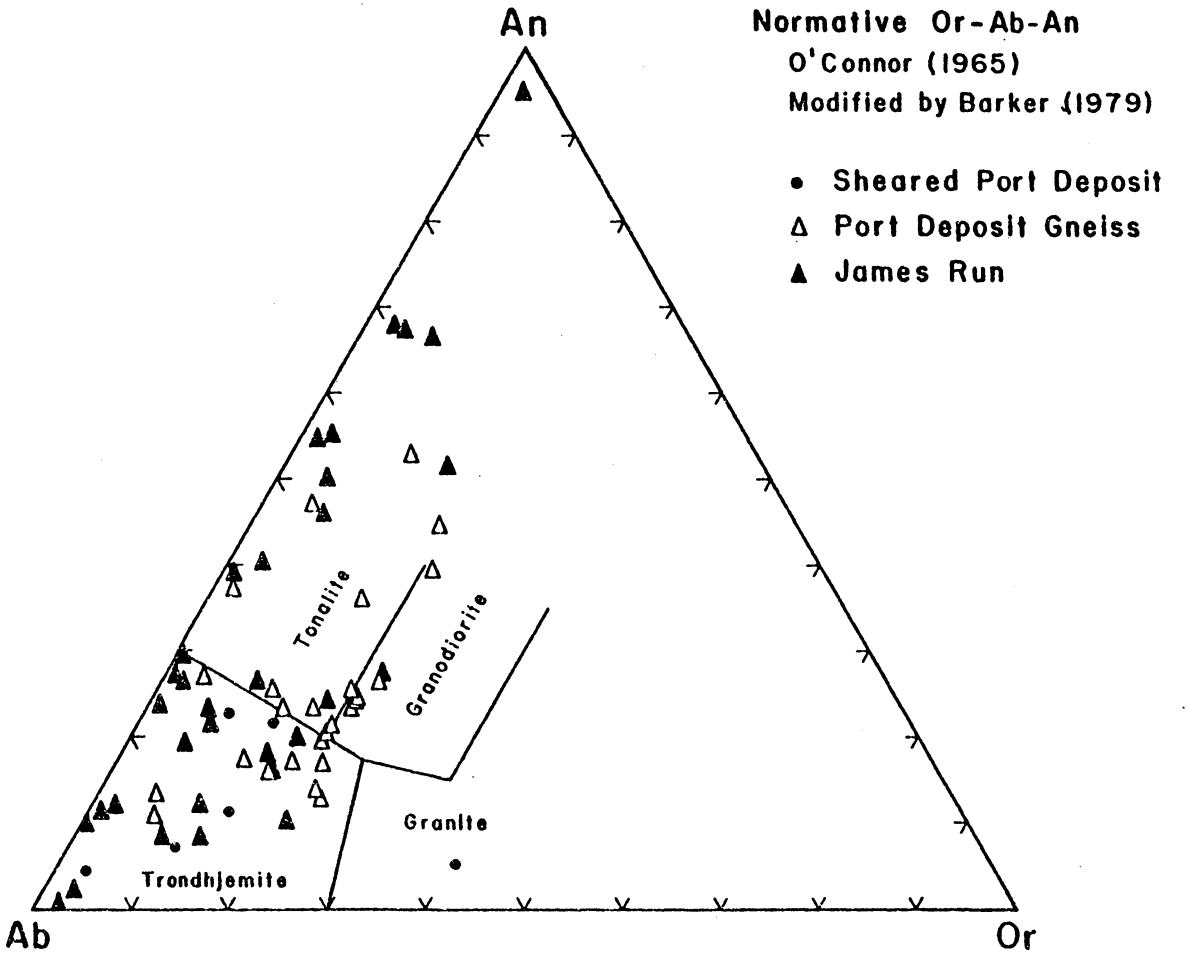
An
Ab
Or
Tonalite
Granodiorite
Granite
Trondhjemite
Normative Or-Ab-An
O'Connor (1965)
Modified by Barker (1979)
Sheared Port Deposit
Port Deposit Gneiss
James Run

Figure 5-C. Harker variation diagrams for the Port Deposit Complex and James Run Formation. Symbols as in Figure 5-B. Data from Southwick (1969), Hanan (1980), and Lesser (this study).

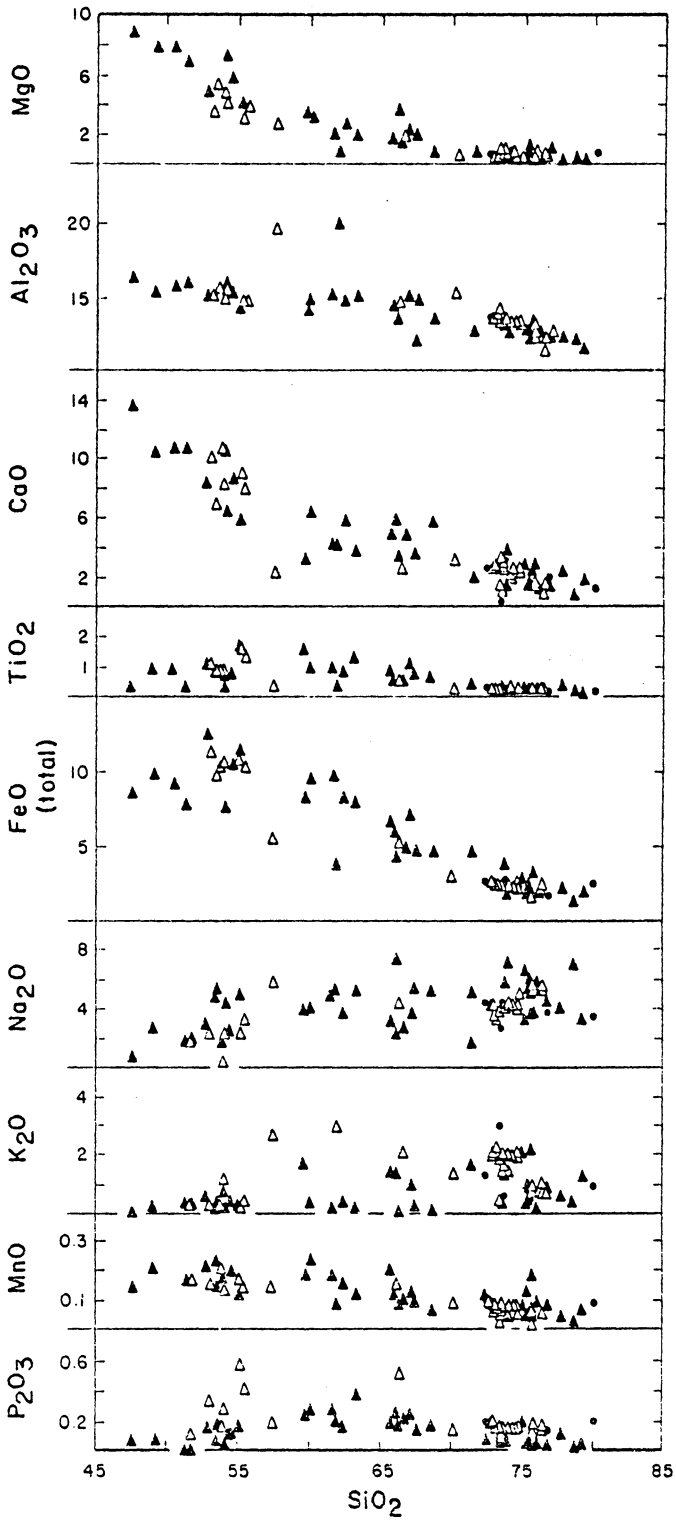
MgO
Al2O3
CaO
TiO2
FeO (total)
Na2O
K2O
MnO
P2O3
SiO2
45
55
65
75
85

Figure 5-D. AFM plot for the Port Deposit Complex and James Run Formation. Symbols as in Figure 5-B. Data for meta-igneous rocks only. Data from Southwick (1969), Hanan (1980), and Lesser (this study).

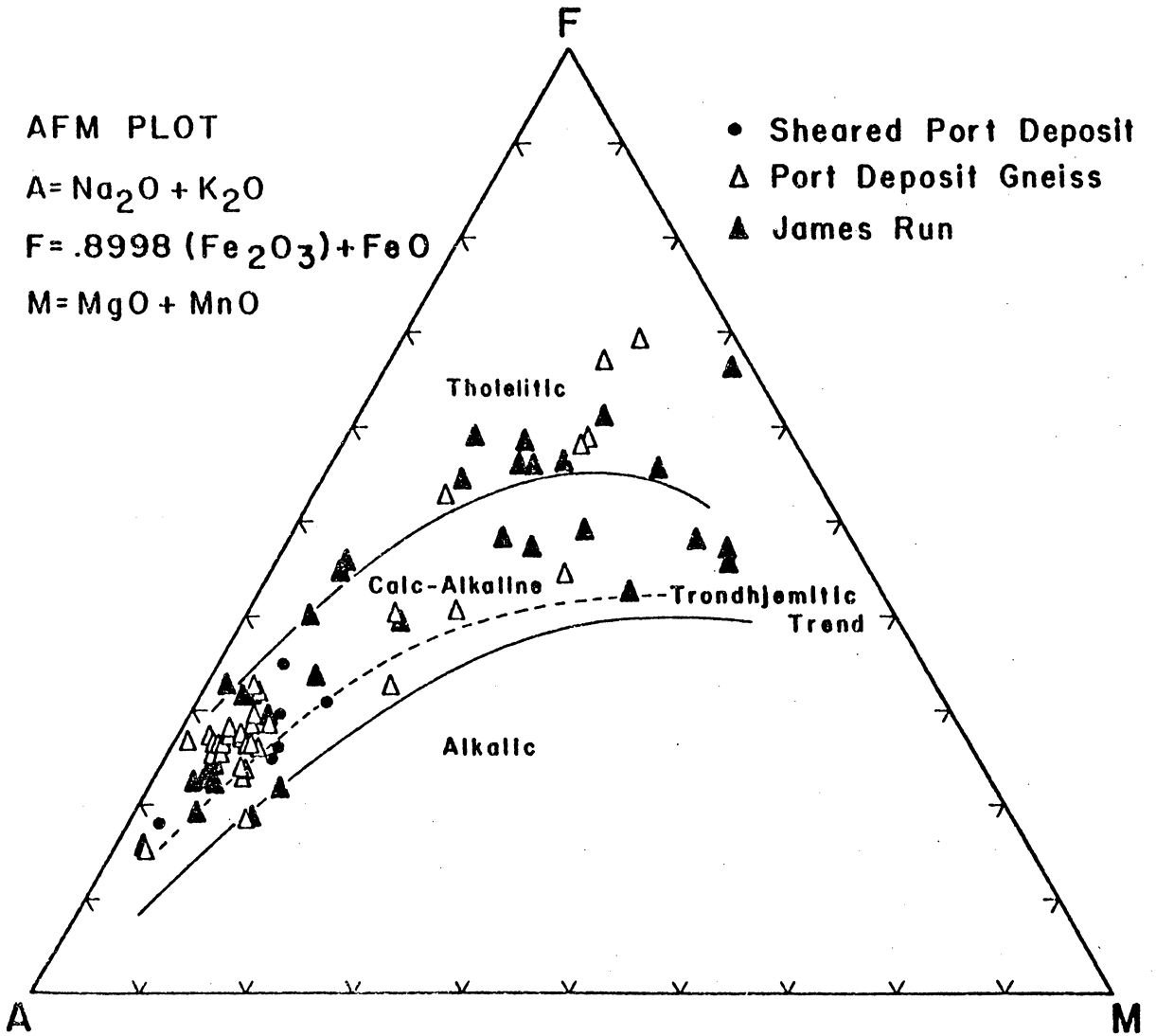
AFM PLOT
A= Na2O + K2O
F= .8998 (Fe2O3)+FeO
M= MgO + MnO
• Sheared Port Deposit
Δ Port Deposit Gneiss
▲ James Run
F
A
M
Tholeiitic
Calc-Alkaline
Trondhjemitic
Trend
Alkalic

of compositions to indicate calc-alkaline, trondhjemitic, or tholeiitic differentiation trends. For the Port Deposit Gneiss, however, bulk chemical and AFM diagrams suggest, but are not diagnostic of, calc-alkaline differentiation trends with trondhjemitic affinities (as defined by Barker and Arth, 1976). The compositional range for silica is 53-77%. All oxides analyzed decrease in concentration with increasing silica except for Na_2O and K_2O. The K_2O versus SiO_2 and Rb versus Sr discrimination diagrams of Coleman (1977) and Coleman and Donato (1979) (Figures 5-E and 5-F) are indicative, but not diagnostic, of continental affinities for these trondhjemitic rocks. In contrast, the trondhjemites are low alumina in the sense of Barker et al. (1976) (Figure 5-C) and imply oceanic affinities for these rocks.

The sheared Port Deposit gneiss is depleted in potassium relative to the Port Deposit gneiss with the same silica concentrations. The sheared rocks are enriched in normative albite relative to normative anorthite and orthoclase, and are higher in normative quartz and orthoclase relative to normative plagioclase (Figures 4, 5-E, and 5-B). The sheared rocks define broader fields on these diagrams than the gneissic rocks. The Rb versus Sr plot in particular (Figure 5-F) shows a greater range for the sheared versus gneissic Port Deposit.

James Run Formation

A silica histogram for the James Run Formation (Figure 5-A) shows a strong bimodality with the felsic rocks (average SiO_2 = 87%, n = 40) dominant over the mafic and intermediate components (average SiO_2 = 57%,

Figure 5-E. Semilog plot of K_2O versus SiO_2 with the tectonic discriminant fields of Coleman (1977). Symbols as for Figure 5-B. Data from Southwick (1969), Hanan (1980), Higgins (1982), and Lesser (this study). Data for meta-igneous rocks only.

A. Continental granophyre

B. Continental trondhjemite

C. Oceanic plagiogranite

D. Continental tholeiitic basalt

E. Sub-alkaline basalts

F. Cumulate gabbro

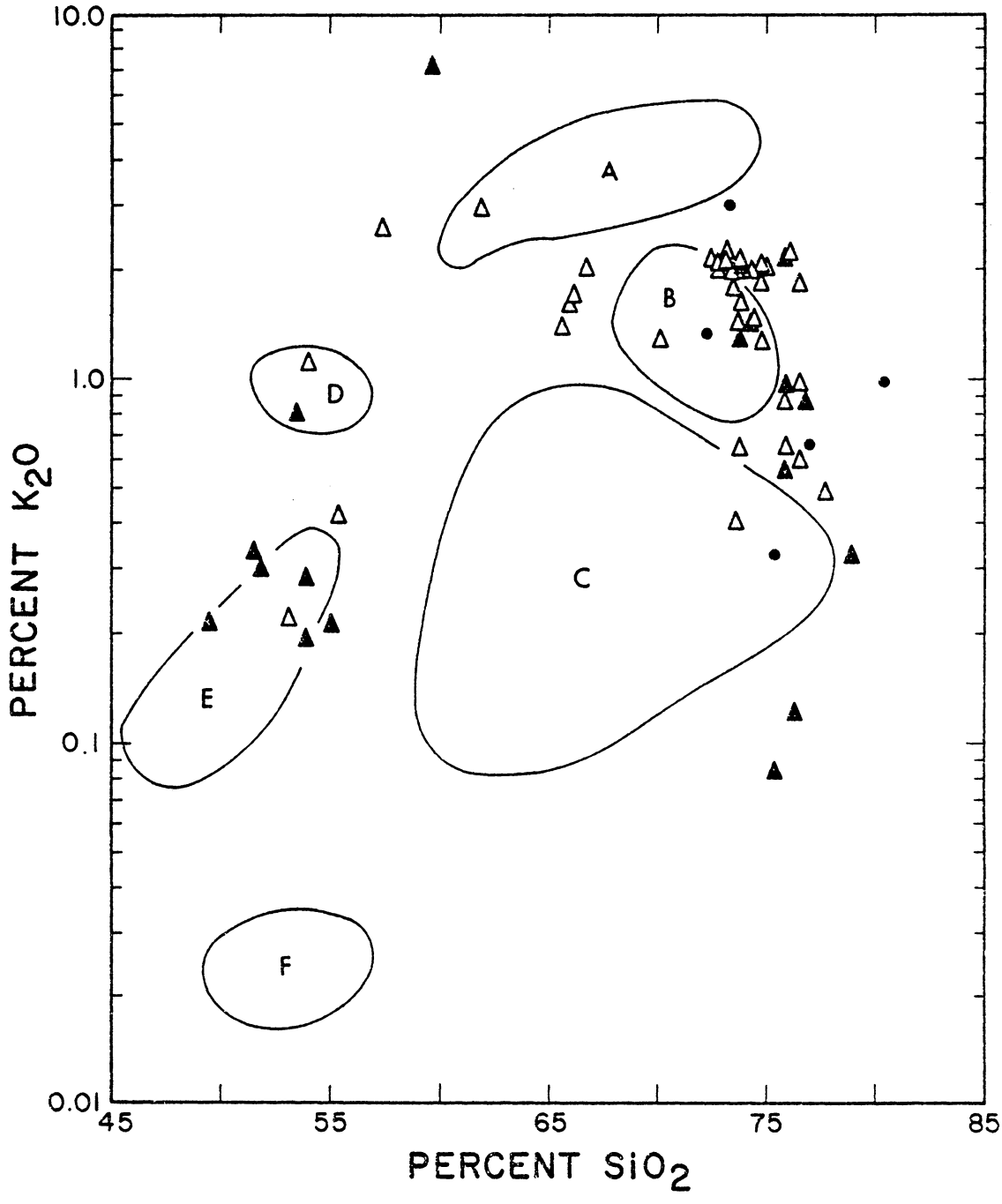
10.0
1.0
0.1
0.01
PERCENT K_2O
45
55
65
75
85
PERCENT SiO_2
A
B
C
D
E
F

Figure 5-F. Log-log plot of Rb versus Sr with the tectonic discriminant fields of Coleman and Donato (1979) as modified from Coleman and Peterman (1975) for the Port Deposit Complex and James Run Formation. Data for meta-igneous rocks only. Data from Hanan (1980) and Lesser (this study). Symbols for analyses of less than 10 ppm Rb are less than analytic uncertainty.

A. Continental granophyre and Red Sea granophyre

B. Continental trondhjemites

C. Oceanic plagiogranite

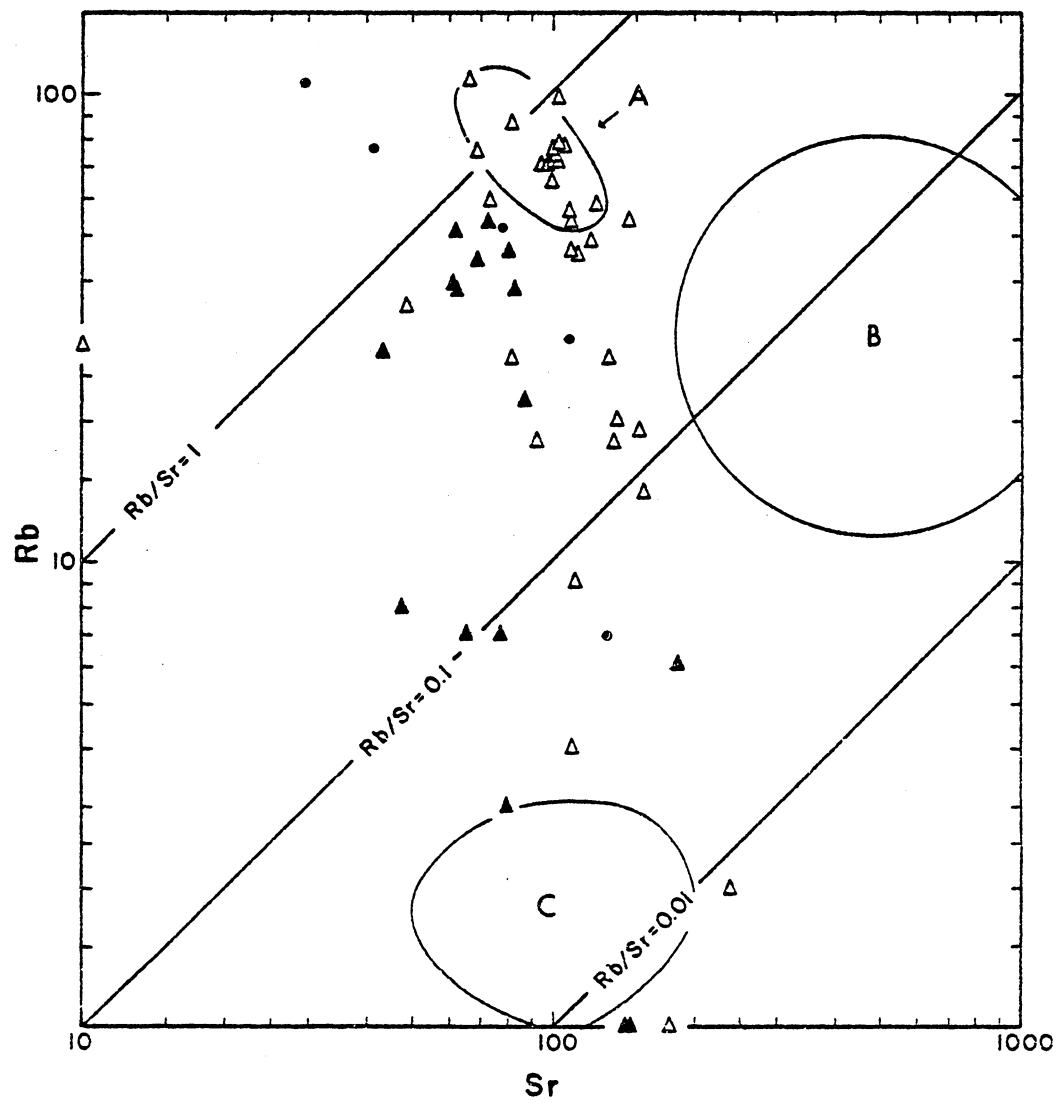
100
10
Rb
10
100
1000
Sr
A
B
C
Rb/Sr=1
Rb/Sr=0.1
Rb/Sr=0.01

n = 35). The felsite/amphibolite ratio estimated in the field approaches 5/1.

The James Run felsites fit the chemical definition of trondhjemite as given by Barker (1979b) (Figure 5-B). In agreement with Bland (1978) and Bland and Blackburn (1980), the metabasalts are low potassium tholeiites by the classification of Pearce (1976) (Figure 5-G). Bulk chemical and AFM plots (Figure 5-D) indicate calc-alkaline differentiation trends with trondhjemitic affinities and parallel the Port Deposit; the Peacock Index is calcic (Figure 5-H). SiO_2 ranges from 46-75%. All oxides decrease with increasing silica except Na_2O and K_2O. The K_2O versus SiO_2 and Rb versus Sr tectonic discriminant diagrams (Figures 5-E and 5-F) show no confinement to any particular field. The James Run rocks are low alumina in the sense of Barker et al. (1976) and imply an oceanic tectonic affinity.

Discussion

Evaluation of chemical data from sheared and metamorphosed igneous rocks has proved difficult. Hopson (1964), Southwick (1969, 1979) and Higgins (1972) interpreted the James Run/Port Deposit bulk chemistries as representative of subsolidus alteration during initial cooling and subsequent metamorphism. For a presentation of any tectonic model which includes the James Run/Port Deposit rocks, bulk chemical variations as a result of shearing and metamorphism must be limited.

To test the possible relation of secondary mineral development with alteration (Augustithus, 1973; Southwick, 1979), Figure 6-A plots the modal percentages of secondary minerals found in cleavages against the

Figure 5-G. Tectonic discriminant diagram of Pearce (1976) for the Port Deposit Complex and James Run Formation. Symbols as in Figure 5-B. Data from Lesser (this study).

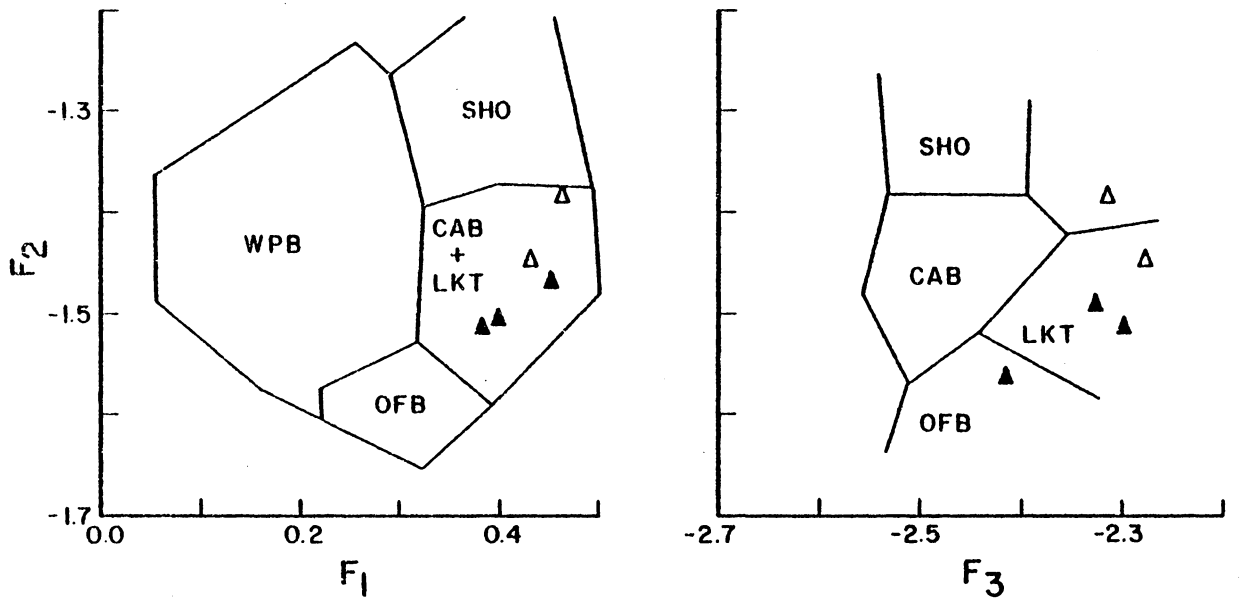
SHO
WPB
CAB
+
LKT
OFB
-1.3
-1.5
-1.7
0.0
0.2
0.4
F2
F1
SHO
CAB
LKT
OFB
-2.7
-2.5
-2.3
F3

Figure 5-H. Peacock (1931) index for the James Run Formation; the Peacock Index is calcic. Data for meta-igneous rocks only. CaO (▲), and $Na_2O + K_2O$ = (△). Data from Southwick (1969), Higgins (1972), Hanan (1980), and Lesser (this study).

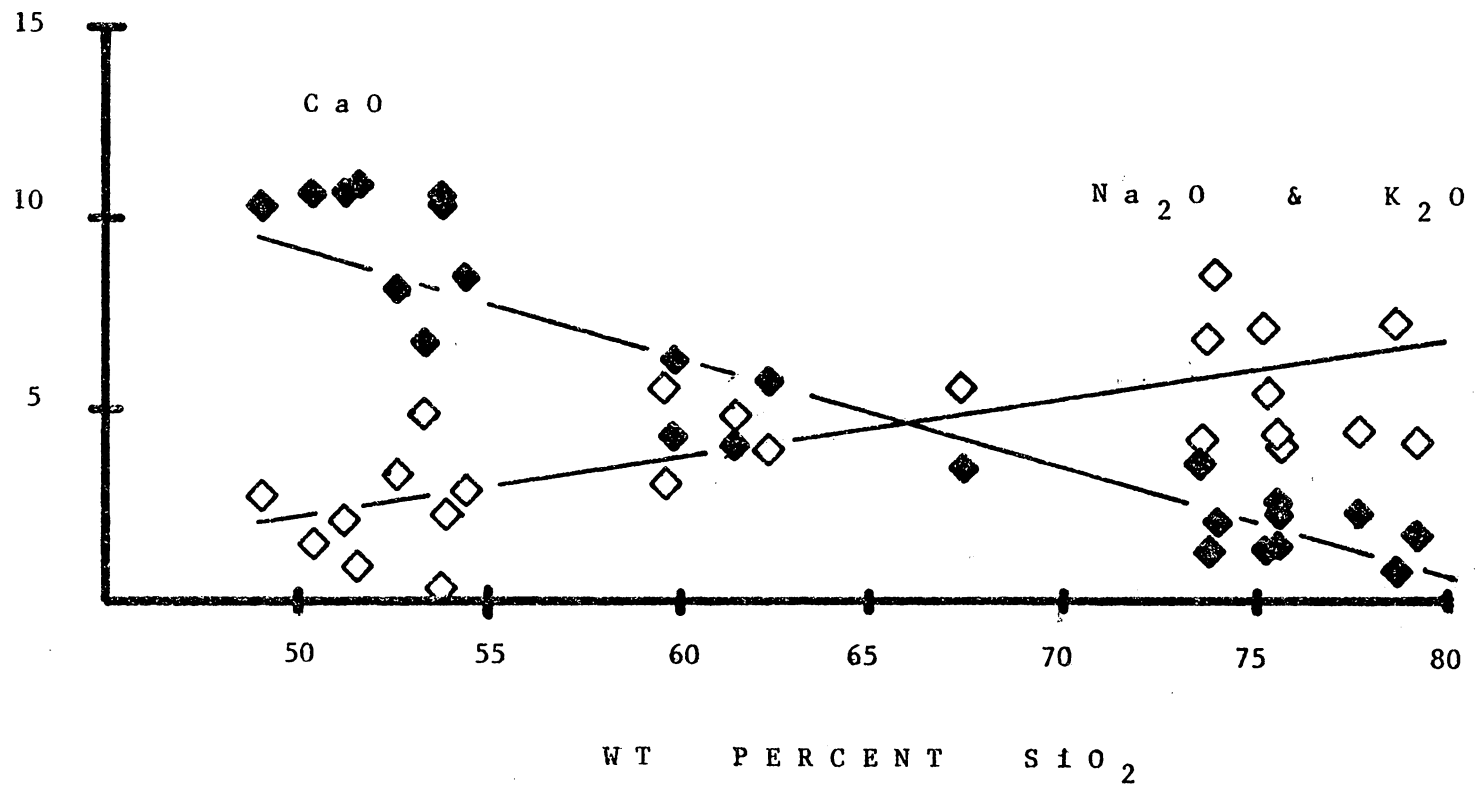
15
10
5
CaO
Na2O & K2O
50
55
60
65
70
75
80
WT PERCENT SiO2

Figure 6-A. Variations of Fe_2O_3, Al_2O_3, and K_2O with respect to silica as a function of dysjunctive cleavage development. Symbols as in Figure 5-B. All data from Lesser (this study).

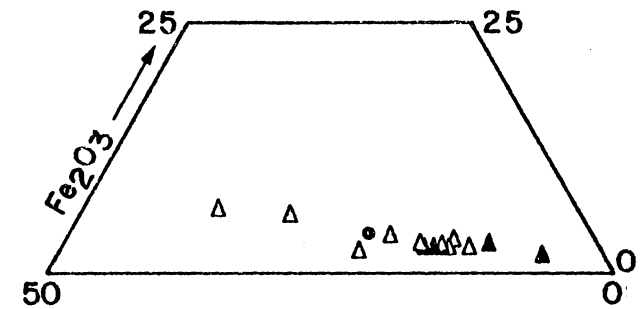

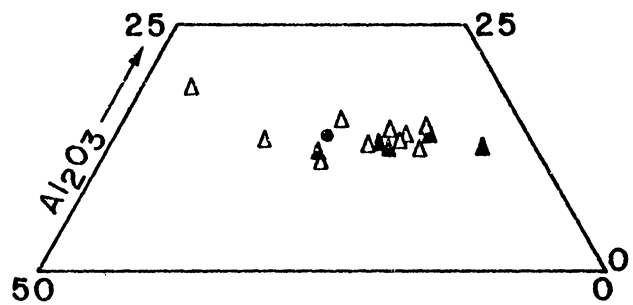

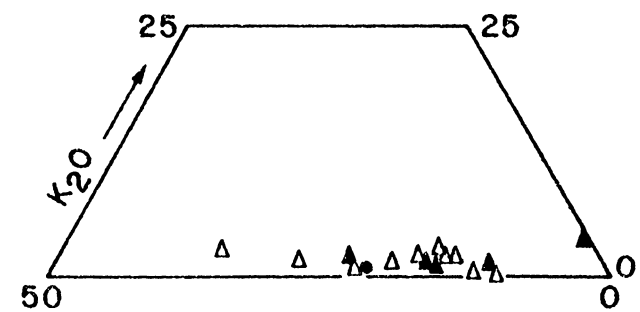

Bio + Ep + Chl + Musc.

SiO_2

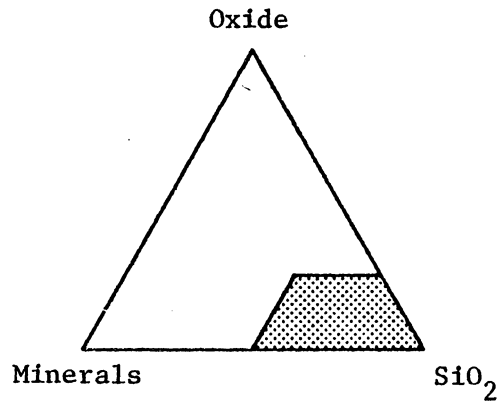

- ● Sheared Port Deposit
- △ Port Deposit Gneiss
- ▲ James Run

variation of selected chemical components with respect to silica. These ternary diagrams show that the James Run metavolcanic and Port Deposit gneissic rocks follow parallel trends, and that the weight proportions of alumina, iron, and potassium are not significantly affected by increasing secondary mineral development.

To test the possible relation of gneissosity with chemical variabilities: Figure 5-D shows the Port Deposit Gneiss has more normative orthoclase with respect to albite and anorthite than the James Run metavolcanics. K_2O versus SiO_2 (Figure 5-E) plots show an increase in K_2O for the Port Deposit Gneiss relative to the James Run, suggesting the higher length/width ratios for the quartz and feldspar domains are associated with higher potassium concentrations. The sheared Port Deposit Gneiss is depleted in K_2O relative to the Port Deposit Gneiss, but its concentrations are not much different than the unsheared James Run felsites.

A Rb versus Sr (Figure 5-G) and a K versus Rb (Figure 6-B) plot shows subtle differences between sheared, gneissic, and meta-volcanic rocks. The Port Deposit Gneiss is enriched in alkalies over the James Run, and the sheared Port Deposit Gneiss defines a much broader field on these plots with a slight depletion of alkalies. The K versus Rb plot shows little deviation from the igneous K versus Rb fractionation trends of Shaw (1968), implying that either K and Rb were mobile and metamorphic redistribution trends are no different than igneous fractionation trends, or that K and Rb were not significantly mobile.

These alkali and alkaline earth systematics can be attributed to a small primary igneous variation, as the James Run metavolcanics and

Figure 6-B. Log-log weight percent K versus ppm Rb for the Port Deposit Complex and James Run Formation. Igneous fractionation trends as outlined by Shaw (1968) vary between K/Rb of 300 to 500. All data from Hanan (1980) and Lesser (this study). Symbols as in Figure 5-B. Symbols for data of less than 10 ppm Rb less than the analytic uncertainty.

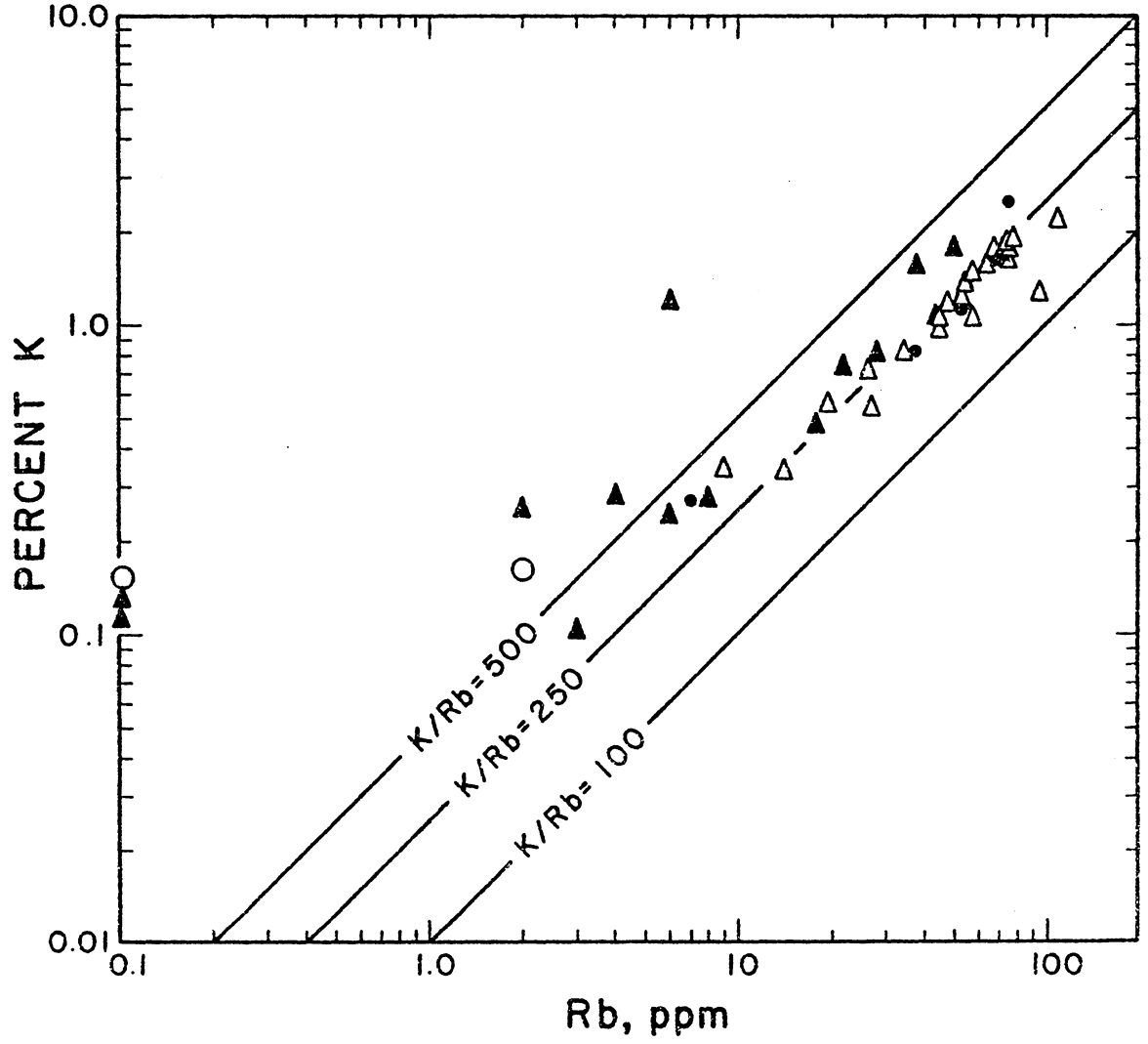
10.0
1.0
0.1
0.01
PERCENT K
0.1
1.0
10
100
Rb, ppm
K/Rb=500
K/Rb=250
K/Rb=100

the Port Deposit pluton need not be consanguineous. The scatter of chemical data for the sheared Port Deposit Gneiss relative to the Port Deposit Gneiss or James Run felsites may be indicative of limited open system chemical behavior, but not an influx or outflux of chemical components during metamorphism and deformation.

Figure 6-C shows K_2O/Na_2O ratios for all rocks analyzed with respect to silica. Such a range is commonly ascribed to open system behavior during initial cooling and subsequent metamorphism (Hopson, 1964; Southwick, 1969; Higgins, 1972; Southwick, 1979). However, if meta-igneous rocks are distinguished from volcaniclastic, epiclastic, and amygdaloidal rocks then two contrasting discriminant fields are defined. The volcaniclastic, epiclastic, and amygdaloidal rocks are distinguished because their measured compositions cannot directly reflect a composition which crystallized as an igneous melt. The volcaniclastic rocks contain mixed components of amphibolite and felsic material initially mixed during an explosive volcanic eruption. Epiclastic rocks are sedimentary in nature and were exposed to weathering processes at the time of deposition. Amygdaloidal rocks are infilled with albite, zoisite, magnetite, and epidote which cause measured whole rock compositions to be enriched in the chemical components which constitute these minerals. In addition, the possibility of hydrothermal alteration of the groundmass is high. These rocks display high Na_2O/K_2O ratios whereas the meta-igneous rocks are not extremely different from the ranges for typical unaltered rocks of the Cenozoic (data from Carmichael et al., 1974; Ewart, 1979). The Sheared Port Deposit rocks show Na_2O/K_2O ratios higher than the Port Deposit Gneiss or James Run meta-volcanics: K_2O is

Figure 6-C. Na_2O/K_2O versus SiO_2 plot. Symbols as in Figure 5-D. Data from Hanan (1980), Higgins (1982), and Lesser (this study).

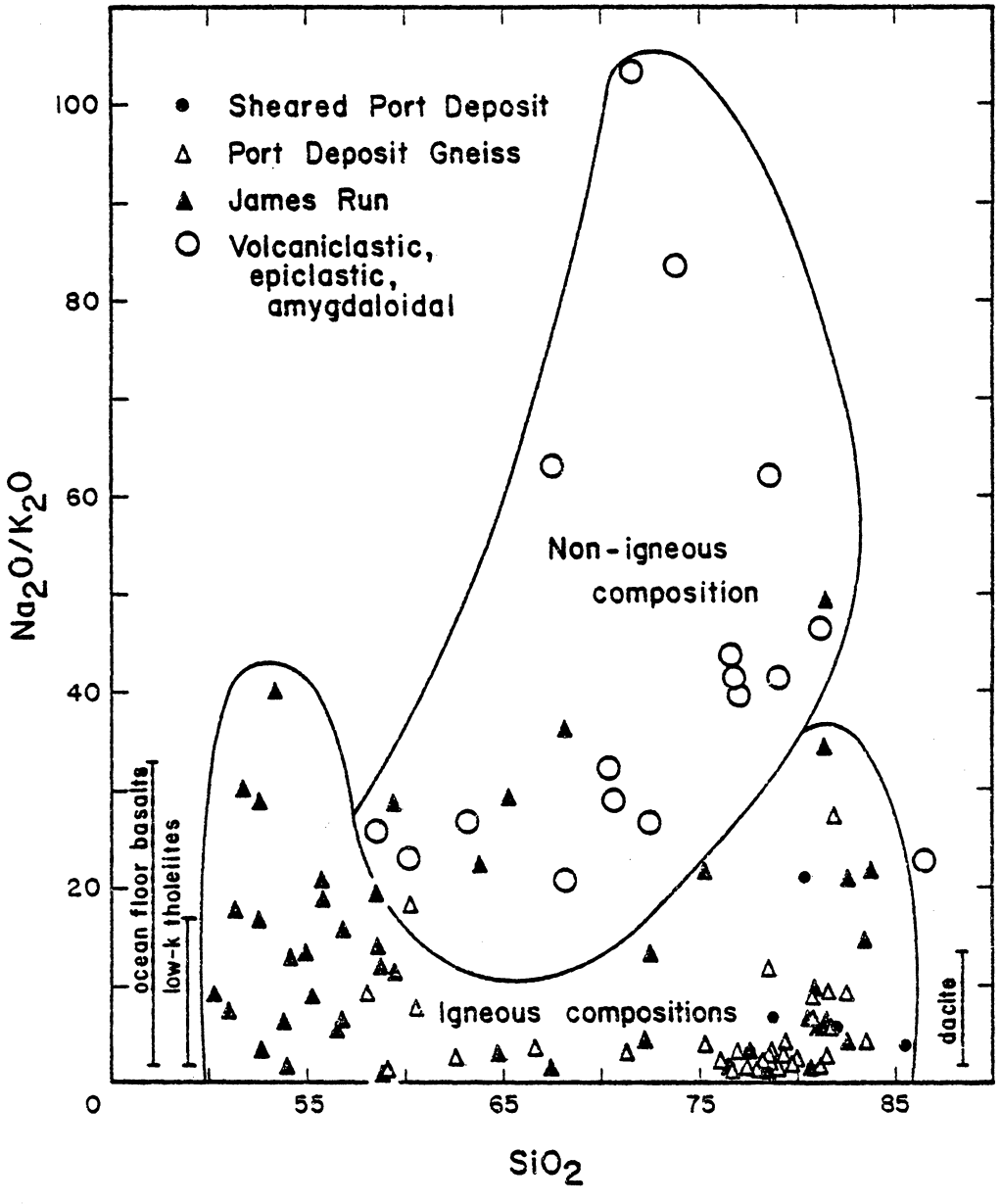
Sheared Port Deposit
Port Deposit Gneiss
James Run
Volcaniclastic, epiclastic, amygdaloidal
Non-igneous composition
Igneous compositions
ocean floor basalts
low-k tholeiites
dacite
Na_2O/K_2O
SiO_2
0
20
40
60
80
100
55
65
75
85

lower in the sheared rocks but Na_2O is similar. It is considered significant that these heavily sheared rocks present values that are not extremely different from unaltered Cenozoic rocks and that these non-igneous versus igneous contrasting fields have remained distinct during shearing and metamorphism. Open system chemical behavior could have obscured these trends.

Since chemical compositions for the meta-igneous rocks of the James Run Formation and Port Deposit Complex have not systematically changed with either shearing or secondary mineral development, and these compositions are not unlike primary Cenozoic igneous rocks, then it may be inferred that these compositions reflect the compositions of their premetamorphic protoliths rather than large scale alteration processes. This conclusion does not imply isochemical behavior during metamorphism, but rather that igneous variation trends and felsic/mafic ratios can be reliably measured. A tectonic model in accord with premetamorphic features can be presented for the James Run and Port Deposit rocks.

ISOTOPE GEOCHEMISTRY

Table 4 presents Rb-Sr data gathered in this study. Values for accepted USGS rock standards and replicate analyses, with an evaluation of analytic uncertainty, are presented in Appendix V. Figure 7 is an isotopic Rb-Sr evolution diagram for all whole rock samples analyzed.

Six evolutionary trends are defined by the six lithologies analyzed. The Conowingo Diamictite produced a whole rock scatterchron age of 473 $\pm$ 38 Ma, $^{87}Sr/^{86}Sr)_o$ = 0.7107 $\pm$ 3, MSRS = 3.9, n = 5. The Wissahickon/Port Deposit fault contact yielded a four-point field from four closely spaced ships with no possible age significance (see Appendix V). The sheared Port Deposit gneiss samples produced a scatterchron with an MSRS of 59. The Port Deposit Gneiss defined two trends: gneissic Port Deposit samples with no relict plutonic textures produced an isochron age of 467 $\pm$ 21 Ma, $^{87}Sr/^{86}Sr)_o$ = 0.7096 $\pm$ 3, MSRS = 0.8, n = 18. Amphibolites and Port Deposit gneisses with relict plutonic fabrics define a scatterchron of 457 $\pm$ 21 Ma, $^{87}Sr/^{86}Sr)_o$ = 0.7068 $\pm$ 2, MSRS = 5.7, n = 8 below this isochron. The James Run metavolcanic rocks yielded a whole rock scatterchron with an age of 430 $\pm$ 21, $^{87}Sr/^{86}Sr)_o$ = 0.7082 $\pm$ 2, MSRS = 4.0, n = 9. Amphibolites and gneisses with relict plutonic fabrics from the Port Deposit fall within the range of scatter for the unsheared James Run rocks.

Table 4 includes Rb-Sr data for biotite separates. Hart et al. (1964) studied the contact aureole of the Eldora Stock in Colorado and concluded that Rb-Sr biotite model ages may represent the time of cooling below 350°C. A biotite separate from the Conowingo Diamictite

Table IV. Rb-Sr and $^{87}Sr/^{86}Sr$ systematics for all samples analyzed in this study.

Sample	Rb	Sr	$^{87}Rb/^{86}Sr$	$^{87}Sr/^{86}Sr$
		Conowingo Diamictite		
RL-80-3	23	205	0.325	0.71357(08)
RL-80-5	74	131	1.637	0.72215(10)
RL-80-6	96	120	2.319	0.72644(08)
RL-80-11	50	185	0.783	0.71523(08)
RL-80-20	45	126	1.034	0.71698(10)
		Port Deposit		
RL-80-32	59	74	2.310	0.72259(07)
RL-80-33	46	111	1.200	0.71814(08)
RL-80-37	35	49	2.070	0.72418(14)
RL-80-39	65	100	1.883	0.72179(30)
RL-80-40	20	138	0.420	0.71225(10)
RL-80-41	76	82	2.687	0.72728(08)
RL-80-42A	n.d.	2		
RL-80-42B	3	8		
RL-80-42C	10	28		
RL-80-46	27	82	0.953	0.71408(08)
RL-80-48	14	154	0.263	0.70929(06)
RL-80-49	2	240	0.024	0.70759(12)
RL-80-53	54	111	1.409	0.71865(08)
RL-81-12	45	113	1.153	0.71327(08)
RL-81-13	70	95	2.135	0.72383(06)
RL-81-17	72	103	2.025	0.72264(11)
RL-81-18	73	101	2.094	0.72300(09)
RL-81-21	48	122	1.139	0.71706(09)
RL-81-24	1	176	0.016	0.70627(08)
RL-81-26	9	112	0.232	0.70732(09)
RL-81-27	7	131	0.155	0.70945(08)
RL-81-28	70	97	2.091	0.72286(13)
RL-81-29	97	104	2.705	0.72735(12)
RL-81-40	n.d.	146		
RL-81-43	72	103		
RL-81-44	54	79	1.980	0.71702(08)
RL-81-45	27	133	0.588	0.71403(12)
RL-81-45S	77	42	5.321	0.73924(12)
RL-81-46	39	63	1.771	0.72232(12)
RL-81-47	30	107		
MJ 8142	75	69		
MJ 8143	76	101	2.181	0.72411(06)
MJ 8144	71	103	1.997	0.72318(08)
MJ 8146	59	124		
MJ 8147	77	106	2.105	0.72383(06)

Table IV (continued).

Sample	Rb	Sr	$^{87}Rb/^{86}Sr$	$^{87}Sr/^{86}Sr$
MJ 8148	111	66	4.881	0.73860(08)
MJ 8148R	111	66		
MJ 8151	73	102	2.074	0.72365(08)
MJ 8152	56	109	1.488	0.71978(08)
MJ 8154A	18	136	0.383	0.71198(08)
MJ 8154B	54	107		
MJ 8155	78	103		
MJ 8156	2	119	0.049	0.70718(08)
MJ 8157	18	94		
MJ 8158	4	109		
		James Run		
RL-80-57	6	53	0.328	0.71076(10)
RL-80-62	44	70	1.821	0.71860(08)
RL-80-63	51	63	2.346	0.72324(08)
RL-80-65	8	48	0.482	0.71192(38)
RL-80-66	2	176	0.033	0.70894(10)
RL-80-68	1	138	0.021	0.70759(10)
RL-80-68'	6	187	0.093	0.70800(10)
RL-81-4	n.d.	144		
RL-81-15	n.d.	144		
RL-81-16	n.d.	187		
MJ 8165	38	63		
MJ 8165R	38	63		
MJ 8168	28	44		
MJ 8169	39	62	1.822	0.71955(06)
MJ 8170	46	82	1.625	0.71731(06)
MJ 8171	3	80		
MJ 8172	7	66		
MJ 8173	7	78		
MJ 8174	53	73		
MJ 8175	38	82		
MJ 8175R	38	82		
MJ 8176	22	88		
		Port Deposit/Wissahickon Contact		
RL-80-29C/3-1	60	190	0.909	0.71754(18)
RL-80-29C/3-2	24	222	0.312	0.71346(22)
RL-80-29C/3-3	9	256	0.106	0.71302(16)
RL-80-29C/3-4	22	216	0.296	0.71420(08)

Table IV (continued).

Sample	Rb	Sr	$^{87}Rb/^{86}Sr$	$^{87}Sr/^{86}Sr$
		Biotite Separates		
RL-80-11	325	43	22.250	0.84217(28)
	UNIT:	Conowingo Diamictite		
	AGE:	399 Ma		
RL-80-33	491	41	34.883	0.90688(18)
	UNIT:	Port Deposit Gneiss		
	AGE:	380 Ma		
RL-80-62	393	161	7.078	0.74149(18)
	UNIT:	James Run Formation		
	AGE:	287 Ma		
RL-81-43	699	72	28.586	0.83873(26)
	UNIT:	Port Deposit Gneiss		
	AGE:	316 Ma		
MJ 8116	402	23	52.785	0.960 (20)
	UNIT:	Sykesville Formation		
	AGE:	333 Ma		
MJ 8117	119	78	4.428	0.73496(06)
	UNIT:	Sykesville Formation		
	AGE:	396 Ma		

n.d. = not detectable.

Figure 7. Rb-Sr evolution diagram. Conowingo Diamictite (⟹), Port Deposit Complex/Wissahickon Contact (⟹), Sheared Port Deposit Gneiss (⟹), Port Deposit Gneiss (⟹), Port Deposit Gneiss with relict igneous textures, and amphibolites of the Port Deposit (⟹), James Run Formation (⟹). All data from Lesser (this study). Symbols exceed analytical uncertainty.

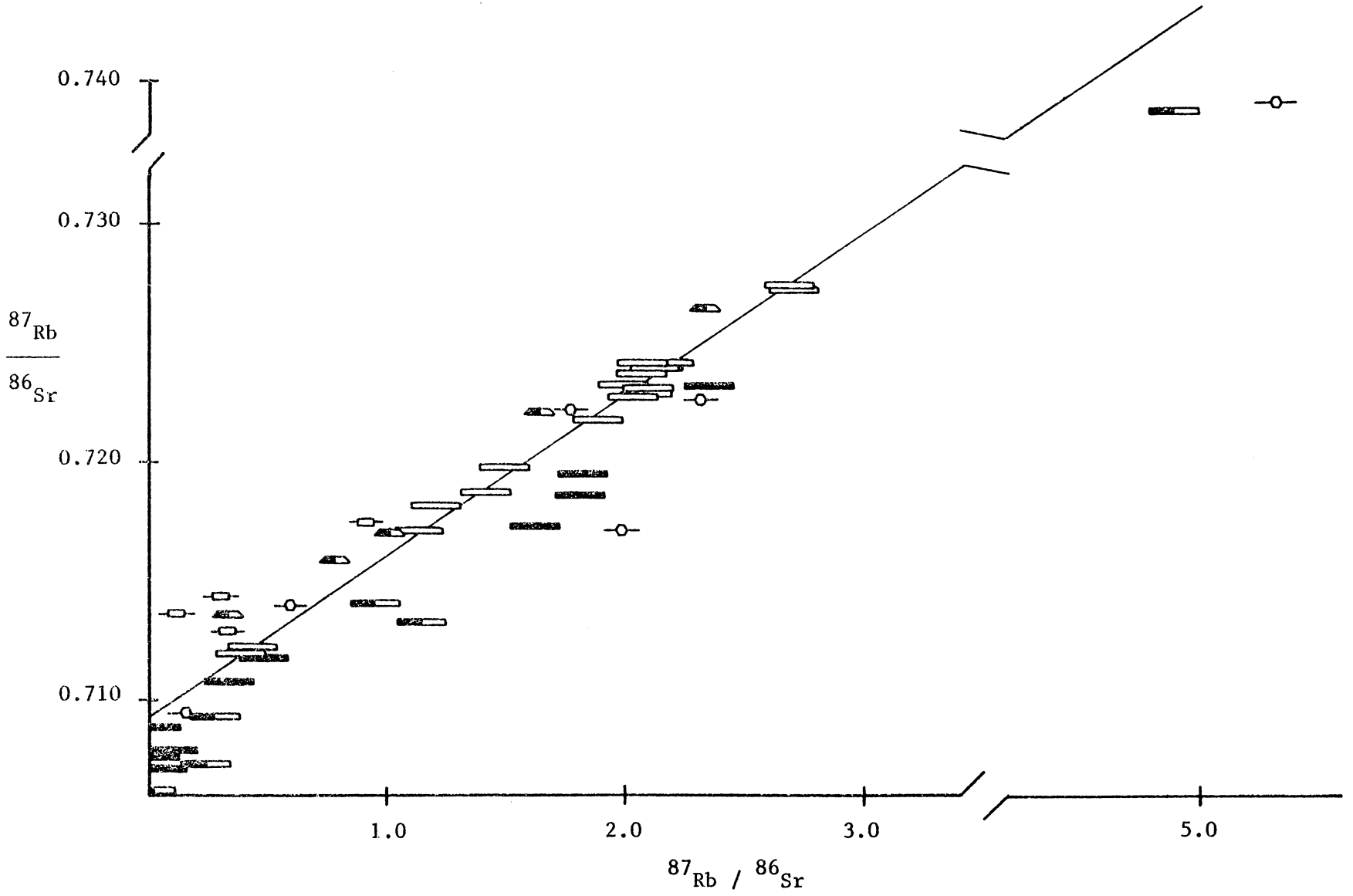
0.740
0.730
0.720
0.710
$\frac{^{87}Rb}{^{86}Sr}$
1.0
2.0
3.0
5.0
^{87}Rb / ^{86}Sr

yielded an age of 400 Ma. The Port Deposit provided two biotite model ages of 380 and 315 Ma, and a James Run metadacite yielded a model biotite age of 290 Ma. Biotite separates from the Sykesville diamictite 30 km northwest of Conowingo Dam gave model ages of 400 Ma for the felsic matrix and 330 Ma for an amphibolite inclusion with secondary biotites. Neither petrographic distinctions nor sample locations can be associated with these ages.

Sinha et al. (1971) found U-Pb zircon upper intercept ages between 1300-1500 Ma for the Conowingo Diamictite. Zircon data from Tilton et al. (1970) recalculated with the U decay constants of Steiger and Jager (1977) gave a U-Pb upper intercept zircon of 516 for the James Run. Sinha (unpublished data) found a zircon upper intercept age of 525 Ma for the Port Deposit Gneiss.

Discussion

Evaluation of data from several isotopic systems in polymetamorphosed and polydeformed terranes has been challenging (Cliff, 1971; Higgins et al., 1977; Sinha and Glover, 1978; Montgomery and Hurley, 1978; Corfu, 1980; Field and Raheim, 1980; Mose and Nagel, 1982). Current consensus holds that the U-Pb zircon upper intercept ages for the Paleozoic Appalachians are misleading, due to a high probability of older, xenocrystic zircons (Higgins et al., 1977; Zartman, 1978). A recent study by Mose and Nagel (1982) presented Rb-Sr whole rock ages for central Virginia as primary phenomenon, where the U-Pb zircon upper intercepts were not considered as concrete indicators of the time of igneous consolidation.

In the evaluation of the available isotopic data for the early Paleozoic Appalachians, these possibilities must be considered:

(1) Zircon upper intercept ages are offset due to inherited lead components, and Rb-Sr whole rock ages may reflect the time of igneous consolidation.

(2) Zircon upper intercept ages represent the time of igneous consolidation, and the Rb-Sr whole rock ages, if significantly lower, represent a time of metamorphism.

It is proposed that these criteria be used in evaluations of isotopic ages in this part of the Appalachians:

(1) Suspected igneous crystallization ages should not be changed by igneous fractionation processes or subsequent metamorphic/structural phenomena.

(2) Suspected metamorphic recrystallization ages should be closely associated with field and petrographic phenomena produced during a metamorphism.

The accessibility of exposures along the Susquehanna River corridor allowed a detailed sampling study and the application of these criteria: These criteria hinge on the lithologic and petrographic divisions outlined above. Field, geochemical, and U-Pb zircon evidence (discussed below) establish the Port Deposit and James Run as temporal, tectonic equivalents (Higgins, 1970, 1982; Lesser, this study). The Rb-Sr data in the James Run and Port Deposit is most easily related to metamorphic and deformational characteristics which clearly postdate igneous consolidation: Relatively unsheared Port Deposit gneisses and meta-volcanic James Run samples produce a scatterchron, whereas the

gneissic phase of the Port Deposit Complex yields an isochron age of 467 $\pm$ 21 Ma. This age is taken as representative of the time of structural emplacement for the James Run/Port Deposit block into this area of the Wissahickon terrane and Baltimore Mafic Complex. The 430 Ma scatterchron age for the James Run and the 473 Ma scatterchron age for the diamictite are lent no singular temporal significance, as these rocks do not satisfy the requirements of a uniform $^{87}Sr/^{86}Sr$ at t_o. However, the similarity of these ages with the Port Deposit Gneiss isochron age substantiates the idea of a regional middle to late Ordovician structural event for the eastern Maryland Piedmont (cf. Rodgers, 1971; Rankin, 1975; Morgan, 1977; Read, 1980; Drake, 1980; Mussman, 1982). The large scatter of data for the sheared Port Deposit gneiss (MSRS = 59) precludes any temporal interpretation.

Previous discussion held that the Port Deposit and James Run did not experience open system chemical behavior for the major oxides. Roddick and Compsten (1977) modeled the phenomenon of apparent trace element mobility without alteration of major element concentrations. They postulated that a suspected open system could be subdivided into a number of smaller domains which possess a $^{87}Sr/^{86}Sr$ average ratio identical to the $^{87}Sr/^{86}Sr$ of the bulk system. Sr homogenization within these smaller domains would produce an effective resetting of the Sr isotopes throughout the larger system.

A calculation of the amount of ^{87}Sr produced by decay of ^{87}Rb in the James Run/Port Deposit association between 525 Ma (the maximum age of igneous crystallization) and 467 Ma (the time of deformation) shows the $^{87}Sr/^{86}Sr$ at t = 467 Ma for the James Run/Port Deposit block could

not have been produced solely by decay of ^{87}Rb since the time of igneous consolidation, where the lowest $^{87}Sr/^{86}Sr)_o$ for the Port Deposit of 0.7063 is assumed to be the $^{87}Sr/^{86}Sr)_{525\ Ma}$ unless Rb left the system between 525 and 467 Ma. More likely, ^{87}Sr was introduced from outside the James Run/Port Deposit system during the 467 Ma deformation event.

Faure (1977) described the mixing relations that result from simple mixing of two isotopically distinct end members in an open chemical system. The $^{87}Sr/^{86}Sr$ ratio calculated for a suspected time of mixing should yield a linear relation between the calculated $^{87}Sr/^{86}Sr)_o$ and the reciprocal of the Sr concentrations. To test this possibility, the $^{87}Sr/^{86}Sr$ ratio at 467, 420, and 300 Ma (the age of deformation and the thermal events of Sinha et al., 1980) was calculated for all rocks analyzed. A mixing relation was not found. This is consistent with the conclusion that the K_2O versus SiO_2, Rb versus Sr, K versus Rb, and Na_2O/K_2O versus SiO_2 diagrams are not suggestive of open system metasomatic processes, but inconsistent with the calculated additions of ^{87}Sr subsequent to igneous consolidation.

Hanan (1980) modelled the phenomenon of Sr isotopic alteration without the production of Sr mixing trends by suggesting that Sr mixing may occur without concomitant Sr addition. He also showed that trace elements are more sensitive to alteration processes than major elements. Indeed, the sheared Port Deposit rocks do not yield a mixing relation, and their bulk chemistries are not significantly offset from the less sheared Port Deposit and James Run rocks.

This model may explain the apparent isotopic homogenization of the felsic Port Deposit Gneiss. Samples with relict plutonic textures were

not reequilibrated during shearing and so fall within the range of scatter for the less sheared James Run rocks. Amphibolites from the Port Deposit have relatively high Sr concentrations which did not allow homogenization with the surrounding felsic gneiss; these rocks also fall within the range of scatter for the less sheared James Run felsic and amphibolitic rocks.

Rb-Sr model biotite ages are most easily interpreted as metamorphic cooling phenomena during the middle and late Paleozoic. They are correlative with the 420 Ma event (Sinha et al., 1980; Pavlides et al., 1982) and the 300 Ma event (Sinha and Zieta, 1982) which produced anatexis in the Maryland and Virginia Piedmonts.

REGIONAL CORRELATIONS

Central Appalachians

Figure 8 is a regional geologic correlations map for the central Appalachian Piedmont. After the fashion of Higgins (1972), the Wilmington Complex, Baltimore Paragneiss, Relay Quartz Diorite, Kensington Quartz Diorite, Chopawamsic Formation, and the Occoquan, Dale City, and Columbia plutons will be considered here. Although considerable work has been done, fundamental disagreement on the tectonic significance and timing of events still exists.

Sinha et al. (1980) consider the meta-volcanic James Run to be the product of ensialic volcanism, whereas Pavlides (1981) considers relations in the Chopawamsic Formation of Virginia as the product of ensimatic volcanism. Higgins (1972) and Seiders et al. (1975) used U-Pb upper intercept ages in their correlation, although Higgins et al. (1977) subsequently questioned the validity of such data. Seiders et al. (1975) and Higgins (1972) thought the plutonic rocks were intrusive into the Wissahickon terrane. Hanan (1980), Higgins (1982), and Lesser (this study) consider the James Run and Port Deposit to be allochthonous above the Wissahickon, and Lesser (this study) interprets the Rb-Sr whole rock isochron age of 467 Ma as the time of emplacement. Mose and Nagel (1982) consider Rb-Sr whole rock ages from correlative rocks to the south as primary, igneous ages. Muth et al. (1979) suggested major tectonism evidenced in the Potomac River Gorge had ceased by 469 Ma (Rb-Sr model mica ages). Pavlides et al. (1982) indicated nappe formation in the Fredericksburg, VA, area was post-410 Ma. Table V presents comparative

Table V. Comparative data from the central Appalachian volcanic/plutonic province of Higgins (1972). Where necessary Rb-Sr and U-Pb ages have been recalculated with the new decay constants of Steiger and Jager (1977).

	James Run Formation	Port Deposit Pluton	Baltimore Paragneiss	Raley Quartz Diorite	Kensington Quartz Diorite	Chopawamsic Formation	Occoquan Pluton	Dale City Pluton	Columbia Pluton
Outcrop Area	350 km^2	140 km^2	25 km^2	5 km^2	9 km^2	900 km^2	260 km^2	1x10^5 m^2	
Rock Types	basalt	qtz. diorite	basalt	basalt	tonalite (trondhjem.)	basalt	tonalite (trondhjem.)	tonalite	tonalite
	andesite	tonalite	dacite	dacite		andesite	granodiorite	granodiorite	granodiorite
(Meta-igneous)	dacite (trondhjem.)	granodiorite				dacite (trondhjem.)	granite		granite
Textures: primary	volcanic plutonic	plutonic	volcanic	volcanic plutonic	plutonic	volcanic	plutonic	plutonic	
secondary	gneissic lepidoblastic	gneissic blasto-mylonitic	gneissic	gneissic	gneissic	granoblastic	gneissic	gneissic	gneissic lepidoblastic
SiO_2, range	46-80%	53-80%	66-78%	72-78%		47-80%	53-76%		
K_2O, range	0.1-2.2%	0.2-3.0%	0.2-2.0%	0.8-1.1%		0.2-6.7%	1.3-5.4%		
Rb-Sr whole rock	430 ± 21	467 ± 21					494 ± 28		454 ±18
$^{87}Sr/^{86}Sr)_o$	0.7082 ± 2	0.7096 ± 3					0.7118 ±8	0.7045 (model T = 500 Ma)	0.7059 ± 6
MSWD	4.0	0.8					3.9		3.0
errors x	2.0%	2.0%					2.0%		2.0%
y	0.05%	0.05%					0.04%		0.04%
Rb-Sr minerals	333	401 320			469 ± 20 (Bear Isl.) 300				300
U-Pb zircon upper int.	516	525	--	--	531	533	558	550	557
			Hopson, 1964	Hopson, 1964	Hopson, 1964	Southwick et al., 1971			
	Hershey, 1937	Hershey, 1937	Tilton et al., 1970	Steiger and Hopson, 1964	Wetherill et al., 1966				
	Southwick, 1969	Southwick, 1969 Steiger and Hopson, 1964							
	Tilton et al., 1970								
	Higgins, 1972	Higgins, 1972	Higgins, 1972	Higgins, 1972	Higgins, 1972 Muth et al., 1979 Sinha et al., 1980	Higgins, 1972 Seiders et al., 1975 Higgins et al., 1977	Higgins, 1972 Seiders et al., 1975	Higgins, 1972 Seiders et al., 1975	Higgins, 1972 Bourland, 1976
		Southwick, 1979 Sinha et al., 1980							
	Hanan, 1980		Hanan, 1980	Hanan, 1980		Pavlides, 1981			
	Higgins, 1982	Higgins, 1982					Mose and Nagel, 1982	Mose and Nagel, 1982	Mose and Nagel, 1982

Figure 8-A. Regional correlations map for the Central Appalachian Piedmont.

L I T H O L O G Y K E Y

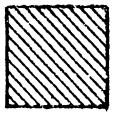

Quantico and Arvonia Slates

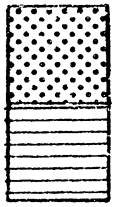

Wissahickon Flysch

Wissahickon Diamictite

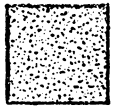

Wissahickon Pelagic Metasediments

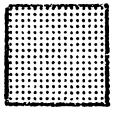

Pre-Cambrian Basement

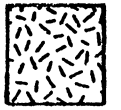

Ellisville and Ellicott Plutons

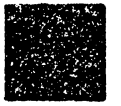

Baltimore Mafic Complex

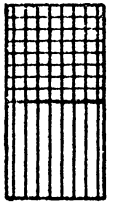

Columbia, Occoquan, and Port Deposit Plutons

James Run and correlative metavolcanics

GENERALIZED GEOLOGIC MAP OF THE CENTRAL APPALACHIAN PIEDMONT

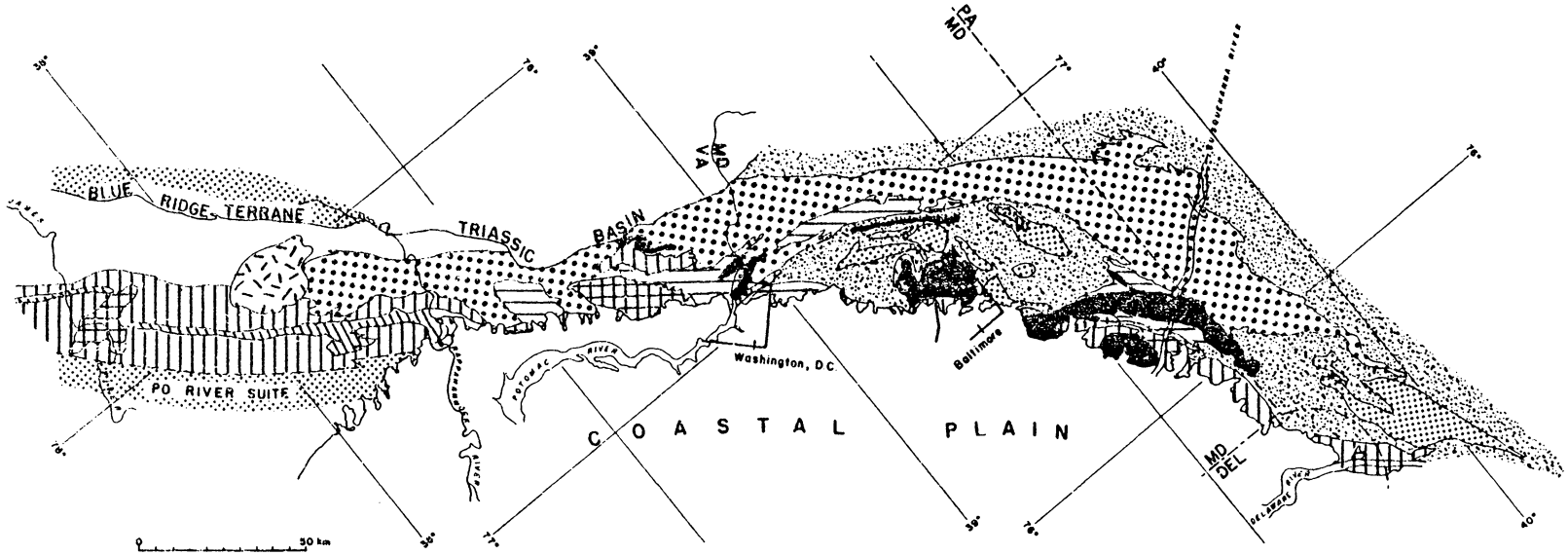

Figure 8-B. Credit key for the regional correlations map (cf. Figure 8-A).

KEY

1) Ward, 1959
2) Spoljaric and Jordan, 1966
3) Higgins, 1982
4) Southwick and Owens, 1968
5) Crowley et al., 1976
6) Hopson, 1964
7) Fisher, 1970
8) Drake and Lyttle, 1981
9) Drake and Morgan, 1981
10) Pavlides et al., 1980
11) Pavlides et al., 1982
12) Pavlides, 1980
13) Bobyarchick et al., 1981
14) Bourland, 1976

In addition:

Pavlides et al., 1974

Zietz et al., 1977

Fisher et al., 1979

Hanan, 1980

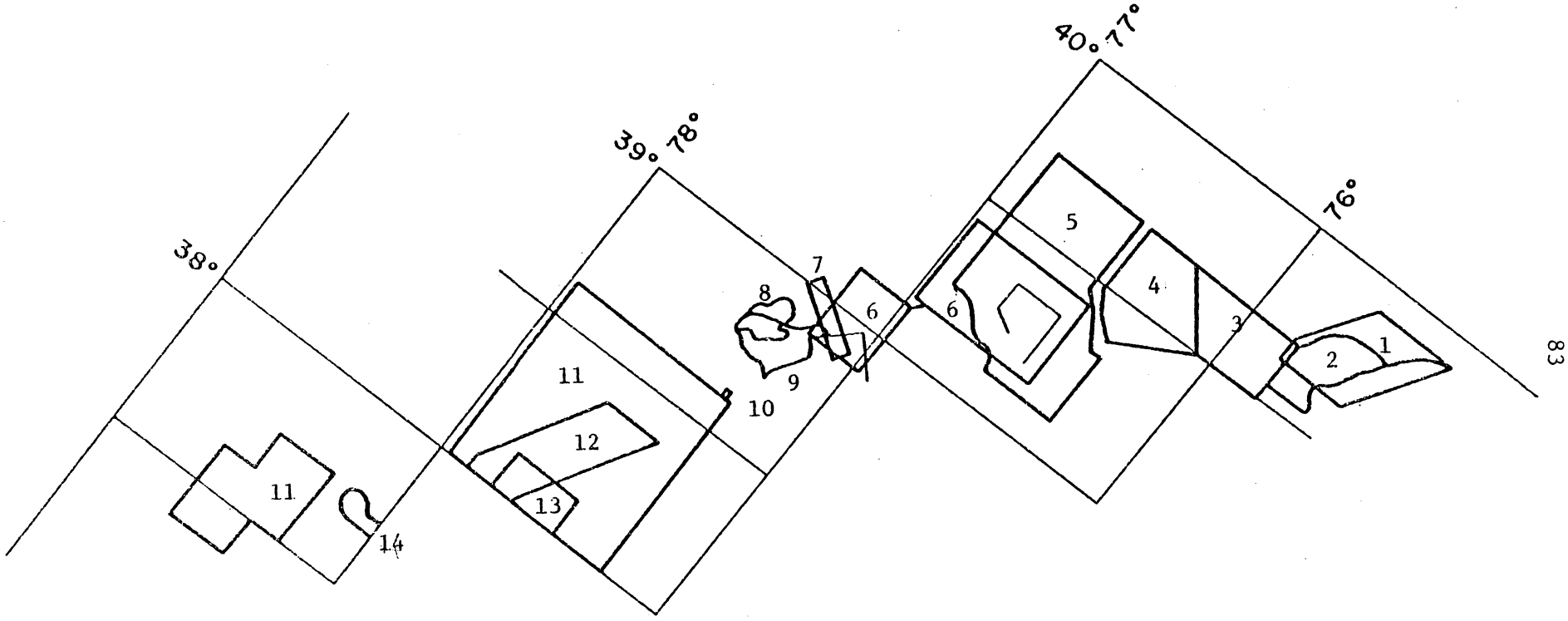
40° 77°
39° 78°
38°
76°
1
2
3
4
5
6
6
7
8
9
10
11
12
13
11
14

compositional and geochronologic data from these aenigmatic rocks. These points merit consideration:

1) Foland and Muessig (1978) discussed the anorthositic-charnockitic character of the 502 Ma (Rb-Sr whole rock) Arden pluton and its tectonic significance. No such compositions exist from other suspected correlative areas to the south. Grauert and Wagner (1974, 1975) dated the granulite grade metamorphism in the Wilmington at 441 Ma (±10%). Granulite metamorphism can disturb Rb-Sr isotopic systems as well as zircon upper intercept ages (Faure, 1977). A Wilmington-James Run correlation as suggested by Ward (1959) will not be considered here.

The geochemistries of the James Run and Port Deposit place constraints on the tectonic environments which produced them. Figure 9 and Table V show the mineralogic and chemical variabilities of their correlative rocks as suggested by Higgins (1972). The rocks are bimodal tholeiite meta-dacite/meta-tonalite suites with trondhjemitic affinities. Work on the James Run/Port Deposit association suggests these compositions are primary.

2) The validity of primary versus metamorphic radiometric ages for the igneous rocks and the nature of their contact with the Wissahickon terrane places a constraint on the age of deposition for that part of the Wissahickon.

Figure 10 is a time-line for plutonic and metamorphic events which affected the meta-igneous rocks in Maryland and northern Virginia. Plutonic events occurred at 540, 420 and 320 Ma (cf. Sinha et al., 1980). The Rb-Sr whole rock dates for the 420 and 320 Ma plutons agree with the zircon dates. There are no U-Pb zircon upper intercept dates

Figure 9. Modal quartz-plagioclase-potassium feldspar for the central Appalachian volcanic/plutonic province of Higgins (1972). Volcanic rocks (▲) and plutonic rocks (△). Data from Hopson (1964), Brown (1969), Seiders et al. (1975), and Bourland (1976).

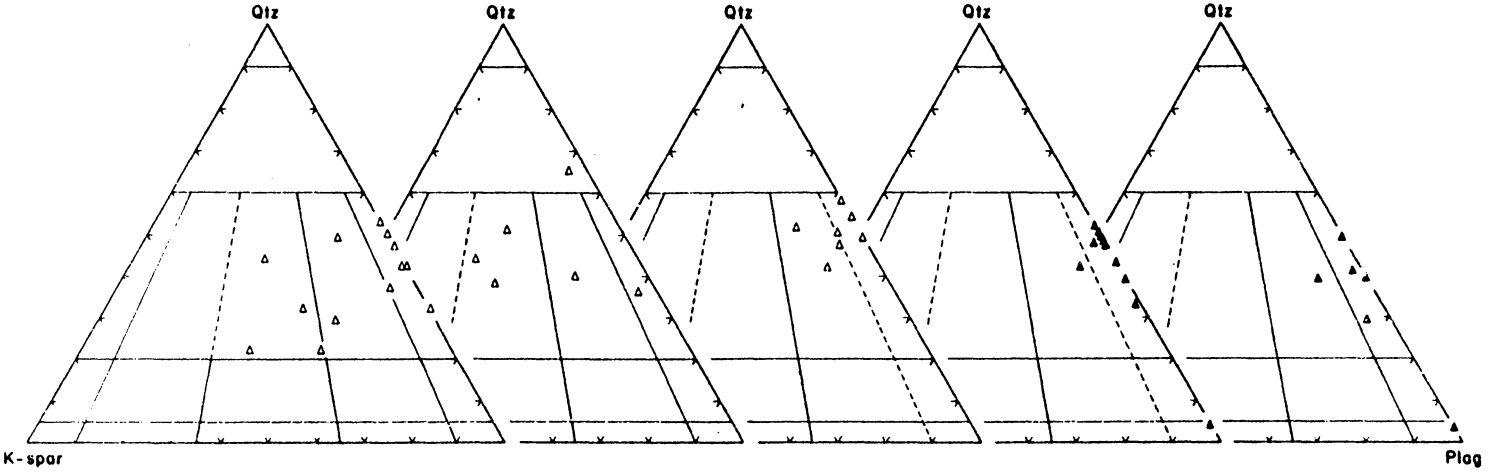

Columbia | Occoquan/ Dale City | Kensington | Relay | Baltimore Paragneiss

Figure 10. Time-line of thermal events in the central Appalachian Piedmont. Each block corresponds to a radiometric date and its corresponding error bar. The associated numerals are keyed to the corresponding rock unit and literature reference.

KEY

	Unit	Reference
1)	Columbia Pluton	Sinha (unpublished data) Mose and Nagel, 1982
2)	Dale City Pluton	Seiders et al., 1975 Mose and Nagel, 1982
3)	Occoquan Pluton	Seiders et al., 1975 Higgins et al., 1977 Mose and Nagel, 1982
4)	Chopawamsic Formation	Higgins et al., 1977
5)	Potomac Gorge Pegmatite	Muth et al., 1979
6)	Kensington Quartz Diorite	Wetherill et al., 1966 Sinha et al., 1980
9)	James Run Formation	Tilton et al., 1970 Lesser (this study)
10)	Port Deposit Pluton	Sinha (unpublished data) Lesser (this study)
11)	Falls Run Intrusive Suite	Pavlides et al., 1982
12)	Guilford Pluton	Wetherill et al., 1966 Sinha et al., 1980
13)	Ellicott Pluton	Wetherill et al., 1966 Sinha et al., 1980
14)	Woodstock Pluton	Wetherill et al., 1966
15)	Petersburg Pluton	Wright et al., 1975 Sinha (unpublished data)
16)	Falmouth Intrusive Suite	Pavlides et al., 1982
17)	Gunpowder Pluton	Grauert, 1973 Sinha et al., 1980

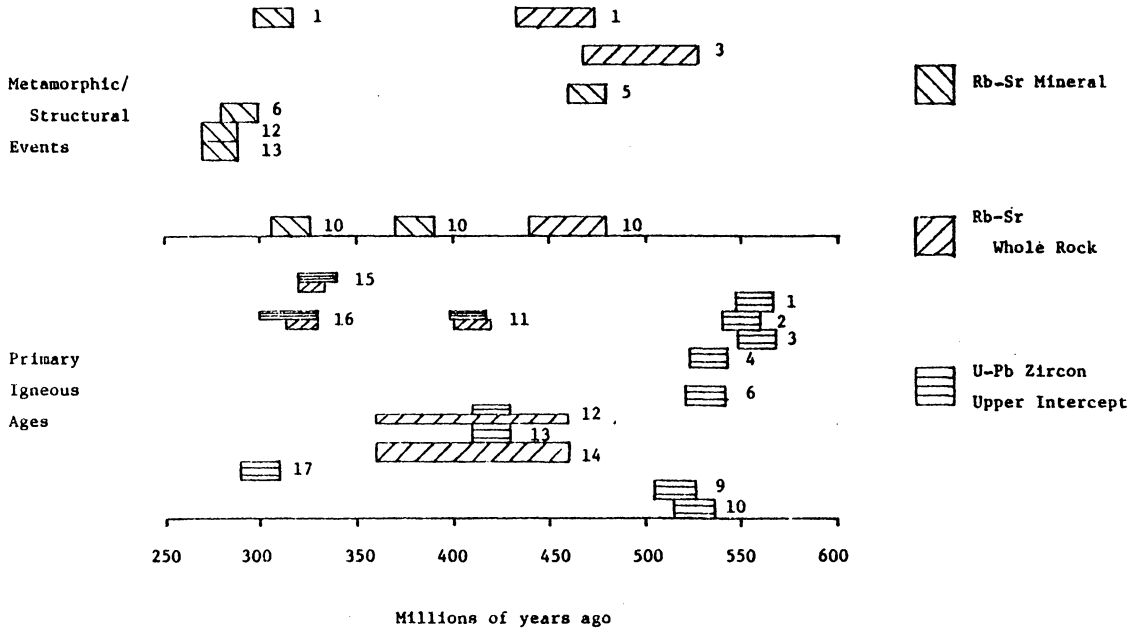
Metamorphic/
Structural
Events
Primary
Igneous
Ages
Rb-Sr Mineral
Rb-Sr
Whole Rock
U-Pb Zircon
Upper Intercept
250
300
350
400
450
500
550
600
Millions of years ago

associated with middle Ordovician Rb-Sr whole rock ages, but rather these rocks yield U-Pb zircon upper intercept ages of approximately 540 Ma. Petrographic considerations from the Port Deposit suggests that the Rb-Sr whole rock age from these rocks represents a deformation episode.

Peterman (1979) derived a mantle Sr-evolution trend from tonalitic and trondhjemitic rocks. The $^{87}Sr/^{86}Sr$ of the mantle between 500 and 450 Ma was less than 0.7035. The $^{87}Sr/^{86}Sr)_o$ for the Appalachian tonalitic rocks range from 0.7045 (Dale City) to 0.7118 (Occoquan) and are clearly higher than Peterman's primitive values. Although crustal contamination may be cited to explain these Sr systematics, tonalitic rocks are not generally found in areas of thick, ancient sialic crust (Moore, 1958). Metamorphic redistribution of Sr seems indicated.

U-Pb zircon upper intercept ages for the central Appalachian volcanic/plutonic association of Higgins (1972) are similar from unit to unit. These rocks range from quartz diorite to tonalite-trondjhemite and granodiorite compositions. Fractionation or fractional crystallization of restitic phases, or introduction of xenocrystic zircons by crustal contamination would upset the proportions of new and old zircon components in the intermediate and final differentiation products, creating scatter in these ages (Higgins et al., 1977). Subsequent thermal events would upset U-Pb zircon upper intercept ages and create poorly defined events. This area has experienced two periods of anatexis and yet the U-Pb zircon upper intercept ages do not vary. Higgins et al. (1977) used this similarity to substantiate a regional correlation without implying the validity of these upper intercepts. In addition, plutons from the 420 and 320 Ma plutons yield identical

Rb-Sr and U-Pb zircon ages. Although more work is needed, the possibility remains that the zircon upper intercept dates represent igneous consolidation events.

3) Crowley (1976) and Fisher et al. (1979) proposed a relation between thrusting of the Baltimore Mafic Complex and James Run Formation composite allochthon and the sedimentation patterns in the Glenarm Series. The Glenarm records a transition from shallow water deposition in a stable tectonic environment to deep water pelagic sedimentation (Figure 8-A, Unit B). Emplacement of the composite allochthon triggered deposition of flysch and diamictite (Figure 8-A, Unit C). In contrast, Drake and Lyttle (1981) mapped several distinct allochthonous units within the northern Virginia flysch terrane and inferred that telescoping of the Wissahickon terrane considerably complicates the picture.

Figure 11 is a modal quartz-plagioclase-potassium feldspar plot for the diamictites associated with thrusting of the Baltimore Mafic Complex in comparision with the Conwingo Diamictite. The Conowingo rocks are higher in potassium feldspar than the other Maryland diamictites; Dickenson (1970) used plagioclase/potassium feldspar ratios as indicators of the provenance for arkosic sedimentary rocks. Sinha et al. (1971) found a U-Pb upper intercept of 1300-1500 Ma for the Conowingo unit, implying a pre-Grenville provenance. Higgins (1972) interpreted the Norbeck Quartz Diorite (not shown in Figure 8-A) as a member of the Sykesville diamictite associated with thrusting of the Baltimore Mafic Complex. The U-Pb upper intercept of approximately 550 Ma precludes a provenance of pre-Grenville basements. Therefore, compositional and zircon dissimilarities between the Conowingo Diamictite and the other

Figure 11. Modal quartz-plagioclase-potassium feldspar diagram. Conowingo Diamictite (▲) and the Sykesville and Laurel Formations (△). Data from Hopson (1964) and Lesser (this study).

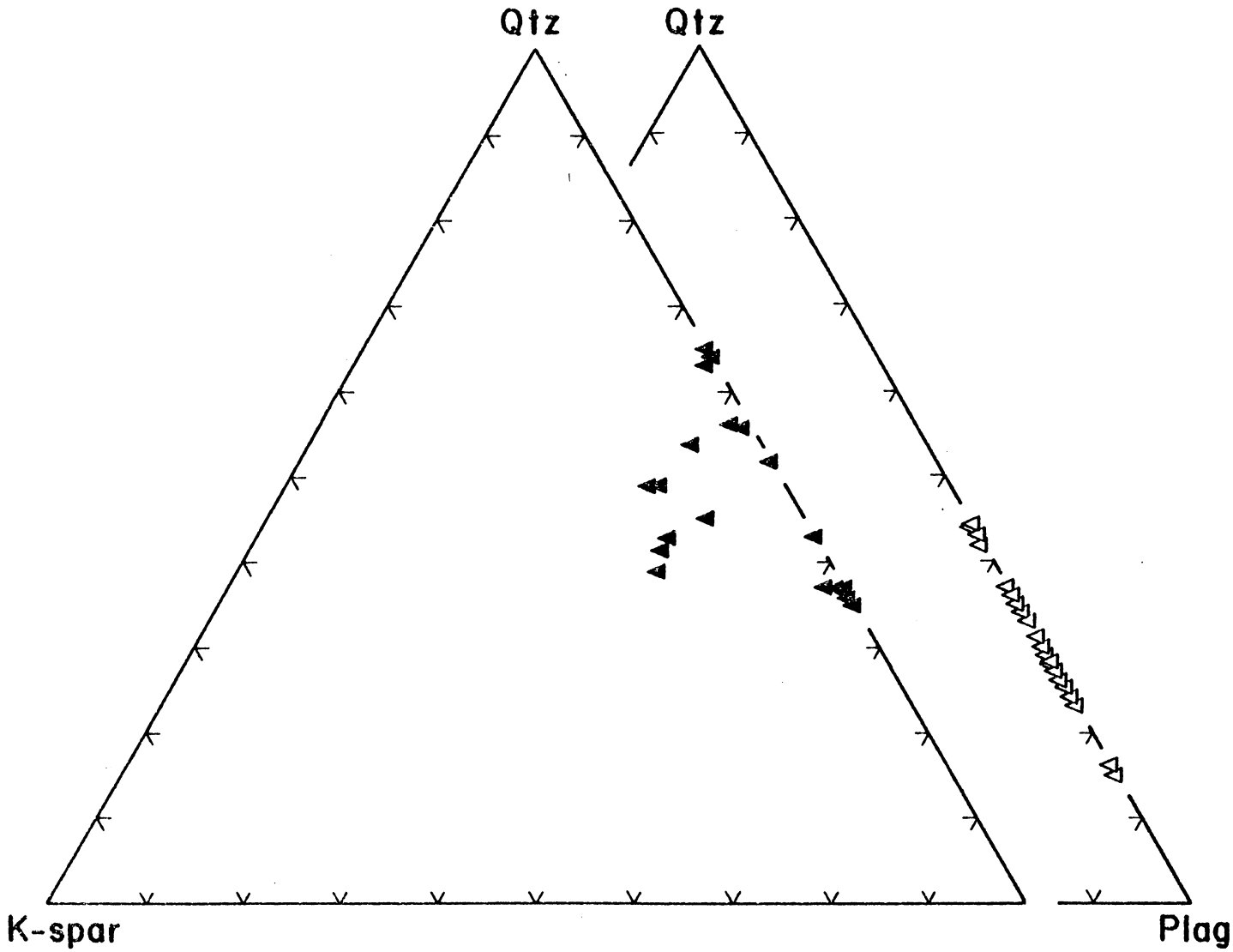
Qtz
Qtz
K-spar
Plag

Maryland diamictites indicate a time-stratigraphic correlation may not be justified.

The 467 age of deformation for the James Run/Port Deposit thrust block cannot be directly associated with the deposition of the Sykesville and Laurel diamictites or the other associated flysch metasediments of the Wissahickon terrane. However, if the Conowingo rocks are a depositional time-equivalent for the James Run/Port Deposit emplacement event, then this particular flysch facies of the Wissahickon was deposited immediately prior to or coincident with the 467 Ma deformation episode; the source terrane of the Conowingo rocks is not currently exposed.

4) The thrust contact between the James Run/Port Deposit block and the Baltimore Mafic Complex discourages a relation between the two. Sinha (unpublished data) found a zircon Pb-Pb age of 480 for plagiogranitic dikes in the Baltimore Mafic Complex. Shaw et al. (1982) presented a Nd-Sm age of 490 $\pm$ 30 Ma for the Baltimore Mafic Complex and suggested the mafic rocks were intruded into continental countryrock and do not represent oceanic or back arc basin material. It is possible that the intrusion of the Baltimore Mafic Complex was associated with thrusting of the James Run/Port Deposit association during Ordovician times.

CONCLUSIONS

The James Run/Port Deposit association may be characterized by:

(1) A bimodal silica distribution, with the felsic/mafic ratio being at least 5/1. However, the Coastal Plain overlap does not permit a full areal coverage of the James Run rocks. Data from Pavlides (1981) suggests a bimodal distribution in the correlative Chopawamsic Formation.

(2) Tonalitic and dacitic differentiates with trondhjemitic affinities. Primary minerals include plagioclase, quartz, magnetite, and possibly garnet and allanite.

Bimodal tholeiite-trondhjemite suites similar to the James Run have received considerable attention for their possible role in the evolution of sialic crust (Barker, 1979a). These rock types are associated with compressional and extensional tectonics in ensialic and ensimatic crustal environments. It is recognized that the types and amounts of differentiates in any tectonic situation reflect a variety of factors, including source terrane-wall rock compositions and the extent of their interaction, as well as the extent of partial fusion and fractional crystallization processes. However, the preponderance of trondhjemitic rocks in the Archean (Barker and Arth, 1976), their frequency in Paleozoic continental margin terranes (Hietanen, 1973, 1976; Malpas, 1979; Barker et al., 1979), their infrequency in the Mesozoic (Hotz, 1971), and their scarcity in the Cenozoic (Chivas et al., 1982) suggests that the James Run trondhjemites may not have originated in an ordinary

Figure 12. Comparative variation diagrams for Viti Levu, Fiji (Gill, 1970, Gill and Storck, 1979), Cloudy Pass Pluton (Peck, 1964), Tonga-Kermadec-New Zealand (Ewart, 1966; Ewart and Stipp, 1968; Ewart et al., 1977), the Green Tuff region of Japan (Aramaki et al., 1972; Aramaki and Nozawa, 1978), and the Port Deposit Complex/James Run Formation meta-igneous differentiation trends (see Figure 5-C).

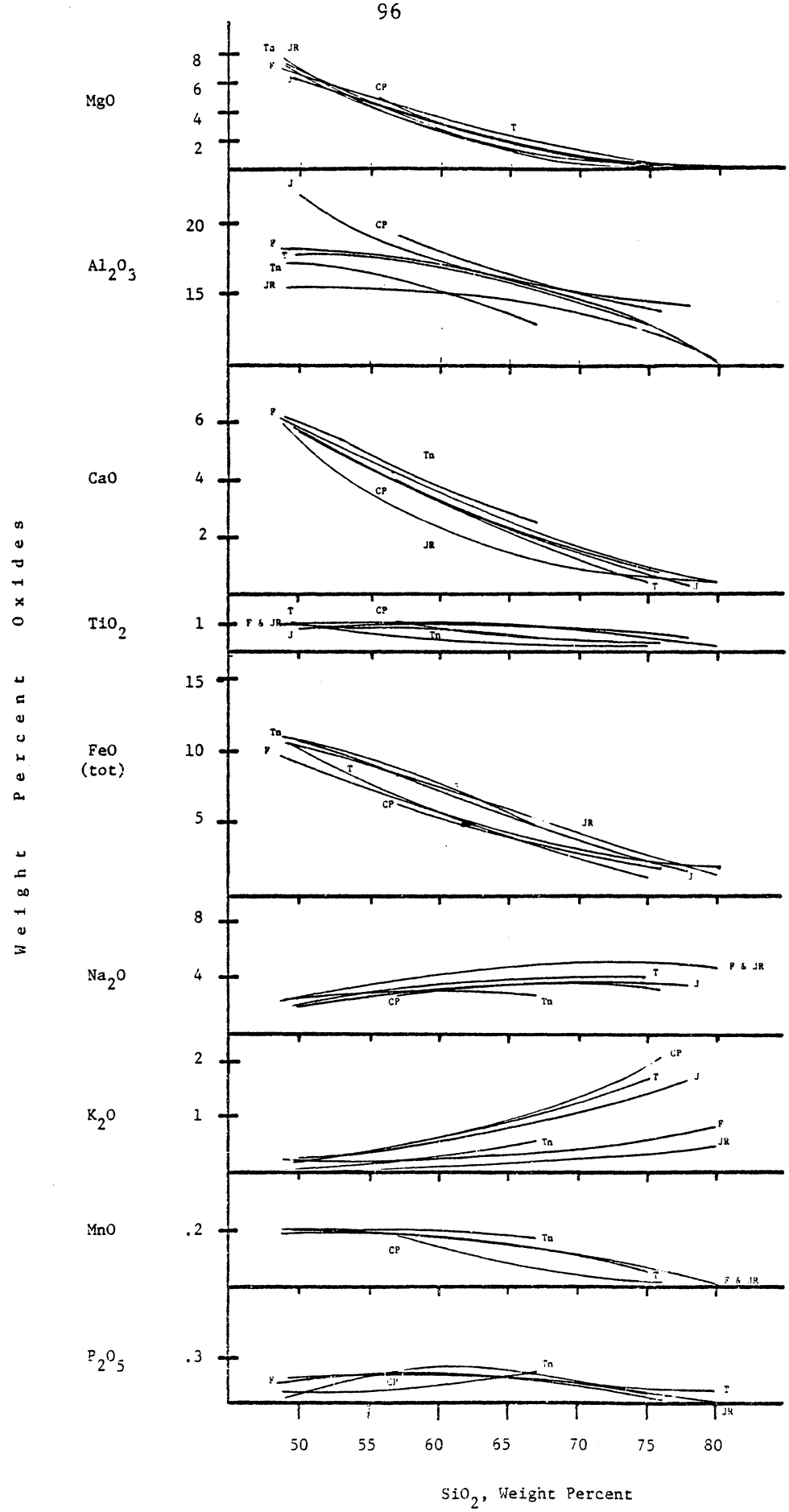
MgO
8
6
4
2
Ta JR
F
J
CP
T
Al2O3
20
15
J
CP
F
T
Ta
JR
CaO
6
4
2
F
Tn
CP
JR
T
J
TiO2
1
T
CP
F & JR
J
Tn
FeO (tot)
15
10
5
Tn
F
T
CP
JR
J
Na2O
8
4
T
J
F & JR
CP
Tn
K2O
2
1
CP
T
J
F
Tn
JR
MnO
.2
Tn
CP
T
F & JR
P2O5
.3
Tn
F
CP
T
JR
50
55
60
65
70
75
80
Weight Percent Oxides
SiO2, Weight Percent

ensimatic island arc as proposed by Hopson (1964), Southwick (1969), Higgins (1972), and Pavlides (1981).

Extensional tectonic regimes, whether in ensialic or ensimatic crust, do not produce differentiates with the characteristics of the James Run (Aumento, 1969; Macdonald, 1974). Figure 12 presents Harker variation trends for rocks from these compressional tectonic regimes:

(1) The continental margin Cloudy Pass pluton, western Cascades, USA,

(2) mature island arc volcanics from the Green Tuff Region of Japan,

(3) the ensialic Taupo Volcanic Zone, New Zealand,

(4) the ensimatic Tongan Islands, immediately north of New Zealand,

(5) the "dilemma" of Viti Levu, Fiji,

in a comparison with the differentiation trends of the James Run/Port Deposit association.

These points merit further consideration:

(1) Given the scatter for the James Run and Port Deposit rocks, only the ensimatic Tongan rocks may be excluded as a tectonic analogue. Data from Ewart (1979) precludes Cenozoic ensimatic island arcs in general as possible tectonic analogues: Siliceous rocks similar to the James Run are too infrequent in these recent terranes (Bryan, 1979).

(2) The Cloudy Pass pluton, the Green Tuff region, and the Taupo zone show roughly similar differentiation trends as the James Run. In addition, siliceous rocks predominate over mafic rocks in these terranes.

However, the bimodal Fijian suite is the only association to have produced dacitic-tonalitic rocks with trondhjemitic affinities.

The tectonic environment of Fiji has been described as "a dilemma to Jakes and Gill (1976)" by Gill and Storck (1979), who prefer to highlight Fiji's geochemical similarities with Archean regimes. Barker and Arth (1976) present a model for these Archean rock types where partial fusion of meta-basalt by mantle-derived melts produce a trondhjemitic differentiate (Helz, 1976) which is then extruded with continued basaltic volcanism.

Comparative data are equivocal, but the preferred model for the petrogenesis of the James Run involves the Fijian analogue and the petrogenetic presentation of Barker and Arth (1976). The notion that the Appalachian volcanic/plutonic belt is the product of ensimatic island arc volcanism is not supported by evaluation of rocks with broadly similar chemical compositions. Thrusting and deformation occurred at approximately 467 Ma and juxtaposed the James Run/Port Deposit thrust block with the Baltimore Mafic Complex (cf. Crowley, 1976); concurrent anatexis of felsic basement in the area is not evident. The Conowingo Diamictite facies of the Wissahickon terrane is cut by this fault, and therefore, it must have been deposited prior to or coincident with this deformation event.

REFERENCES

Aramaki, S., Hirayama, K., and Nozawa, T., 1972. Chemical composition of Japanese granites, Part 2. Variation trends and average composition of 1200 analyses. J. Geol. Society of Japan 78, 39-49.

Aramaki, S. and Nozawa, T., 1978. A reference book of chemical data for Japanese granites. Contribution from Geodynamics Project of Japan 78-1, 88 pp.

Arth, J. G. and Hanson, G. N., 1975. Geochemistry and origin of the early Precambrian crust of northeastern Minnesota. Geochim. Cosmochim. Acta 39, 325-362.

Augustithus, S. S., 1973. Atlas of the Textural Patterns of Granites, Gneisses, and Associated Rock Types. Elsevier Scientific Publishing Company, Amsterdam, 378 pp.

Aumento, F., 1969. Diorites from the Mid-Atlantic Ridge at 450°N. Science 165, 1112-1113.

Barker, F. (ed.), 1979a. Trondhjemites, Dacites, and Related Rocks. Elsevier Publishing Co., New York, 659 pp.

Barker, F., 1979b. Trondhjemite: definition, environment and hypotheses of origin. In: F. Barker (ed.), Trondhjemites, Dacites, and Related Rocks, Elsevier Publishing Co., New York, p. 1-11.

Barker, F. and Arth, J. G., 1976. Generation of trondhjemitic-tonalitic liquids and Archean bimodal trondhjemite-basalt suites. Geology 4, 596-600.

Barker, F., Arth, J. G., Peterman, Z. E., and Friedman, I., 1976. The 1.1-1.8 b.y. old trondhjemite of southwestern Colorado and northern New Mexico: Geochemistry and depths of genesis. Geol. Soc. Am. Bull. 87, 189-198.

Barker, F., Millard, A. T., Jr., and Knight, R. J., 1979. Reconnaissance geochemistry of Devonian island-arc volcanic and intrusive rocks, west Shasta district, California. In: F. Barker (ed.), Trondhjemites, Dacites, and Related Rocks, Elsevier Publishing Co., New York, p. 531-546.

Beach, A., 1979. Pressure solution as a metamorphic process in deformed terrigenous sedimentary rocks. Lithos 12, 51-58.

Bland, A. E., 1978. Trace element-geochemistry of volcanic sequences of Maryland, Virginia and North Carolina and its bearing on the tectonic evolution of the Central Appalachians. Unpublished Ph.D. dissertation, University of Kentucky, 333 pp.

Bland, A. E. and Blackburn, W. H., 1980. Geochemical studies on the greenstones of the Atlantic Seaboard Volcanic Province, south-central Appalachians. In: D. R. Wones (ed.), The Caledonides in the U.S.A.," I.G.C.P. Project 27: Caledonide Orogen, VPI & SU Memoir No. 2, 263-270.

Bobyarchick, A. R., Pavlides, L., and Wier, K., 1981. Piedmont geology of the Ladysmith and Lake Anna East Quadrangles, and vicinity, Virginia. USGS Miscellaneous Investigations Map I-1282.

Bourland, W. C., 1976. Tectogenesis and metamorphism of the Piedmont from Columbia to Westview, Virginia, along the James River. Unpublished M.S. thesis, VPI & SU, 114 pp.

Brown, W. R., 1969. Geology of the Dillwyn Quadrangle, Virginia. Virginia Division of Mineral Resources, Report of Investigations 10, 77 pp.

Brown, W. R. and Pavlides, L., 1981. Melange terrane in the Central Virginia Piedmont: Geol. Soc. Am. Abstracts with Programs 13, p. 419.

Bryan, W. B., 1979. Low K_2O dacite from the Tonga-Kermadec island arc: petrography, chemistry andpetrogenesis. In: F. Barker (ed.), Trondhjemites, Dacites, and Related Rocks, Elsevier Publishing Co., New York, p. 581-600.

Carmichael, I. S. E., Turner, F. J., and Verhoogen, J., 1974. Igneous Petrology, McGraw-Hill Book Company, New York, 739 pp.

Cater, F. W., 1969. The Cloudy Pass epizonal batholith and associated subvolcanic rocks. Geol. Soc. Am. Spec. Pap. 116, 54 pp.

Chivas, R., Andrew, A. S., and O'Neill, J. R., 1982. Geochemistry of a Pliocene-Pleistocene oceanic-arc plutonic complex, Guadalcanal. Nature (in press).

Cliff, R. A., 1971. Sr isotope distribution in a regionally metamorphosed granite from the Zentralgneiss, southeast Tauernfenster, Austria. Contrib. Mineral. Petrol. 32, 274-288.

Coleman, R. G., 1977. Ophiolites. Springer-Verlag, Berlin, 299 pp.

Coleman, R. G. and Donato, M. M., 1979. Oceanic plagiogranite revisited. In: F. Barker (ed.), Trondhjemites, Dacites, and Related Rocks, Elsevier Publishing Co., New York, p. 149-165.

Coleman, R. G. and Peterman, Z. E., 1975. Oceanic plagiogranite. J. Geophys. Res. 80, 1099-1108.

Corfu, F., 1980. U-Pb and Rb-Sr systematics in a polyorogenic segment of the Precambrian shield, central southern Norway. Lithos 13, 305-323.

Crowley, W. P., 1976. The geology of the crystalline rocks near Baltimore and its bearing on the evolution of the eastern Maryland Piedmont. Md. Geol. Surv. Report of Investigations No. 27, 40 pp.

Crowley, W. P., Reinhardt, J., and Cleaves, E. T., 1976. Geologic map of Baltimore County and vicinity. Md. Geol. Surv., scale 1:62,500.

Davis, G. L., Tilton, G. R., Aldrich, L. T., Hart, S. R., and Steiger, R. H., 1965. The minimum age of the Glenarm Series, Baltimore, Maryland. Carnegie Inst. Wash. Yearbook 64, 174-177.

Dickinson, W. R., 1970. Interpreting detrital modes of greywacke and arkose. J. Sed. Petrol. 40, 695-707.

Drake, A. A., Jr., 1980. The taconides, acadides, and alleghenides in the Central Appalachians. In: D. R. Wones (ed.), The Caldeonides in the U.S.A., VPI & SU Memoir No. 2, 179-188.

Drake, A. A. and Lyttle, P. T., 1981. The Accotink Schist, Lake Barcroft Metasandstone, and Popes Head Formation--keys to understanding of the tectonic evolution of the northern Virginia Piedmont. USGS Prof. Paper 1205, 15 pp.

Drake, A. A., Jr. and Morgan, B., 1981. The Piney Branch Complex--a metamorphosed fragment of the central Appalachian ophiolite in northern Virginia. Am. J. Sci. 281, 484-508.

Ewart, A., 1966. Review of mineralogy and chemistry of the acidic volcanic rocks of Taupo volcanic zone, New Zealand. Bull. Volc. 2, 1147-1171.

Ewart, A., 1979. A review of the mineralogy and chemistry of Tertiary--Recent dacitic, latitic, rhyolitic, and related salic volcanic rocks. In: F. Barker (ed.), Trondhjemites, Dacites, and Related Rocks, Elsevier Publishing Co., New York, p. 13-122.

Ewart, A. and Stipp, J. J., 1968. Petrogenesis of the volcanic rocks of the Central North Island, New Zealand, as indicated by a study of $^{87}Sr/^{86}Sr$ ratios, and Sr, Rb, K, U, and Th abundances. Geochim. Cosmochim. Acta 32, 699-736.

Ewart, A., Brothers, R. N., and Mateen, A., 1977. An outline of the geology and geochemistry, and the possible petrogenetic evolution of the volcanic rocks of the Tonga-Kermadec-New Zealand island arc. J. Volcan. and Geotherm. Res. 2, 205-250.

Faure, G., 1977. Principles of Isotope Geology. John Wiley and Sons, New York, 464 pp.

Field, D. and Raheim, A., 1980. Secondary geologically meaningless Rb-Sr isochrons, low $^{87}Sr/^{86}Sr$ initial ratios and crustal residence times of high grade gneisses. Lithos 13, 295-304.

Fisher, G. W., 1970. The metamorphosed sedimentary rocks along the Potomac River, near Washington, D. C. In: G. W. Fisher, F. J. Pettijohn, J. C. Reed, and K. N. Weaver (eds.), Studies of Appalachian Geology: Central and Southern. Wiley Interscience, New York, 460 pp.

Fisher, G. W., Higgins, M. W., and Zietz, I., 1979. Geological interpretations of aeromagnetic maps of the crystalline rocks in the Appalachians, northern Virginia to New Jersey. Md. Geol. Surv. Report of Investigations 32, 43 pp.

Foland, K. A. and Muessig, K. W., 1978. A Paleozoic age for some charnockitic-anorthositic rocks. Geology 6, 143-146.

Gill, J. B., 1979. Geochemistry of Viti Levu, Fiji, and its evolution as an island arc. Contrib. Mineral. Petrol. 27, 179-203.

Gill, J. B. and Storck, A. L., 1979. Miocene low-K dacites and trondhjemites of Fiji. In: F. Barker (ed.), Trondhjemites, Dacites, and Related Rocks, Elsevier Publishing Co., New York, p. 629-649.

Grauert, B. W., 1973. U-Pb isotopic studies of zircons from the Gunpowder granite, Baltimore County, Maryland. Carnegie Inst. Wash., Yearbook 72, 288-290.

Grauert, B. and Wagner, M. E., 1974. Age of the granulite facies metamorphism of the Wilmington Complex, Delaware-Pennsylvania Piedmont. Carnegie Inst. Wash., Yearbook 73, 997-998.

Grauert, B. and Wagner, M. E., 1975. Age of the granulite facies metamorphism of the Wilmington Complex, Delaware-Pennsylvania Piedmont. Am. J. Sci. 275, 683-691.

Gulson, B. L. and Krogh, T. E., 1973. Old lead components in the young Bergell Massif, southeast Swiss Alps. Contrib. Mineral. Petrol. 40, 239-252.

Hanan, B., 1980. The petrology and geochemistry of the Baltimore Mafic Complex, Maryland. Unpublished Ph.D. thesis, VPI & SU, 218 pp.

Hart, S. R., Davis, G. L., Steiger, R. H., and Tilton, G. R., 1968. A comparison of the isotopic mineral age variations and petrologic changes induced by contact metamorphism. In: E. I. Hanilton and R. M. Farquhar (eds.), Radiometric Dating for Geologists, Interscience Publ., New York, p. 73-110.

Harvey, P. K., Taylor, D. M., Hendry, R. D., and Bancroft, F., 1973. An accurate fusion method for the analysis of rocks and chemically related materials by x-ray fluorescence spectrometry. X-Ray Spectrometry 2, 33-44.

Helz, R. T., 1976. Phase relations of basalts in their melting range at PH_2O = 5 kb as a function of oxygen fugacity, Part II. Melt compositions. J. Petrol. 17, 139-193.

Hershey, H. G., 1937. Structure and age of the Port Deposit granodiorite complex. Maryland Geol. Surv. 13, 109-148.

Hietanen, A., 1973. Geology of the Pulga and Bucks Lake Quadrangles, Butte and Plumas Counties, California. USGS Prof. Paper 731, 66 pp.

Hietanen, A., 1976. Metamorphism and plutonism around the middle and south forks of the Feather River, California. USGS Prof. Paper 731, 30 pp.

Higgins, M. W., 1970. Metavolcanic rocks and epizonal plutons in the Cecil County Piedmont, Maryland. In: New Interpretations of the Eastern Piedmont Geology of Maryland, Guidebook for the 35th Annual Field Conference of Pennsylvania Geologists, 60 pp.

Higgins, M. W., 1971. Depth of emplacement of James Run Formation pillow basalts, and the depth of deposition of part of the Wissahickon Formation, Appalachian Piedmont, Maryland. Am. J. Sci. 271, 321-332.

Higgins, M. W., 1972. Age, origin, regional relations, and nomenclature of the Glenarm Series, central Appalachian Piedmont: a reinterpretation. Geol. Soc. Am. Bull. 83, 989-1026.

Higgins, M. W., 1982. Pre-publication manuscript and map of the geology of Cecil County, scale 1:62,500.

Higgins, M. W., Sinha, A. K., Tilton, G. R., and Kirk, W. S., 1971. Correlation of metavolcanic rocks in the Maryland, Delaware, and Virginia Piedmont (abstr.). Geol. Soc. Am. Abstracts with Programs 3, 320-321.

Higgins, M. W., Sinha, A. K., Zartman, R. E., and Kirk, W. S., 1977. U-Pb zircon dates from the central Appalachian Piedmont: a possible case of inherited radiogenic lead. Geol. Soc. Am. Bull. 88, 125-132.

Hobbs, B. E., Means, W. D., and Williams, P. F., 1976. An Outline of Structural Geology. John Wiley and Sons, Inc., New York, 571 pp.

Hopson, C. A., 1960. The Port Deposit Granodiorite Complex (stop 1), and Conowingo Contact Zone, Port Deposit Granodiorite (stop 2). In: D. U. Wise and M. E. Kauffman (eds.), Some Tectonic and Structural Problems of the Appalachian Piedmont along the Susquehanna River, Pennsylvania Geologists Guidebook, 25th Field Conf., Lancaster, p. 26-33.

Hopson, C. A., 1964. The crystalline rocks of Howard and Montgomery Counties. In: The Geology of Howard and Montgomery Counties, Maryland Geol. Surv., p. 27-215.

Hotz, P. E., 1971. Plutonic rocks of the Klamath Mountains, California and Oregon. USGS Prof. Paper 684-B, 20 pp.

Jakes, P. and Gill, J., 1970. Rare earth elements and the island arc tholeiitic series. Earth Planet. Sci. Lett. 9, 17-28.

Malpas, J., 1979. Two contrasting trondhjemite associations from transported ophiolites in western Newfoundland: initial report. In: F. Barker (ed.), Trondhjemites, Dacites, and Related Rocks, Elsevier Publishing Co., New York, p. 465-488.

Macdonald, R., 1974. Tectonic settings and magma associations. Bull. Volc. 38, 575-593.

McBryde, E. F., 1963. A classification of common sandstones. J. Sed. Petrol. 33, 664-669.

Mitra, G., 1978. Ductile deformation zones and mylonites: the mechanical process involved in the deformation of crystalline basement rocks. Am. J. Sci. 278, 1057-1084.

Montgomery, C. W. and Hurley, P. M., 1978. Total rock U-Pb and Rb-Sr systematics in the Imataca series, Guayana Shield, Venezuela. Earth Planet. Sci. Lett. 39, 281-290.

Moore, J. G., 1958. The quartz diorite boundary line in the western United States. J. Geol. 66, 198-210.

Morgan, B. A., 1977. The Baltimore Complex, Maryland, Pennsylvania, and Virginia: In: R. G. Coleman and W. P. Irwin (eds.), North American Ophiolites, State of Oregon Dept. Geol. and Min. Industires, Bull. 95, 41-49.

Mose, D. C. and Nagel, M. S., 1982. Plutonic events in the Piedmont of Virginia. Southeastern Geology 23, 25-39.

Mussman, B., 1982. The Middle Ordovician Knox Unconformity, Virginia Appalachians. Unpublished M.S. thesis, VPI & SU, 160 pp.

Muth, K. G., Arth, J. G., and Reed, J. C., Jr., 1979. A minimum age for high-grade metamorphism and granite intrusion in the Piedmont of the Potomac River Gorge near Washington, D. C. Geology 7, 349-350.

Norrish, K. and Hutton, J. T., 1969. An accurate spectrographic method for the analysis of a wide range of geological samples. Geochim. Cosmochim. Acta 33, 431-453.

Norrish, K. and Chappell, B. W., 1977. X-ray fluorescence spectrometry. In: J. Zussman (ed.), Physical Methods in Determinative Mineralogy, p. 201-272.

O'Connor, J. T., 1965. A classification for quartz-rich igneous rocks based on feldspar ratios. U. S. Geol. Surv. Prof. Paper 525-B, B79-B84.

Pavlides, L., 1980. Revised nomenclature and stratigraphic relationships of the Fredericksburg Complex and Quantico Formation of the Virginia Piedmont. USGS Prof. Paper 1146, 29 pp.

Pavlides, L., 1981. The Central Virginia Volcanic-Plutonic Belt: An island arc of Cambrian(?) age. U. S. Geol. Surv. Prof. Paper 1231-A, 34 pp.

Pavlides, L., Sylvester, K. A., Daniels, D. L., and Bates, R. G., 1974. Correlation between geophysical data and rock types in the Piedmont and Coastal Plain of northeast Virginia and related areas. J. Res. U. S. Geol. Surv. 2, 569-580.

Pavlides, L., Pojeta, J., Jr., Gordon, M., Jr., Parsley, R. L., and Bobyarchick, A. R., 1980. New evidence for the age of the Quantico Formation of Virginia. Geology 8, 286-290.

Pavlides, L., Gair, J. E., and Cranford, S. L., 1982a. Central Virginia volcanic-plutonic belt as a host for massive sulfide deposits. Econ. Geol. 77, 233-272.

Pavlides, L., Stern, T. W., Arth, J. G., Muth, K. G., and Newell, M. R., 1982b. Middle and Upper Paleozoic granitic rocks in the Piedmont near Fredericksburg, VA: Geochronology. U. S. Geol. Surv. Prof. Paper 1231-B, 9 pp.

Peacock, M. A., 1931. Classification of igneous rock series. J. Geol. 39, 54-67.

Pearce, J. A., 1976. Statistical analysis of major element patterns in basalts. J. Petrol. 17, 15-43.

Peck, D. L., Griggs, A. B., Schlicker, H. G., Wells, F. G., and Dole, H. M., 1964. Geology of the central and northern parts of the western Cascade Range in Oregon. U. S. Geol. Surv. Prof. Paper 449, 56 pp.

Peterman, Z. E., 1979. Strontium isotope geochemistry of late Archean to late Cretaceous tonalites and trondhjemites. In: F. Barker (ed.), Trondhjemites, Dacites, and Related Rocks, Elsevier Publishing Co., New York, p. 133-145.

Pidgeon, R. T., Koppel, V., and Grunenfelder, M., 1970. U-Pb isotopic relationships in zircon suites from a para- and ortho-gneiss from the Ceneri Zone, southern Switzerland. Contrib. Mineral. Petrol. 26, 1-11.

Rankin, D. W., 1975. The continental margin of eastern North America in the southern Appalachians: the opening and closing of the proto-Atlantic Ocean. Am. J. Sci. 275-A, 298-336.

Read, J. R., 1980. Depocenters, carbonate facies and foreland basin evolution, middle Ordovician, Virginia. In: D. R. Wones (ed.), The Caledonides in the U.S.A., VPI & SU Memoir No. 2, 19-26.

Roddick, J. C. and Compston, W., 1972. Strontium isotopic equilibration: a solution to a paradox. Earth Planet. Sci. Lett. 34, 238-246.

Rodgers, J., 1971. The taconic orogeny. Geol. Soc. Am. Bull. 82, 1141-1177.

Seiders, V. M., Mixon, R. B., Stern, T. W., Newell, M. F., and Thomas, C. B., Jr., 1975. Age of plutonism and tectonism and a new minimum age limit on the Glenarm series in the northeast Virginia Piedmont near Occoquan. Am. J. Sci. 275, 481-511.

Shaw, D. M., 1968. A review of K-Rb fractionation trends by covariance analysis. Geochim. Cosmochim. Acta 32, 573-601.

Shaw, H., Wasserburg, G. J., and Albee, A. C., 1982. Isotopic constraints on the origin of Appalachian Mafic Complexes. Geol. Soc. Am. Abstracts with Programs, 392.

Sibson, R. H., 1977. Fault rocks and fault mechanism. J. Geol. Soc. London 133, 191-213.

Sinha, A. K. and Glover, L., III, 1978. U-Pb systematics of zircons during dynamic metamorphism. Contrib. Mineral. Petrol. 66, 305-310.

Sinha, A. K., Hanan, B. B., Sans, J. R., and Hall, S. T., 1980. Igneous rocks of the Maryland Piedmont: indicators of crustal evolution. In: D. R. Wones (ed.), The Caledonides in the U.S.A., VPI & SU Memoir No. 2, 131-135.

Sinha, A. K., Higgins, M. W., Davis, G. L., Hart, S. R., and Kirk, W. S., 1971. The Glenarm series and related rocks. Carnegie Inst. Wash., Yearbook 69, 412-413.

Sinha, A. K. and Zietz, I., 1982. Geophysical and geochemical evidence for a Hercynian magmatic arc, Maryland to Georgia. Geology, pre-publication manuscript.

Southwick, D. L., 1969. Crystalline rocks of Harford County. In: The Geology of Harford County, Maryland. Maryland Geol. Surv., 1-76.

Southwick, D. L., 1979. The Port Deposit Gneiss revisited. Southeastern Geology 20, 101-119.

Southwick, D. L. and Owens, J. P., 1968. Geologic map of Harford County. Maryland Geol. Surv., scale 1:62,500.

Southwick, D. L., Reed, J. C., Jr., and Mixon, R. B., 1971. The Chopawamsic Formation--a stratigraphic unit in the Piedmont of northeastern Virginia. U. S. Geol. Surv. Bull. 1324-D, D1-D11.

Spoljaric, N. and Jordan, R. R., 1966. Generalized geologic map of Delaware. Delaware Geol. Surv.

Steiger, R. H. and Hopson, C. A., 1964. Minimum age of the Glenarm Series, Baltimore, Maryland (abstr.). Geol. Soc. Am. Spec. Paper 82, pp. 194-195.

Steiger, R. H. and Jager, E., 1977. Subcommission on geochronology: convention and use of decay constants in geo- and cosmochronology. Earth Planet. Sci. Lett., 359-362.

Stern, T. W., Newell, M. F., Kistler, R. W., and Shawe, D. R., 1965. Zircon uranium-lead and thorium-lead and mineral potassium-argon ages of La Sal Mountains rocks, Utah. J. Geophys. Res. 70, 1503-1507.

Streckeisen, A. L., 1973. Plutonic rocks: classification and nomenclature recommended by the IUGS Subcommission on the Systematics of Igneous Rocks. Geotimes 18, 26-30.

Streckeisen, A. L., 1979. Classification and nomenclature of volcanic rocks, lamprophyres, carbonatites, and melilitic rocks: Recommendations and suggestions of the IUGS Subcommission on the Systematics of Igneous Rocks. Geology 7, 331-335.

Tilton, G. R., Doe, B. R., and Hopson, C. A., 1970. Zircon age measurements in the Maryland Piedmont, with special reference to Baltimore Gneiss problems. In: G. W. Fisher and others (eds.), Studies of Appalachian Geology--Central and Southern. Interscience Publishers, New York, p. 429-434.

Ward, R. F., 1959. Petrology and metamorphism of the Wilmington Complex, Delaware, Pennsylvania, and Maryland. Geol. Soc. Am. Bull. 70, 1425-1458.

Wetherill, G. W., Tilton, G. R., Davis, G. L., Hart, S. R., and Hopson, C. A., 1966. Age measurements in the Maryland Piedmont. J. Geophys. Res. 71, 2139-2155.

Wright, J. E., Sinha, A. K., and Glover, L., III, 1975. Age of zircons from the Petersburg granite, Virginia: with comments on belts of plutons in the Piedmont. Am. J. Sci. 275, 848-856.

Yamada, N., Nozawa, T., Hayama, Y., and Yamada, T., 1977. Guidebook for Excursion 4. Mesozoic felsic igneous activity and related metamorphism in the Central Japan, from Nagoya to Toyama. Geol. Surv. of Japan. Sumitomo Printing and Publishing Co., Ltd.

York, D., 1966. Least-squares fitting of a straight line. Canadian J. Phys. 44, 1079-1086.

Zartman, R. E., 1978. U-Pb zircon dates from the central Appalachian Piedmont: a possible case of inherited radiogenic lead: Reply. Geol. Soc. Am. Bull. 89, 1115-1117.

Zietz, I., Calver, J. L., Johnson, S. S., and Kirby, J. R., 1977. Aeromagnetic map of Virginia. USGS Geophysical Investigations Map GP-915.

APPENDIX I

SAMPLE LOCATIONS

INDEX TO SAMPLE LOCATIONS

Stop #1

Location: 100 meters downstream of Conowingo Dam on the northeast bank of the Susquehanna River, Cecil County, Conowingo Dam Quadrangle.
Unit: Wissahickon Formation, Conowingo Diamictite Facies
Sample #: RL-80-2
RL-80-3

Stop #2

Location: 0.8 km southeast of Conowingo Dam along the Conrail Railroad Tracks, northeast bank of Susquehanna River, Cecil County, Conowingo Dam Quadrangle
Unit: Wissahickon Formation, Conowingo Diamictite Facies

Stop #3

Location: 1.25 km southeast of Conowingo Dam along the Conrail Railroad Tracks, northeast bank of Susquehanna River, Cecil County, Conowingo Dam Quadrangle
Unit: Wissahickon Formation, Conowingo Diamictite Facies

Stop #4

Location: Below bridge for Basin Run Road in the streambed of Basin Run, Cecil County, Conowingo Dam Quadrangle
Unit: Wissahickon Formation, Conowingo Diamictite Facies
Sample #: RL-80-4

Stop #5

Location: Large cliffs along Basin Run, 0.45 km southeast of Octoraro Creek, in the town of Rowlandsville, Cecil County, Conowingo Dam Quadrangle
Unit: Wissahickon Formation, Conowingo Diamictite Facies
Sample #: RL-80-5
RL-80-6

Stop #6

Location: 1 km south of Rowlandsville along Dr. Jack Road, Cecil County, Conowingo Dam Quadrangle
Unit: Wissahickon Formation, Conowingo Diamictite Facies
Sample #: RL-80-6'

Stop #7

Location: 0.4 km north of Harmony Chapel along Dr. Jack Road, Cecil County, Conowingo Dam Quadrangle
Unit: Wissahickon Formation, Conowingo Diamictite Facies
Sample #: RL-80-7

Stop #8

Location: The dead-end road spur between Harmony Chapel and Route 269, Cecil County, Conowingo Dam Quadrangle
Unit: Wissahickon Formation, Conowingo Diamictite Facies

Stop #9

Location: 2.6 km southeast of Conowingo Dam along the Conrail Railroad Tracks, northeast bank of the Susquehanna River, Cecil County, Conowingo Dam Quadrangle
Unit: Wissahickon Formation, Conowingo Diamictite Facies

Stop #10

Location: 15 meters southeast of utility pole #178 along the Conrail Railroad Tracks, northeast bank of the Susquehanna River, Cecil County, Conowingo Dam Quadrangle
Unit: Wissahickon Formation, Conowingo Diamictite Facies
Sample #: RL-80-8

Stop #11

Location: 50 meters northwest of mile-post 8, along the Conrail Railroad Tracks, northeast bank of the Susquehanna River, Cecil County, Conowingo Dam Quadrangle
Unit: Wissahickon Formation, Conowingo Diamictite Facies

Stop #12

Location: 15 meters southeast of utility pole #178 along the Conrail Railroad Tracks, northeast bank of Susquehanna River, Cecil County, Conowingo Dam Quadrangle
Sample #: RL-80-10

Stop #13

Location: 25 meters southeast of utility pole #175 along the Conrail Railroad Tracks, northeast bank of Susquehanna River, 2006 meters southeast of Conowingo Dam, Cecil County, Conwingo Dam Quadrangle
Unit: Wissahickon Formation, Conowingo Diamictite Facies
Sample #: RL-80-11

Stop #14

Location: 15 meters southeast of utility pole #178 along the Conrail Railroad Tracks, northeast bank of the Susquehanna River, Cecil County, Conowingo Dam Quadrangle
Unit: Wissahickon Formation, Conowingo Diamictite Facies
Sample #: RL-80-12

Stop #15

Location: 15 meters southeast of utility pole #140 along the Conrail Railroad Tracks, northeast bank of the Susquehanna River, Cecil County, Conowingo Dam Quadrangle
Unit: Wissahickon Formation, Conowingo Diamictite Facies
Sample #: RL-80-13

Stop #16

Location: At utility pole #142 along the Conrail Railroad Tracks, northeast bank of the Susquehanna River, Cecil County, Conowingo Dam Quadrangle
Unit: Wissahickon Formation, Conowingo Diamictite Facies
Sample #: RL-80-15

Stop #17

Location: At utility pole #143 along the Conrail Railroad Tracks, northeast bank of the Susquehanna River, Cecil County, Conowingo Dam Quadrangle
Unit: Wissahickon Formation, Conowingo Diamictite Facies
Sample #: RL-80-19

Stop #20

Location: Along the Conrail Railroad Tracks, northeast bank of the Susquehanna River, 3185 meters southeast of Conowingo Dam (as measured on map), Cecil County
Unit: Wissahickon Formation, Conowingo Diamictite Facies
Sample #: RL-80-20

Stop #21

Location: At utility pole #156 along the Conrail Railroad Tracks, northeast bank of the Susquehanna River, Cecil County, Conowingo Dam Quadrangle
Unit: Wissahickon Formation, Conowingo Diamictite Facies
Sample #: RL-80-26

Stop #22

Location: 10 meters southeast of utility pole #154 along the Conrail Railroad Tracks, northeast bank of the Susquehanna River, Cecil County, Conowingo Dam Quadrangle
Unit: Wissahickon Formation, Conowingo Diamictite Facies
Sample #: RL-80-22

Stop #23

Location: Between utility poles #151 and #152 along the Conrail Railroad Tracks, northeast bank of the Susquehanna River, Cecil County, Conowingo Dam Quadrangle
Unit: Wissahickon Formation, Conowingo Diamictite Facies
Sample #: RL-80-23

Stop #24

Location: Near mile post #7 along the Conrail Railroad Tracks, northeast bank of the Susquehanna River, Cecil County, Conowingo Dam Quadrangle
Unit: Wissahickon Formation, Conowingo Diamictite Facies

Stop #25

Location: At utility pole #145 along the Conrail Railroad Tracks, northeast bank of the Susquehanna River, Cecil County, Conowingo Dam Quadrangle
Unit: Wissahickon Formation, Conowingo Diamictite Facies
Sample #: RL-80-24

Stop #27

Location: At utility pole #130 along the Conrail Railroad Tracks, northeast bank of the Susquehanna River, Cecil County, Aberdeen Quadrangle
Unit: Wissahickon Formation, Conowingo Diamictite Facies
Sample #: RL-80-27
RL-80-28

Stop #29

Location: At mile post #6, between utility poles #125 and #126, along the Conrail Railroad Tracks, northeast bank of the Susquehanna River, Cecil County, Aberdeen Quadrangle
Unit: Port Deposit Complex, Sheared Port Deposit
Sample #: RL-80-29

Stop #30

Location: Midway between utility poles #128 and #129 along the Conrail Railroad Tracks, northeast bank of the Susquehanna River, 50 meters northeast from these tracks on the southeast side of the unnamed stream, Aberdeen Quadrangle
Unit: Sheared Port Deposit and Wissahickon Formation (Metagreywacke Facies) - Contact Zone
Sample #: RL-80-29C
RL-80-30
RL-80-31
RL-80-34
RL-80-35
RL-81-44
RL-81-45
RL-81-45S
RL-81-46
RL-81-47

Stop #32

Location: 30 meters northwest of the entrance to the Port Deposit Quarry along the Conrail Railroad Tracks, Cecil County, Aberdeen Qudrangle
Unit: Port Deposit Gneiss
Sample #: RL-80-32
MJ 8142

Stop #33

Location: Southwest corner of the Port Deposit Quarry, Cecil County, Aberdeen Quadrangle
Unit: Port Deposit Gneiss
Sample #: RL-80-33
RL-81-43
MJ 8142
MJ 8143

Stop #34

Location: Northwest face of the Port Deposit Quarry, Cecil County, Aberdeen Quadrangle
Unit: Port Deposit Gneiss
Sample #: RL-80-36
RL-80-37
RL-80-39
RL-80-40

Stop #35

Location: Northern face of the Port Deposit Quarry, Cecil County
Unit: Port Deposit Complex, Port Deposit Gneiss
Sample #: RL-80-41
MJ 8144
MJ 8145
MJ 8147
MJ 8148
MJ 8151
MJ 8152

Stop #36

Location: Northern face of the Port Deposit Quarry, 20 meters east of stop #35, Cecil County, Aberdeen Quadrangle
Unit: Port Deposit Complex, Port Deposit Gneiss
Sample #: RL-80-43

Stop #38

Location: Northwest of Route 222 at northern edge of Port Deposit Town, Cecil County, Aberdeen Quadrangle
Unit: Port Deposit Complex, Port Deposit Gneiss
Sample #: MJ 8154A
MJ 8154B
MJ 8155

Stop #40

Location: Yard behind house at 252 Main Street, Port Deposit Town, Cecil County, Havre de Grace Quadrangle
Unit: Port Deposit Complex, Port Deposit Gneiss
Sample #: RL-80-44

Stop #42

Location: Behind Keetley Motors, southeast end of Port Deposit Town, Cecil County, Havre de Grace Quadrangle
Unit: Port Deposit Complex, Port Deposit Gneiss
Sample #: RL-80-46
RL-80-47

Stop #43

Location: 0.10 km southeast of Route 276, on hill overlooking the boat construction facilities on the northwest bank of the Susquehanna River, Cecil County, Havre de Grace Quadrangle
Unit: Port Deposit Gneiss
Sample #: RL-80-48
RL-80-49
RL-80-50

Stop #44

Location: 0.15 km northeast of Route 222 on Route 269, on the banks of the small unnamed stream, Cecil County, Havre de Grace Quadrangle
Unit: Port Deposit Gneiss
Sample #: RL-80-51

Stop #45

Location: 210 Main Street, Port Deposit Town, Cecil County, Havre de Grace Quadrangle
Unit: Port Deposit Gneiss
Sample #: RL-80-52

Stop #47

Location: 186 Main Street, Port Deposit Town, Cecil County, Havre de Grace Quadrangle
Unit: Port Deposit Gneiss
Sample #: RL-80-53

Stop #48

Location: 174 Main Street, Port Deposit Town, Cecil County, Havre de Grace Quadrangle
Unit: Port Deposit Gneiss
Sample #: RL-80-54

Stop #49

Location: 90 Main Street, Port Deposit Town, Cecil County, Havre de Grace Quadrangle
Unit: Port Deposit Gneiss

Stop #50

Location: 98 Main Street, Port Deposit Town, Cecil County, Havre de Grace Quadrangle
Unit: Port Deposit Gnei s
Sample #: RL-80-55
MJ 8156
MJ 8157
MJ 8158

Stop #51

Location: Behind the trailer court 200 meters southeast of the right-angle turn on Route 222, at the southeastern end of Port Deposit Town, Cecil County, Havre de Grace Quadrangle
Unit: Port Deposit Gneiss
Sample #: RL-80-56

Stop #52

Location: At utility pole #85 along the Conrail Railroad Tracks, northeast bank of the Susquehanna River, Cecil County, Havre de Grace Quadrangle
Unit: James Run Formation, Happy Valley Branch Member
Sample #: RL-80-57

Stop #53

Location: 1410 meters northwest of the I-95 bridge along the Conrail Railroad Tracks, northeast bank of the Susquehanna River, Cecil County, Havre de Grace Quadrangle
Unit: James Run Formation, Happy Valley Branch Member
Sample #: RL-80-60
MJ 8174

Stop #54

Location: In Happy Valley Creek, just upstream from the Conrail Railroad Tracks, northeast bank of the Susquehanna River, Cecil County, Havre de Grace Quadrangle
Unit: James Run Formation, Happy Valley Branch Member
Sample #: MJ 8173

Stop #55

Location: 9754 meters southeast of Conowingo Dam, along the Conrail Railroad Tracks, northeast bank of the Susquehanna River, Cecil County, Havre de Grace Quadrangle
Unit: James Run Formation, Happy Valley Branch Member
Sample #: RL-80-62

Stop #56

Location: 9815 meters southeast of Conowingo Dam along the Conrail Railroad Tracks, northeast bank of the Susquehanna River, Cecil County, Havre de Grace Quadrangle
Unit: James Run Formation, Happy Valley Branch Member
Sample #: RL-80-63
MJ 8172

Stop #57

Location: 9997 meters southeast of Conowingo Dam along the Conrail Railroad Tracks, northeast bank of the Susquehanna River, Cecil County, Havre de Grace Quadrangle
Unit: James Run Formation, Happy Valley Branch Member
Sample #: RL-80-65

Stop #58

Location: 10,196 meters southeast of Conowingo Dam along the Conrail Railroad Tracks (measured on map), northeast bank of the Susquehanna River, Cecil County, Havre de Grace Quadrangle
Unit: James Run Formation, Happy Valley Branch Member
Sample #: RL-80-66

Stop #61

Location: Below the I-95 bridge along the Conrail Railroad Tracks, northeast bank of the Susquehanna River, Cecil County, Havre de Grace Quadrangle
Unit: James Run Formation, Frenchtown Member
Sample #: RL-80-68
RL-80-68'

Stop #62

Location: Below the southwest end of the I-95 bridge over the Susquehanna River, Harford County, Havre de Grace Quadrangle
Unit: James Run Formation, Cecil County Volcanics of Southwick (1969)
Sample #: RL-81-4

Stop #68

Location: Along Herring Run Stream, beneath the Lapidum Road Bridge, Harford County, Aberdeen Quadrangle
Unit: Port Deposit Complex, Port Deposit Gneiss
Sample #: RL-81-12
RL-81-13

Stop #69

Location: Intersection of Gashey's Creek and Chapel Road, in the creek bed, Harford County, Aberdeen Quadrangle
Unit: James Run Formation, Cecil County Volcanics of Southwick (1969)
Sample #: RL-81-15

Stop #70

Location: Intersection of Swan Creek and Aldino Road, in the creek bed, Harford County, Aberdeen Quadrangle
Unit: Aberdeen Metagabbro
Sample #: RL-81-16

Stop #72

Location: Intersection of Rock Run and Rowland Road, in the creek bed, Cecil County, Conowingo Dam Quadrangle
Unit: Port Deposit Complex, Port Deposit Gneiss
Sample #: RL-81-17

Stop #73

Location: Intersection of Rock Creek and Rowland Road, in the creek bed, Cecil County, Rising Sun Quadrangle
Unit: Port Deposit Gneiss
Sample #: RL-81-18

Stop #74

Location: 0.6 km southeast of the power line, along Basin Run Stream, Ceil County, Rising Sun Quadrangle
Unit: Port Deposit Gneiss
Sample #: RL-81-19

Stop #76

Location: Old, small, abandoned quarry 0.1 km southeast of Rock Run along Route 269, Cecil County, Aberdeen Quadrangle
Unit: Port Deposit Gneiss
Sample #: RL-81-21

Stop #77

Location: In unnamed stream bed near the Route 276 bridge, 1.5 km northeast of Port Deposit Town, Havre de Grace Quadrangle
Unit: Port Deposit Gneiss
Sample #: RL-81-22

Stop #78

Location: Along small tributary to Rock Run Stream, between Rock Run Road and Jack Road, where it flows beneath Burlin Road, Cecil County, Rising Sun Quadrangle
Unit: Port Deposit Gneiss
Sample #: RL-81-23
RL-81-24

Stop #79

Location: 0.5 km southwest of Hopewell Church along Post Road, Cecil County, Rising Sun Quadrangle
Unit: Port Deposit Gneiss
Sample #: RL-81-25
RL-81-26

Stop #80

Location: Intersection of Elbow Creek and Route 161, in the stream channel, Harford County, Aberdeen Quadrangle
Unit: Sheared Port Deposit Gneiss
Sample #: RL-80-27

Stop #81

Location: 100 meters inside Susquehanna State Park, along Run Road in Harford County, Aberdeen Quadrangle
Unit: Port Deposit Gneiss
Sample #: RL-81-28

Stop #82

Location: Near the intersection of Wilkinson Road and Run Road in the bed of Rock Run Stream, Cecil County, Aberdeen Quadrangle
Unit: Port Deposit Gneiss
Sample #: RL-81-29

Stop #83

Location: At intersection of Elbow Creek and Wilkinson Road, 100 meters southeast of washed-out bridge, Harford County, Aberdeen Quadrangle
Unit: Sheared Port Deposit Gneiss
Sample #: RL-81-30

Stop #84

Location: At intersection of Palmyra Drive and Bramble Lane, in intermittent stream bed, Bel Air Quadrangle
Unit: Sheared Port Deposit Gneiss
Sample #: RL-81-31

Stop #87

Location: At intersection of McPhail Road and intermittent stream, 0.5 km northwest of Wheel Road, Bel Air Quadrangle
Unit: Sheared Port Deposit Gneiss
Sample #: RL-81-32

Stop #88

Location: At intersection of McPhail Road and Bynton Run, near the Country Glub Golf Course, Bel Air Quadrangle
Unit: Sheared Port Deposit Gneiss
Sample #: RL-81-33

Stop #89

Location: At intersection of Plumtree Run and Plumtree Road, Bel Air Quadrangle
Unit: Sheared Port Deposit Gneiss
Sample #: RL-81-34

Stop #90

Location: Near intersection of Frenchtown Road and the Conrail Railroad Tracks, northeast bank of the Susquehanna River, in the unnamed stream bed, Havre de Grace Quadrangle
Unit: James Run Formation, Frenchtown Member
Sample #: RL-81-35
RL-81-36
RL-81-37

Stop #91

Location: 200 meters north of Frenchtown along Frenchtown Road, Havre de Grace Quadrangle
Unit: James Run Formation, Frenchtown Member

Stop #92

Location: Near intersection of Frenchtown Road and St. Marks Church Road, in the stream bed on the southwestern side of Frenchtown Road, Havre de Grace Quadrangle
Unit: James Run Formation, Frenchtown Member
Sample #: RL-81-38

Stop #93

Location: 0.5 km along Frenchtown Road northwest of Cokebury Road, in bed of unnamed stream, Cecil County, Havre de Grace Quadrangle
Unit: James Run Formation, Frenchtown Member
Sample #: RL-81-39
RL-81-40

Stop #94

Location: Abandoned Frenchtown Quarry, just northwest of the I-95 bridge over the Susquehanna River, Cecil County, Havre de Grace Quadrangle
Unit: James Run Formation, Gilpins Falls Member
Sample #: RL-81-41

Stop #95

Location: Intersection of Happy Valley Branch and Old Frenchtown Road, Cecil County, Havre de Grace Quadrangle
Unit: James Run Formation, Happy Valley Branch Member
Sample #: RL-81-42

Stop #98

Location: Below the Conrail Railway Bridge over Octoraro Creek, Conowingo Dam Quadrangle, Cecil County
Unit: Wissahickon Formation, Conowingo Diamictite Facies
Sample #: RL-81-48

CROSS INDEX TO SAMPLE NUMBERS

Sample Number	Stop Number
RL-80-1	1
RL-80-2	1
RL-80-3	1
RL-80-4	4
RL-80-5	5
RL-80-6	5
RL-80-6'	6
RL-80-7	7
RL-80-8	10
RL-89-9	11
RL-80-10	12
RL-80-11	13
RL-80-12	14
RL-80-13	15
RL-80-14	16
RL-80-15	16
RL-80-16	16
RL-80-17	16
RL-80-18	16
RL-80-19	17
RL-80-20	20
RL-80-21	21
RL-80-22	22
RL-80-23	23
RL-80-24	25
RL-80-26	21
RL-80-27	27
RL-80-28	27
RL-80-29	29
RL-80-29C	30
RL-80-30	30

Sample Number	Stop Number
RL-80-30	30
RL-80-31	30
RL-80-32	32
RL-80-33	33
RL-80-34	30
RL-80-35	30
RL-80-36	34
RL-80-37	34
RL-80-38	34
RL-80-39	34
RL-80-40	34
RL-80-41	35
RL-80-42	35
RL-80-43	36
RL-80-44	40
RL-80-45	42
RL-80-46	42
RL-80-47	42
RL-80-48	43
RL-80-49	43
RL-80-50	43
RL-80-51	44
RL-80-52	45
RL-80-53	47
RL-80-54	48
RL-80-55	50
RL-80-56	51
RL-80-57	52
RL-80-58	52
RL-80-60	53
RL-80-61	54
RL-80-62	55
RL-80-63	56
RL-80-64	57
RL-80-65	57

Sample Number	Stop Number
RL-80-66	58
RL-80-67	57
RL-80-68	61
RL-80-68'	61
RL-81-4	62
RL-81-5	62
RL-81-6	63
RL-81-7	63
RL-81-8	64
RL-81-9	65
RL-81-10	66
RL-81-11	67
RL-81-12	68
RL-81-13	68
RL-81-14	69
RL-81-15	69
RL-81-16	70
RL-81-17	72
RL-81-18	73
RL-81-19	74
RL-81-20	75
RL-81-21	76
RL-81-22	77
RL-81-23	78
RL-81-24	78
RL-81-25	79
RL-81-26	79
RL-81-27	80
RL-81-28	81
RL-81-29	82
RL-81-30	83
RL-80-31	84
RL-81-32	87

Sample Number	Stop Number
RL-81-33	88
RL-81-34	89
RL-81-35	90
RL-81-36	90
RL-81-37	90
RL-81-38	92
RL-81-39	93
RL-81-40	93
RL-81-41	94
RL-81-42	95
RL-81-43	33
RL-81-44	30
RL-81-45	30
RL-81-45S	30
RL-81-46	30
RL-81-47	30
MJ 8142	32
MJ 8143	33
MJ 8144	35
MJ 8146	35
MJ 8147	35
MJ 8148	35
MJ 8151	35
MJ 8152	35
MJ 8154A	38
MJ 8154B	38
MJ 8155	38
MJ 8156	50
MJ 8157	50
MJ 8158	50
MJ 8165	138
MJ 8168	141
MJ 8169	142
MJ 8170	142

Sample Number	Stop Number
MJ 8171	142
MJ 8172	56
MJ 8173	54
MJ 8174	53
MJ 8175	146
MJ 8176	147

Appendix II

FIELD PHOTOGRAPHS

Plate 4. Port Deposit Gneiss in outcrop, showing gneissic fabrics. Block measures approximately 35 centimeters in length. Loose block, Port Deposit Quarry, Field Stop #32.

Plate 5. Interbedded mafic and felsic rocks of the James Run Formation. Height of cliff is approximately 15 meters. Abandoned Frenchtown Quarry, Field Stop #61.

Appendix III

PHOTOMICROGRAPHS

Plate 6. RL-80-11. Conowingo Diamictite. Detrital quartz grain with undulatory extinction. Field of view 3.0 x 2.0 mm.

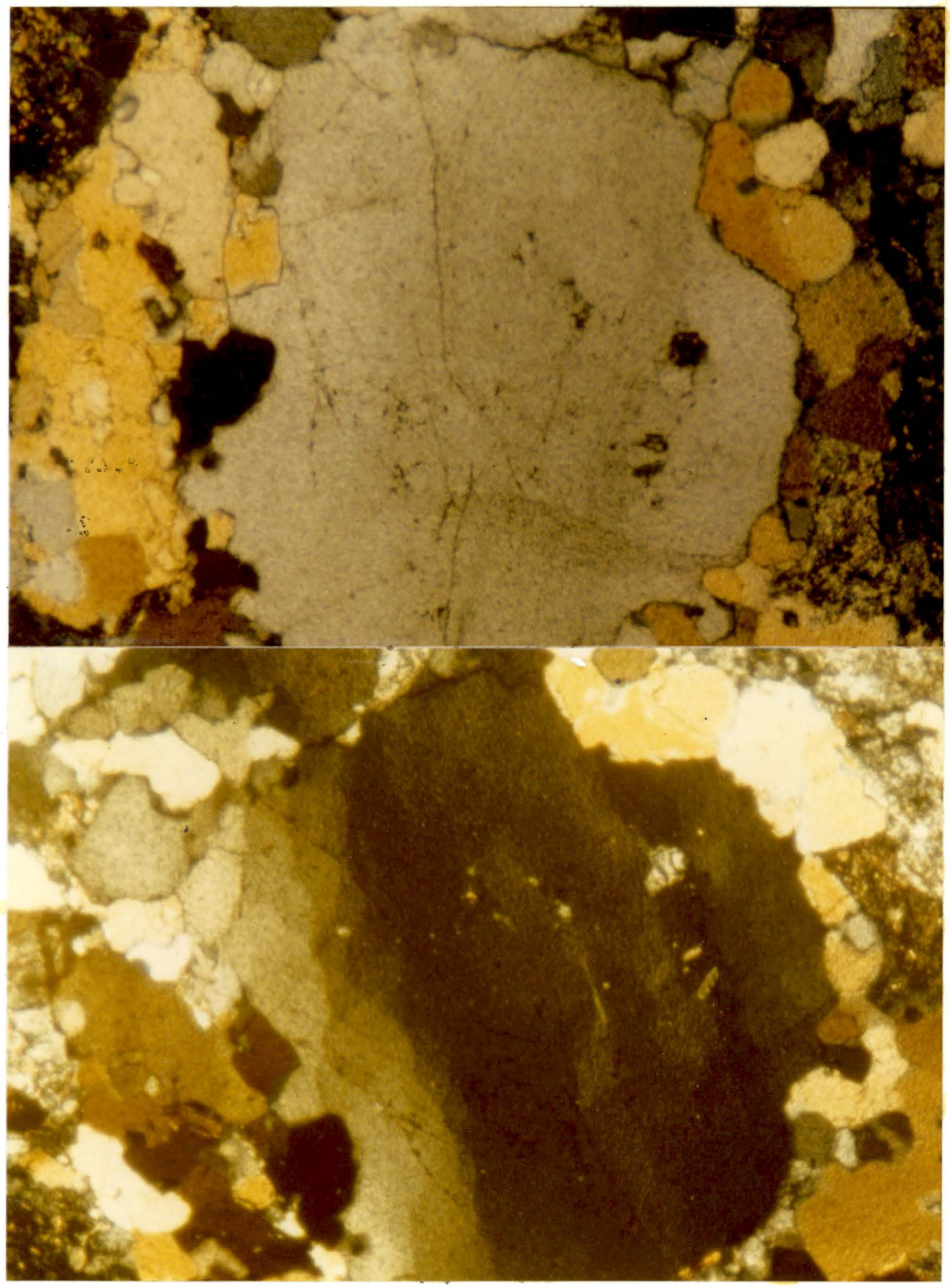

Plate 7. RL-80-29C. Port Deposit Complex/Wissahickon Contact zone. Amphibolite of the Wissahickon Formation in contact with Sheared Port Deposit Gneiss. Field of view 3.0 x 2.0 mm.

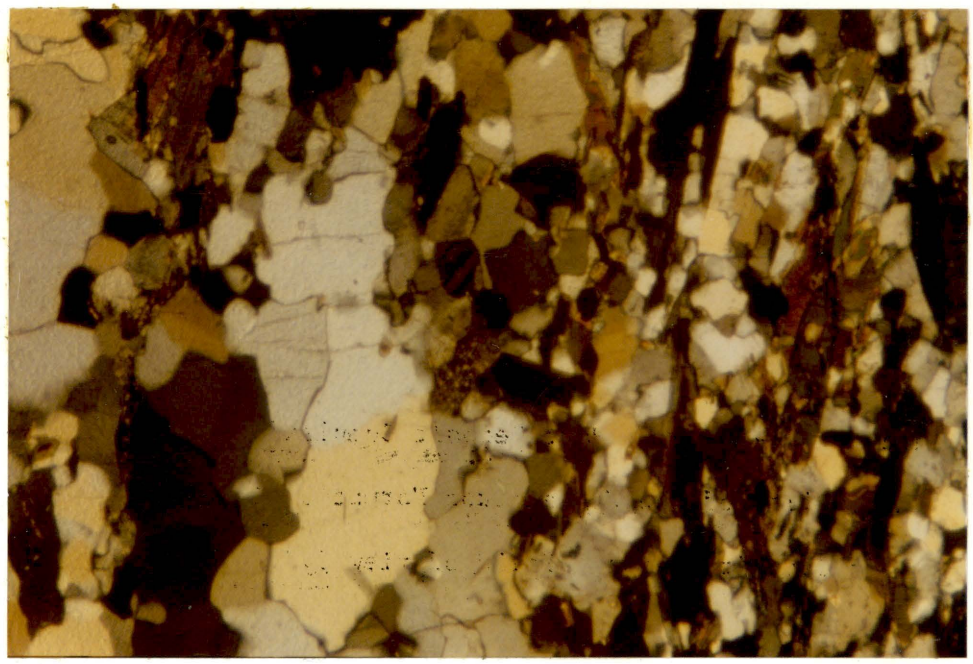

Plate 8. RL-81-45. Sheared Port Deposit Gneiss. Well developed gneissosity, with quartz and feldspar segregated into discrete domains. Field of view 3.0 x 2.0 mm.

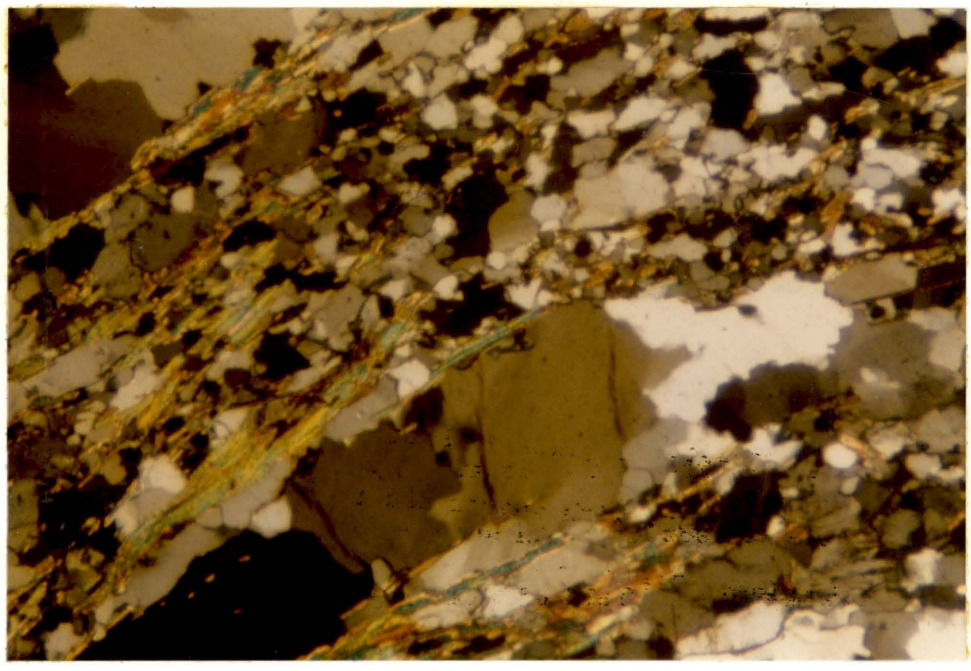

Plate 9. RL-80-30. Sheared Port Deposit Gneiss. Well developed gneissosity and anastomosing fabric. Note two privileged directions for the biotite cleavages. Field of view 3.0 x 2.0 mm.

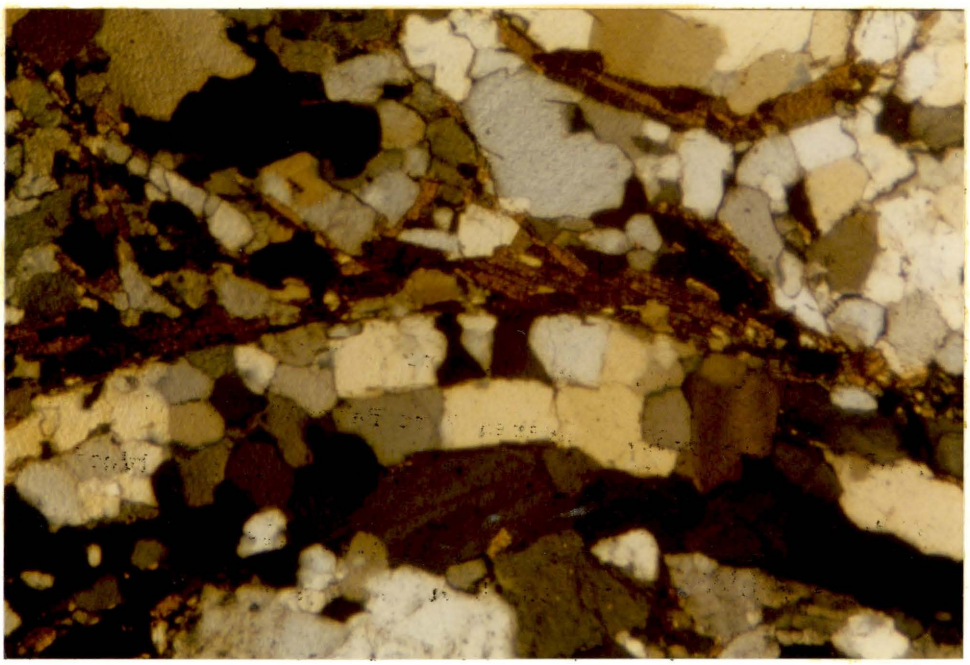

Plate 10. MJ 8143. Port Deposit Gneiss. Symplectitic intergrowths of quartz (extinct) and plagioclase (white interference colors). Field of view 0.5 x 0.3 mm.

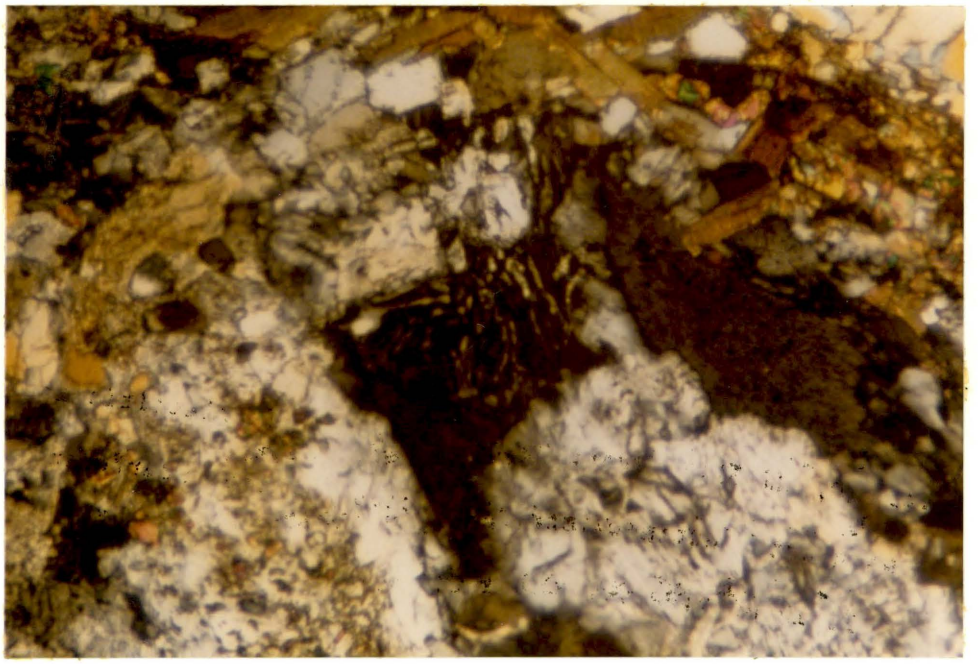

Plate 11. MJ 8146. Port Deposit Gneiss. Quartz (clear) interstitial to plagioclase (cloudy) in a relict plutonic fabric. This section was etched in HF to show the quartz-plagioclase grain relations. Field of view 3.0 x 2.0 mm.

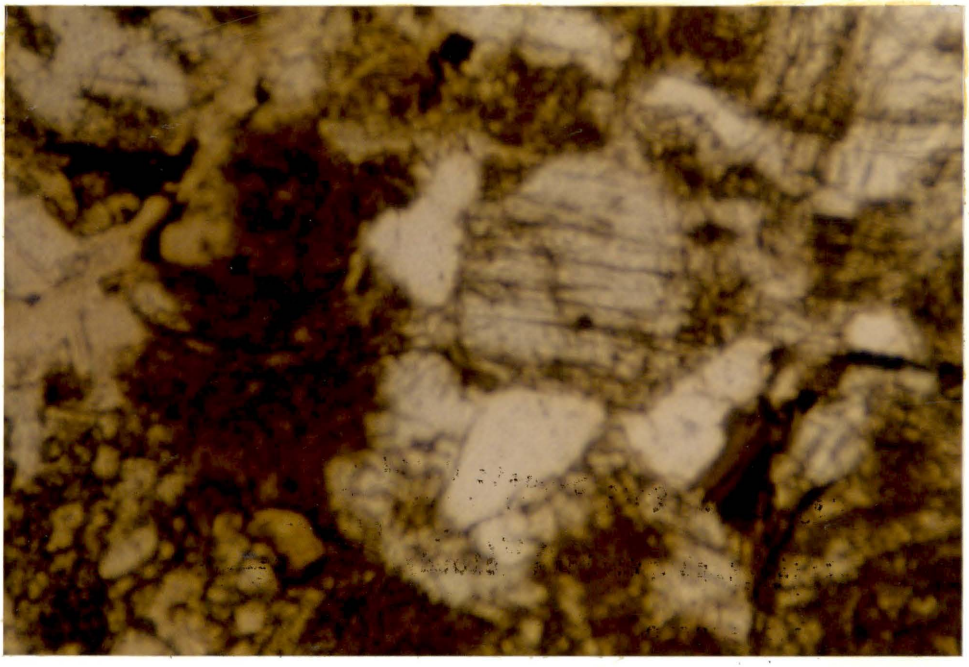

Plate 12. MJ 8175. James Run Formation. Zoned allanite crystal with epidote overgrowths. Biotite and epidote are localized in a pressure shadow of the allanite. Field of view 0.5 x 0.3 mm.

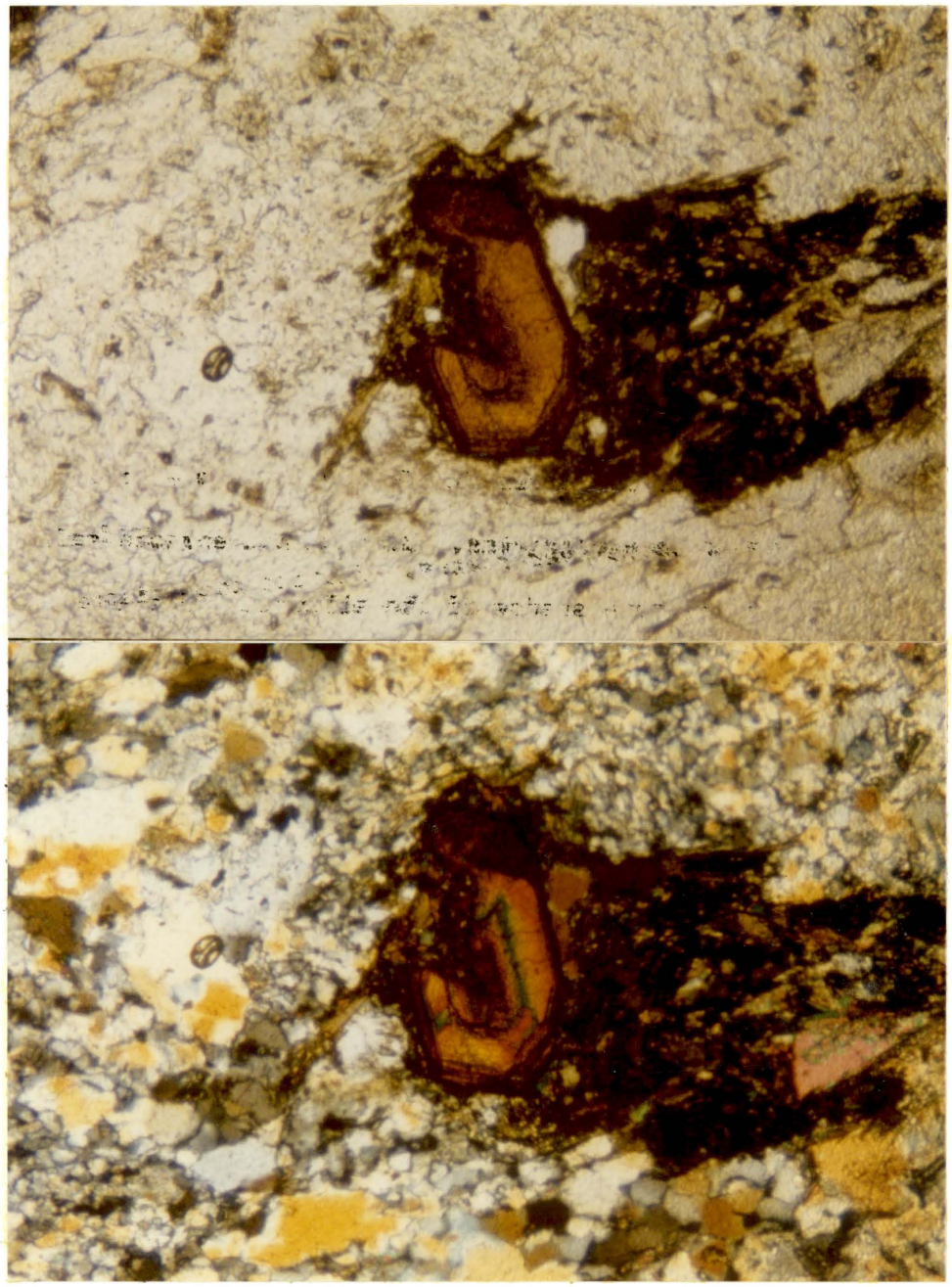

Plate 13. RL-80-60. James Run Formation. Magnetite inclusion (diamond) in plagioclase grain. Transmitted light, plane polarized. Field of view 0.5 x 0.3 mm.

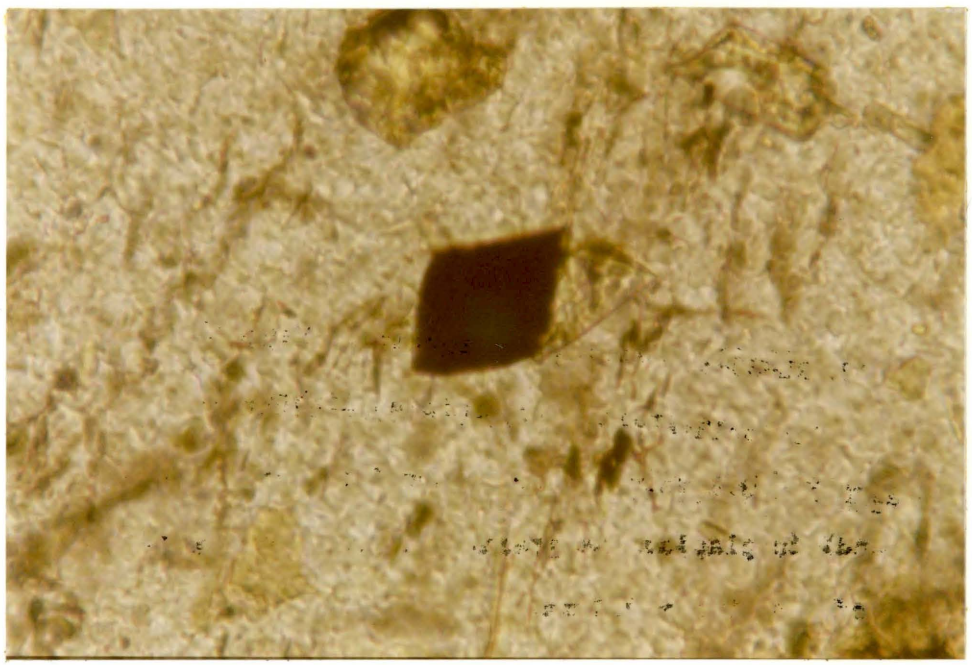

Plate 14. RL-80-66. Relict amygdule of epidote, zoisite, and magnetite in a metabasalt. Field of view 3.0 x 2.0 mm.

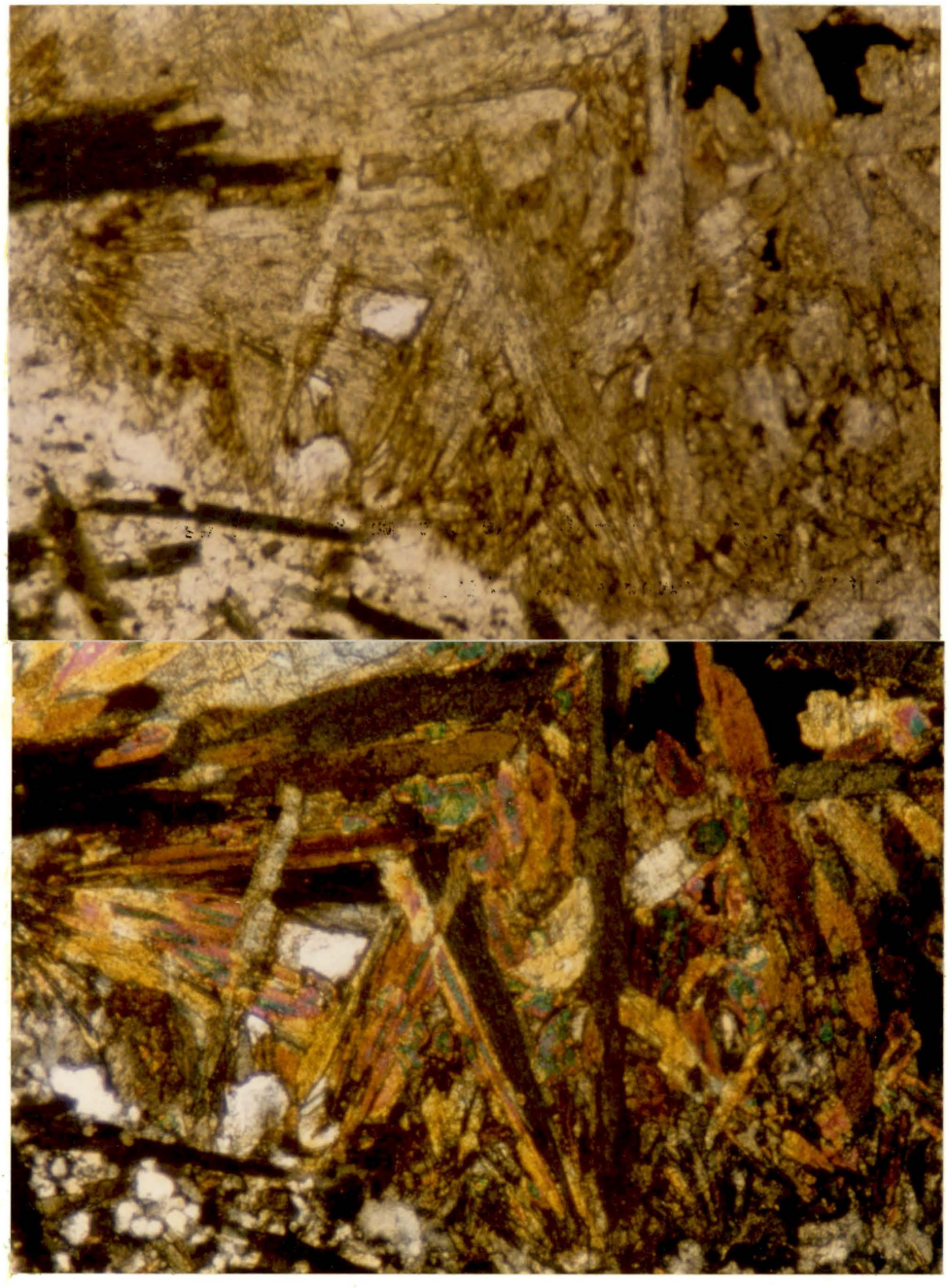

Plate 15. RL-80-67. James Run Formation. Twinned amphibole (grunerite?) in a James Run metabasalt. Field of view 0.5 x 0.3 mm.

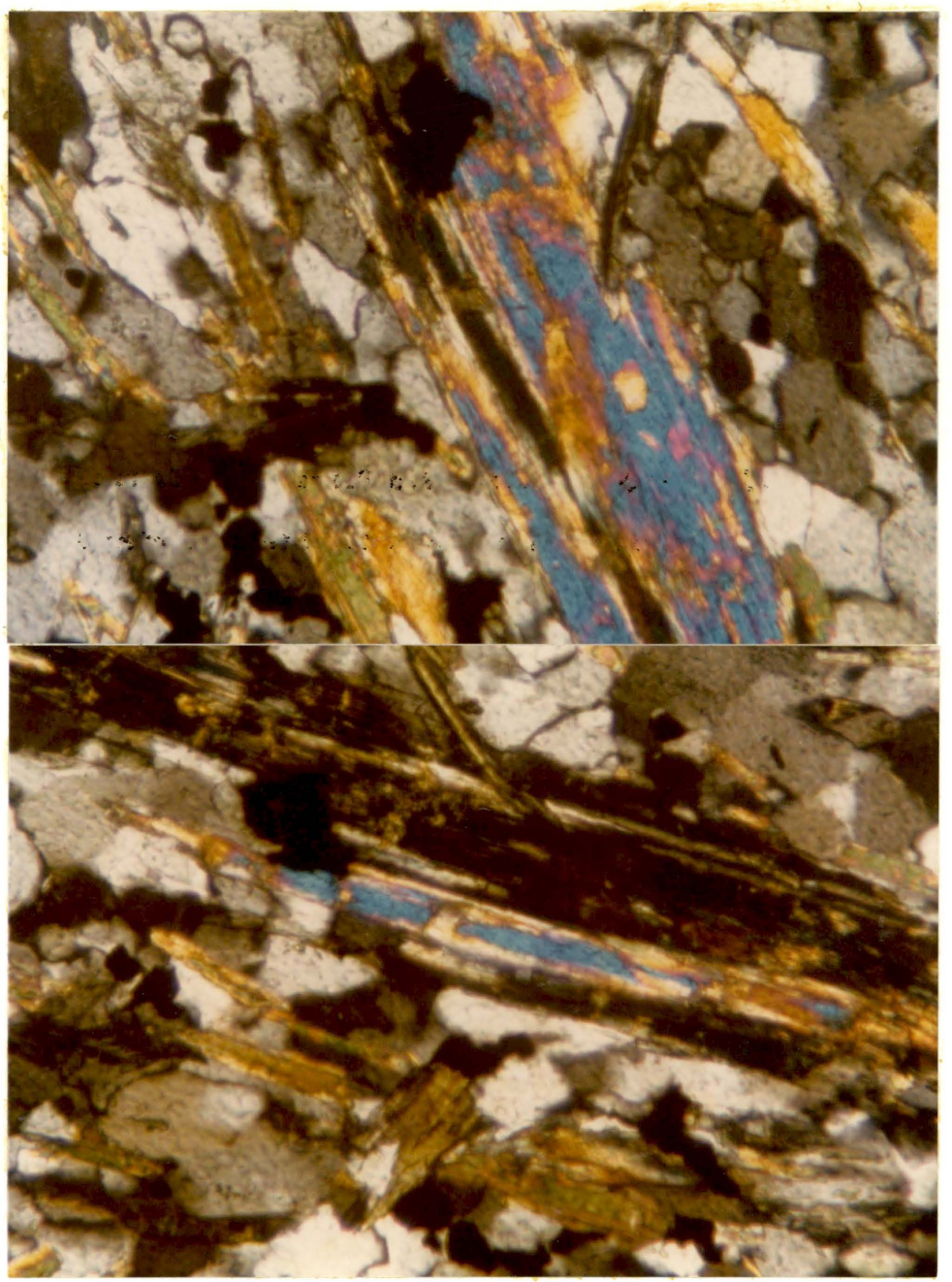

Plate 16. KS-2. Kensington Quartz Diorite of Washington, D. C. Well developed gneissosity. Note similarities to Plates 9 and 10. Field of view 3.0 x 2.0 mm.

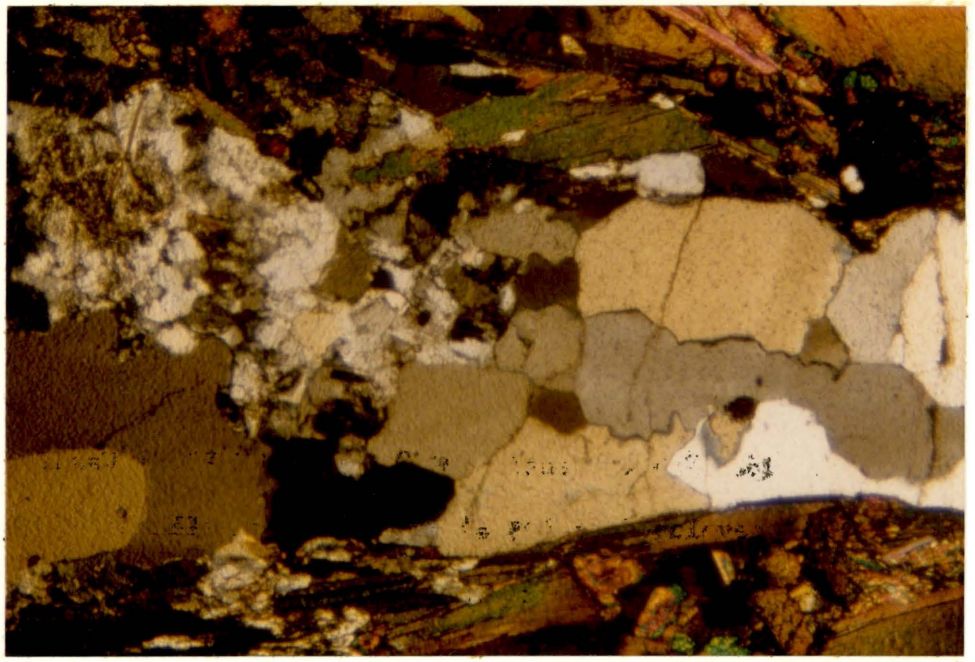

Appendix IV

MODAL DATA

TECHNIQUE

Point counts (1000 points) were performed on stained thin sections 4 x 2 cm^2 in area and on stained slabs 3 x 5 cm^2 in area, depending on the grain size of the specimen. Exceptions to this standard are indicated for the respective analyses. All point count measurements performed for this study are presented below.

Stained slabs, 8 x 5 cm^2

CONOWINGO DIAMICTITE

Sample #	RL-80-3	RL-80-5	RL-80-6	RL-80-6'	RL-80-7	RL-80-8
Phase:						
Plagioclase	39	33	36	29	52	34
Quartz	23	43	37	39	39	31
K-spar	tr	11	13	11	0	14
Mafics	38	14	15	21	9	21
Counts	1000	1000	1000	1000	1000	1000

Stained slabs, 8 x 5 cm^2

CONOWINGO DIAMICTITE

Sample #	RL-80-10	RL-80-11	RL-80-12	RL-80-23	RL-80-26
Phase:					
Plagioclase	37	56	36	44	53
Quartz	38	34	35	47	32
K-spar	8	1	14	tr	2
Mafics	17	9	15	9	13
Counts	1000	1000	1000	1000	1000

Stained slabs, 8 x 5 cm^2

PORT DEPOSIT

Sample #	RL-80-39	RL-80-41	RL-80-48	RL-80-49	RL-80-53	RL-81-44
Phase:						
Plagioclase	42.6	41.4	52.1	19.6	38.1	33.5
Quartz	44.4	35.4	38.5	2.3	40.0	45.8
K-feldspar	1.0	8.8	tr	-	-	1.2
Actinolite	-	-	-	-	-	-
Hornblende	-	-	-	53.6	-	-
Biotite	5.5	10.1	3.7	-	5.1	5.6
Epidote	3.3	1.8	2.3	11.4	2.9	4.7
Piemontite	0.1	tr	tr	-	-	-
Zoisite	-	-	-	8.7	-	-
Zircon	tr	tr	tr	-	tr	tr
Muscovite	2.9	2.5	1.2	2.6	12.8	7.9
Magnetite	tr	tr	1.5	0.8	0.1	0.6
Rutile	-	-	-	-	-	-
Apatite	tr	tr	tr	tr	tr	0.1
Sphene	tr	tr	tr	-	0.1	0.1
Allanite	tr	-	-	-	tr	-
Garnet	0.2	-	tr	-	-	tr
Chlorite	tr	-	0.7	1.0	tr	0.5
Counts	1000	1000	1000	1000	1000	1000

Stained thin sections, 4 x 2 cm^2

PORT DEPOSIT

Sample #	MJ 8146	MJ 8148	MJ 8151	MJ 8154A	MJ 8154B	MJ 8156
Phase:						
Plagioclase	67.6	66.6	52.8	38.1	49.7	23.4
Quartz	15.6	2.3	36.5	51.0	24.5	3.7
K-feldspar	-	0.2	0.1	tr	tr	-
Actinolite	-	-	-	-	-	1.8
Hornblende	-	-	-	-	-	57.9
Biotite	6.0	25.6	4.6	4.2	20.1	0.1
Epidote	7.2	2.6	3.9	3.8	3.8	1.26
Piemontite	-	-	-	tr	-	-
Zoisite	-	-	-	-	-	-
Zircon	tr	tr	-	-	tr	-
Muscovite	2.7	0.9	2.1	0.9	0.2	0.1
Magnetite	0.8	1.7	tr	0.7	1.3	tr
Rutile	-	-	-	-	-	0.1
Apatite	tr	tr	-	tr	tr	-
Sphene	tr	-	-	-	tr	0.3
Allanite	-	-	tr	0.1	tr	-
Garnet	-	-	-	tr	0.2	-
Chlorite	0.1	-	tr	1.2	0.5	-
Counts	1000	1000	1000	1000	1000	1000

Stained slabs, 8 x 5 cm^2

PORT DEPOSIT

Sample #	RL-80-31	RL-80-34	RL-80-36	RL-80-41	RL-80-43	RL-80-47
Phase:						
Plagioclase	59	54	0	54	44	47
Quartz	36	36	100	37	39	39
K-spar	0	0	0	6	8	8
Mafics	5	5	0	4	8	8
Counts	1000	770 ($31\ cm^2$)	1000	1000	1000	1000

Stained slabs, 8 x 5 cm^2

PORT DEPOSIT

Sample #	RL-80-52	RL-80-54A	RL-80-54B	RL-80-55	RL-80-56
Phase:					
Plagioclase	39	46	52	51	39
Quartz	40	41	41	40	45
K-spar	9	7	3	4	12
Mafics	12	7	4	5	4
Counts	1000	398	588	1000	1000
		986 ($39\ cm^2$)			

Stained thin sections, 4 x 2 cm^2

JAMES RUN

Sample #	RL-80-57	RL-80-62	RL-80-63	RL-80-65
Phase:				
Plagioclase	57.8	50.2	42.0	60.0
Quartz	33.6	36.2	36.6	35.2
K-feldspar	-	-	9.9	-
Actinolite	-	-	-	-
Hornblende	-	-	-	-
Biotite	4.0	7.3	4.8	1.5
Epidote	1.1	2.0	2.2	0.6
Piemontite	tr	tr	-	-
Zoisite	-	-	-	-
Zircon	-	-	tr	-
Muscovite	2.9	4.3	4.4	1.0
Magnetite	0.4	tr	tr	0.2
Rutile	-	-	-	-
Apatite	-	tr	-	tr
Sphene	-	-	tr	tr
Allanite	-	tr	0.1	-
Garnet	-	-	-	-
Chlorite	0.2	-	tr	1.5
Counts	1000	1000	1000	1000

Stained slabs, 8 x 5 cm^2

JAMES RUN

Sample #	RL-80-57	RL-80-62
Phase:		
	Phenocrysts:	
Plagioclase	22	49
Quartz	13	27
K-spar	1	6
Mafics	1	18
	Groundmass:	
	63	
Counts	1000	1000

Appendix V

ANALYTICAL TECHNIQUES

AND CHEMICAL AND ISOTOPIC DATA TABLES

ANALYTICAL TECHNIQUES

Samples weighing 2-10 kilograms were crushed, split by the cone and quartering method to one kilogram, powdered in a tungsten carbide mill, and then resplit to 0.25 kilogram for regrinding to an average grainsize of 5.0 microns prior to chemical and isotopic analysis.

Major element determinations were performed with a Phillips Sequential X-Ray Analysis System Model 1450 equipped with a chromium tube. The oxides (SiO_2, TiO_2, Al_2O_3, Fe_2O_3, MnO, MgO, CaO, K_2O, P_2O_5) were measured on fused glass disks 4 cm in diameter. These disks were prepared by fusing 0.9375 grams of dry sample powder with 0.1 grams of dry lithium nitrate and 5.0 grams of Spectroflux 105 in platinum-gold crucibles (Norrish and Hutton, 1969; Harvey et al., 1973; Norrish and Chappell, 1977). Table VIII presents analyses and accepted compositions by Flanagan (1976) for USGS standard powders BCR-1, G-2, and PCC-1. In addition, duplicate processing of selected powders was performed, and results are shown in Table IX to show data reproducibility.

Na_2O determinations were performed with the instrumentation described above on 2.5 cm pressed powder pellets. These pellets were prepared by mixing 0.3 grams of boric acid with three grams of sample. The pellets were supported by a backing of 100% boric acid pressed to 10 tons in a vacuum (Norrish and Chappell, 1977). Table X presents analyses of USGS standard powders BCR-1, G-2, GSP-1, PCC-1, SCO-1, and STM-1 and the accepted compositions of Flanagan (1976).

Table VIII. USGS standards.

	BCR-1		G-2		PCC-1	
	Measured	Flanagan	Measured	Flanagan	Measured	Flanagan
Oxide:						
SiO_2	54.64	54.50	69.44	69.11	41.84	41.90
TiO_2	2.22	2.20	0.48	0.50	0.02	0.02
Al_2O_3	13.56	13.61	15.41	15.40	0.58	0.74
Fe_2O_3	12.24	12.12	2.39	2.42	7.75	7.80
MnO	0.13	0.18	0.08	0.03	0.10	0.12
MgO	3.37	3.46	0.78	0.76	42.38	43.18
CaO	6.91	6.92	1.92	1.94	0.53	0.51
Na_2O*	3.27	3.27	4.13	4.07	0.01	0.01
K_2O	1.71	1.70	4.49	4.51	0.00	0.00
P_2O_5	0.37	0.36	0.13	0.14	0.00	0.00
LOI	0.80	0.80	0.54	0.55	4.68	4.70
Total	99.22	99.12	99.79	99.43	97.89	98.98

*Na_2O values from pressed pellet method.

Flanagan's values compiled by B. Crawford.

Table IX. Replicate Analyses.

Sample #	RL-80-3	RL-80-3/R	RL-80-20	RL-80-20/R	RL-80-40	RL-80-40/R
Oxide:						
SiO_2	62.03	61.49	72.65	73.15	75.84	76.59
TiO_2	1.08	1.07	0.36	0.37	0.23	0.22
Al_2O_3	15.25	14.98	13.87	13.79	12.08	12.11
Fe_2O_3	7.28	7.15	2.92	2.89	2.43	2.46
MnO	0.15	0.18	0.08	0.05	0.06	0.06
MgO	1.86	1.83	0.72	0.84	0.60	0.60
CaO	6.52	6.52	2.09	2.09	1.53	1.51
Na_2O*	2.03	2.03	4.80	4.80	5.45	5.45
K_2O	0.65	0.65	1.50	1.48	0.64	0.62
P_2O_5	0.24	0.25	0.07	0.07	0.06	0.05
LOI	2.58	2.24	1.26	1.03	0.70	0.71
Total	99.67	98.39	100.32	100.56	99.62	99.83

*Na_2O values from pressed pellet method.

Table IX (continued).

Sample #	RL-80-53	RL-80-53/R	RL-80-66	RL-80-66/R	MJ 8163	MJ 8163/R
Oxide:						
SiO_2	74.14	74.12	67.45	67.57	50.45	49.17
TiO_2	0.22	0.22	0.72	0.74	0.91	0.88
Al_2O_3	13.37	13.48	14.67	14.59	15.68	15.24
Fe_2O_3	2.48	2.49	5.26	5.20	10.17	10.88
MnO	0.06	0.05	0.09	0.09	0.21	0.20
MgO	0.48	0.66	1.79	1.77	7.69	7.66
CaO	2.01	2.01	3.54	3.55	10.74	10.33
Na_2O*	4.40	4.40	5.38	5.38	2.71	2.71
K_2O	1.38	1.38	0.20	0.18	0.20	0.21
P_2O_5	0.04	0.05	0.14	0.15	0.04	0.07
LOI	1.58	1.12	0.69	0.43	1.43	1.72
Total	100.17	99.93	99.93	99.65	100.55	99.07

*Na_2O values from pressed pellet method.

Table IX (continued).

Sample #	RL-81-25	RL-81-25/R	RL-81-43	RL-81-43/R
Oxide:				
SiO_2	73.00	73.65	74.83	74.55
TiO_2	0.23	0.23	0.21	0.22
Al_2O_3	13.54	14.15	13.27	13.31
Fe_2O_3	2.60	2.61	2.40	2.44
MnO	0.09	0.08	0.08	0.08
MgO	0.36	0.33	0.33	0.40
CaO	2.74	2.76	2.69	2.69
Na_2O*	4.09	4.09	4.24	4.24
K_2O	2.01	2.00	1.98	2.03
P_2O_5	0.08	0.08	0.05	0.05
LOI	0.80	1.19	0.52	0.55
Total	99.52	101.17	100.27	100.56

*Na_2O values from pressed pellet method.

Table X. Na_2O determinations.

Standard	Measured	Flanagan
BCR-1	3.270	3.270
G-2	4.128	4.070
GSP	2.887	2.800
PCC-1	0.006	0.006
SCO-1	0.591	0.780
STM-1	8.866	8.920

Table XI presents all major and minor element data acquired with the fused disk and pressed pellet methods for samples analyzed in this study.

Rb and Sr analyses were performed on the Phillips instrument using a molybdenum tube. Table XII presents analyses for USGS standard powders G-2, AGV-1, BCR-1, and GSP-1 and the accepted values of Flanagan (1976).

For isotopic analyses, all reagents were distilled in teflon evaporation stills (Mattinson, 1972). Approximately 200 mg of sample were dissolved in HNO_3 and doubly distilled HF. Mineral separates, slabbed specimens, and selected rock powders were spiked with mixed Rb-Sr spike solutions. After dissolution and evaporation, the residue was redissolved in 2 ml of 2.5 N teflon distilled HCl. Rb and Sr were separated using Dowex 50 cation exchange resin packed in a 19 cm, 3 ml volume chromatography column. After evaporation of the elutant, Sr was dissolved in ultra-pure phosphoric acid and loaded onto rhenium filaments with a tantalum oxide matrix. Rb was dissolved in ultra-pure HCl and loaded in the same manner. The analyses were performed on a 35 cm solid source mass spectrometer in a single filament configuration. Data acquisition and processing was performed by an LSI/1 minicomputer using VPI & SU (MASCOS) program routines. Eight Sr blanks averaged 465 picograms and two Rb blanks averaged 75 picograms during the course of data collection. Rb and Sr concentrations determined with the isotope dilution method and replicate values determined by the XRF pressed powder pellet method are shown in Table XIII to demonstrate data replication and accuracy.

Table XI. Comprehensive major element data

Major Element Data

CONOWINGO DIAMICTITE

Sample #	RL-80-3	RL-80-5	RL-80-6	RL-80-11	RL-80-20
Oxide:					
SiO_2	62.03	71.27	71.64	72.11	72.65
TiO_2	1.08	0.40	0.40	0.38	0.36
Al_2O_3	15.25	13.61	13.67	13.59	13.87
Fe_2O_3	7.28	3.38	3.22	3.08	2.92
MnO	0.15	0.05	0.06	0.08	0.08
MgO	1.86	0.82	0.79	0.88	0.72
CaO	6.52	3.04	2.95	2.22	2.09
Na_2O	2.03	3.70	3.25	4.53	4.80
K_2O	0.65	1.92	2.70	1.43	1.50
P_2O_5	0.24	0.08	0.09	0.07	0.07
LOI	2.58	1.26	1.32	0.83	1.26
Total	99.67	99.54	100.10	99.18	100.32
Normative Minerals:					
Q	32.66	35.50	35.60	34.99	33.96
C	0.00	0.11	0.26	0.73	0.72
Or	3.96	11.55	16.15	8.59	8.95
Ab	17.69	31.86	27.84	38.97	41.00
An	31.50	14.82	14.22	10.73	10.01
Wo	0.00	0.00	0.00	0.00	0.00
En	4.77	2.08	1.99	2.23	1.81
Hm	7.50	3.44	3.26	3.13	2.95
Il	0.33	0.11	0.13	0.17	0.17
Tn	0.14	0.00	0.00	0.00	0.00
Ru	0.88	0.35	0.34	0.30	0.27
Ap	0.59	0.19	0.22	0.17	0.17
Total	100.02	100.01	100.01	100.01	100.00
Trace Elements:					
Rb, ppm	23	74	96	50	45
Sr, ppm	205	131	120	185	126

Major Element Data

SHEARED PORT DEPOSIT

Sample #	RL-81-27	RL-81-44	RL-81-45S	RL-81-46	RL-81-47
Oxide:					
SiO_2	75.31	72.48	73.48	80.41	76.91
TiO_2	0.19	0.28	0.24	0.45	0.22
Al_2O_3	12.89	13.81	13.00	8.64	12.65
Fe_2O_3	1.90	3.08	2.66	2.73	1.84
MnO	0.07	0.10	0.08	0.09	0.08
MgO	0.17	0.66	0.79	0.91	0.57
CaO	1.46	2.72	0.52	1.21	2.09
Na_2O	7.00	4.52	2.80	3.57	3.69
K_2O	0.33	1.34	3.00	0.99	0.66
P_2O_5	0.03	0.08	0.04	0.10	0.03
LOI	2.03	0.68	1.40	0.66	0.49
Total	101.38	99.82	98.02	99.75	99.23
Normative Minerals:					
Q	31.16	34.80	45.06	52.82	48.29
C	0.00	0.17	4.45	0.00	2.16
Or	1.96	7.99	18.35	5.90	3.96
Ab	59.62	38.61	24.52	30.48	31.62
An	2.79	13.09	2.40	4.67	10.30
Wo	1.63	0.00	0.00	0.00	0.00
En	0.43	1.66	2.04	2.29	1.44
Hm	1.91	3.11	2.75	2.76	1.86
Il	0.15	0.22	0.18	0.19	0.17
Tn	0.28	0.00	0.00	0.51	0.00
Ru	0.00	0.17	0.16	0.14	0.13
Ap	0.07	0.19	0.10	0.24	0.07
Total	100.00	100.01	100.01	100.00	100.00
Trace Elements:					
Rb, ppm	7	54	77	38.5	107
Sr, ppm	131	79	42	63	30

Major Element Data

PORT DEPOSIT

Sample #	RL-80-33	RL-80-37	RL-80-39	RL-80-40	RL-80-41	RL-80-46	RL-80-48
Oxide:							
SiO_2	74.81	76.40	74.82	75.84	74.12	75.81	73.33
TiO_2	0.23	0.20	0.22	0.23	0.25	0.23	0.25
Al_2O_3	13.28	11.51	13.06	12.08	13.24	12.44	14.18
Fe_2O_3	2.41	2.26	2.48	2.43	2.64	1.75	2.36
MnO	0.08	0.05	0.05	0.06	0.08	0.01	0.03
MgO	0.32	0.68	0.19	0.60	0.68	0.90	0.44
CaO	2.05	0.83	2.34	1.53	1.97	1.46	3.14
Na_2O	4.80	5.18	3.90	5.45	4.10	5.23	4.63
K_2O	1.26	0.96	1.84	0.64	1.99	0.86	0.40
P_2O_5	0.05	0.03	0.04	0.06	0.04	0.03	0.00
LOI	0.86	0.90	0.94	0.70	0.70	0.67	0.84
Total	100.16	98.99	99.89	99.62	99.62	99.40	99.60
			C.I.P.W. Norms				
Q	37.61	40.75	40.34	38.23	37.87	38.20	38.03
C	0.42	0.46	0.50	0.00	0.86	0.33	0.31
Or	7.50	5.71	10.99	3.82	11.37	5.15	2.39
Ab	40.91	44.60	33.35	46.62	35.01	44.83	39.56
An	9.91	4.06	11.47	6.68	9.60	7.14	15.73
Wo	0.00	0.00	0.00	0.01	0.00	0.00	0.00
En	0.80	1.80	0.48	1.51	1.71	2.27	1.31
Hm	2.43	2.30	2.51	2.46	2.66	1.77	2.36
Il	0.17	0.13	0.11	0.13	0.17	0.02	0.11
Tn	0.00	0.00	0.00	0.40	0.00	0.00	0.00
Ru	0.14	0.15	0.17	0.00	0.16	0.22	0.20
Ap	0.12	0.05	0.10	0.14	0.10	0.07	0.00
			Trace Element Data				
Rb, ppm	46	35	65	20	76	27	14
Sr, ppm	111	49	100	138	82	82	154

Major Element Data

PORT DEPOSIT

Sample #	RL-80-49	RL-80-53	RL-81-12	RL-81-17	RL-81-18	RL-81-19	RL-81-21
Oxide:							
SiO_2	53.91	74.14	54.01	72.85	73.63	55.23	73.66
TiO_2	0.79	0.22	0.96	0.24	0.22	1.51	0.24
Al_2O_3	14.84	13.37	15.42	13.58	13.15	14.73	13.68
Fe_2O_3	11.46	2.48	11.69	2.74	2.53	11.89	2.56
MnO	0.20	0.06	0.13	0.09	0.09	0.17	0.09
MgO	4.76	0.48	3.99	0.35	0.33	2.98	0.42
CaO	10.63	2.01	8.15	2.56	2.59	8.86	2.91
Na_2O	0.15	4.40	2.27	4.10	4.18	2.11	4.37
K_2O	0.19	1.38	1.11	1.97	1.98	0.12	1.41
P_2O_5	0.05	0.04	0.14	0.08	0.05	0.46	0.05
LOI	1.95	1.58	0.69	0.89	0.66	0.94	0.58
Total	98.91	100.07	98.56	99.45	99.41	98.99	99.97
			C.I.P.W. Norms				
Q	26.47	38.91	16.24	36.20	36.57	23.10	36.47
C	0.00	1.10	0.00	0.24	0.00	0.00	0.00
Or	1.16	8.27	6.70	11.81	11.85	0.72	8.38
Ab	0.87	37.77	19.63	35.20	35.82	18.21	37.21
An	40.73	9.85	29.23	12.36	11.41	30.97	13.63
Wo	4.72	0.00	3.45	0.00	0.36	2.55	0.03
En	12.23	1.21	10.15	0.88	0.83	7.57	1.05
Hm	11.82	2.52	11.94	2.78	2.56	12.13	2.58
Il	0.44	0.13	0.28	0.20	0.20	0.37	0.19
Tn	1.43	0.00	2.04	0.00	0.30	3.30	0.34
Ru	0.00	0.00	0.00	0.14	0.00	0.00	0.00
Ap	0.12	0.10	0.34	0.19	0.12	1.11	0.12
			Trace Element Data				
Rb, ppm	2	54	45	72	73	1	48
Sr, ppm	240	111	113	103	101	173	122

Major Element Data

PORT DEPOSIT

Sample #	RL-81-24	RL-81-25	RL-81-26	RL-81-28	RL-81-29	RL-81-43	MJ 8142
Oxide:							
SiO_2	53.11	73.00	55.49	73.69	74.50	74.38	73.22
TiO_2	1.01	0.23	1.30	0.23	0.22	0.21	0.24
Al_2O_3	15.10	13.54	14.72	13.17	13.12	13.27	13.20
Fe_2O_3	12.33	2.60	11.37	2.47	2.37	2.40	2.78
MnO	0.15	0.09	0.14	0.09	0.09	0.08	0.07
MgO	3.39	0.36	3.77	0.03	0.29	0.33	0.80
CaO	9.90	2.74	7.82	2.49	2.63	2.69	1.43
Na_2O	2.18	4.09	3.07	4.06	4.32	4.24	4.21
K_2O	0.22	2.01	0.41	2.01	1.46	1.98	2.17
P_2O_5	0.23	0.08	0.30	0.04	0.05	0.05	0.04
LOI	1.21	0.80	0.84	0.79	0.64	0.52	1.05
Total	98.82	99.55	99.22	99.06	99.68	100.27	99.22
			C.I.P.W. Norms				
Q	18.04	35.88	17.33	39.62	39.67	36.53	36.96
C	0.00	0.00	0.00	1.70	1.19	0.00	1.45
Or	1.33	12.03	2.46	11.99	8.66	11.74	13.06
Ab	18.90	35.05	16.40	34.69	36.69	36.01	36.29
An	31.52	12.81	25.59	7.26	8.90	11.37	6.96
Wo	5.95	0.00	3.26	0.00	0.00	0.53	0.00
En	8.65	0.91	9.54	0.08	0.73	0.83	2.03
Hm	12.63	2.63	11.56	2.49	2.38	2.41	2.83
Il	0.33	0.20	0.30	0.19	0.19	0.17	0.15
Tn	2.11	0.30	2.85	0.00	0.00	0.30	0.00
Ru	0.00	0.01	0.00	0.13	0.12	0.00	0.16
Ap	0.56	0.19	0.72	1.89	1.52	0.12	0.10
			Trace Element Data				
Rb, ppm	1	72	9	70	97	72	75
Sr, ppm	176	101	112	97	104	103	69

Major Element Data

PORT DEPOSIT

Sample #	MJ 8143	MJ 8144	MJ 8146	MJ 8148	MJ 8151	MJ 8152	MJ 8154A
Oxide:	73.68	74.77	70.17	57.48	73.40	73.75	76.47
TiO_2	0.22	0.24	0.28	0.32	0.24	0.23	0.22
Al_2O_3	13.38	13.42	15.21	19.55	13.33	13.20	12.11
Fe_2O_3	2.57	2.57	3.32	6.04	2.74	2.55	2.41
MnO	0.08	0.08	0.09	0.14	0.08	0.06	0.07
MgO	0.46	0.36	0.43	2.56	0.55	0.32	0.52
CaO	2.69	2.77	3.19	2.10	2.85	2.75	1.50
Na_2O	3.83	3.73	4.65	5.64	3.65	4.03	5.40
K_2O	2.05	2.02	1.27	2.56	1.94	1.59	0.58
P_2O_5	0.05	0.04	0.03	0.07	0.05	0.05	0.04
LOI	0.71	0.84	1.19	1.64	0.77	0.90	1.00
Total	98.21	100.84	99.84	98.11	99.60	99.41	100.34
			C.I.P.W. Norms				
Q	37.61	38.98	31.30	6.95	38.41	38.58	39.12
C	0.09	0.16	0.46	3.97	0.17	0.00	0.00
Or	12.24	11.94	7.61	15.68	11.60	9.54	3.51
Ab	32.74	31.56	39.89	49.56	31.25	34.61	45.94
An	13.15	13.48	15.85	10.33	13.98	13.43	7.07
Wo	0.00	0.00	0.00	0.00	0.00	0.00	0.00
En	1.16	0.90	1.09	6.61	1.39	0.81	1.55
Hm	2.60	2.57	3.37	6.27	2.77	2.59	2.40
Il	0.17	0.17	0.20	0.31	0.17	0.13	0.11
Tn	0.00	0.00	0.00	0.00	0.00	0.06	0.10
Ru	0.13	0.15	0.18	0.17	0.15	0.14	0.12
Ap	0.12	0.10	0.07	0.17	0.12	0.12	0.10
			Trace Element Data				
Rb, ppm	76	71	59	111	73	56	18
Sr, ppm	101	103	124	66	102	109	136

Major Element Data

PORT DEPOSIT

Sample #	MJ 8154B	MJ 8156	MJ 8157	MJ 8158
Oxide:				
SiO_2	66.29	51.75	75.74	51.41
TiO_2	0.54	0.32	0.25	0.32
Al_2O_3	14.53	15.97	13.28	15.86
Fe_2O_3	5.75	8.79	2.07	8.74
MnO	0.15	0.07	0.04	0.16
MgO	1.62	6.63	0.33	6.79
CaO	2.47	10.95	2.29	10.64
Na_2O	4.28	1.78	5.15	1.21
K_2O	1.69	0.29	0.55	0.33
P_2O_5	0.40	0.00	0.03	0.00
LOI	1.01	2.20	1.07	2.09
Total	98.74	98.84	100.80	98.09
		C.I.P.W. Norms		
Q	29.01	11.56	38.53	11.47
C	2.18	0.00	0.14	0.00
Or	10.22	1.77	3.26	2.03
Ab	37.06	15.58	43.62	15.43
An	9.87	35.93	11.20	35.88
Wo	0.00	8.27	0.00	7.77
En	4.13	17.08	0.82	17.62
Hm	5.88	9.10	2.08	9.10
Il	0.33	0.38	0.09	0.36
Tn	0.00	0.33	0.00	0.36
Ru	0.38	0.00	0.21	0.00
Ap	0.97	0.00	0.07	0.00
		Trace Element Data		
Rb, ppm	54	2	18	4
Sr, ppm	147	119	94	109

Major Element Data

JAMES RUN

Sample #	RL-80-57	RL-80-62	RL-80-63	RL-80-65	RL-80-66	RL-80-68	RL-80-68'
Oxide:							
SiO_2	74.04	73.88	75.68	78.77	67.45	53.46	53.60
TiO_2	0.22	0.24	0.24	0.14	0.72	0.69	1.01
Al_2O_3	13.27	12.48	12.42	11.98	14.67	15.51	16.64
Fe_2O_3	2.45	2.21	2.15	1.43	5.26	10.82	9.80
MnO	0.04	0.04	0.07	0.04	0.09	0.23	0.14
MgO	0.59	0.33	0.42	0.23	1.79	5.20	4.20
CaO	2.01	1.30	1.38	0.78	3.54	6.74	6.18
Na_2O	7.12	5.60	4.88	6.89	5.38	4.66	5.44
K_2O	1.38	1.29	2.14	0.32	0.20	0.18	0.28
P_2O_5	0.04	0.06	0.03	0.02	0.14	0.07	0.18
LOI	0.63	0.99	0.81	0.71	0.69	0.68	0.96
Total	101.80	98.41	100.22	101.31	99.93	98.24	98.44
			C.I.P.W. Norms				
Q	52.88	34.35	36.03	36.39	26.02	6.44	4.01
C	4.78	0.00	0.00	0.00	0.00	0.00	0.00
Or	8.47	7.82	12.72	1.88	1.19	1.09	1.70
Ab	19.34	48.64	41.54	57.25	45.87	40.42	47.23
An	10.09	5.24	5.70	1.21	15.41	21.39	20.68
Wo	0.00	0.12	0.18	0.91	0.00	4.54	2.72
En	1.52	0.34	1.05	0.57	4.49	13.28	10.73
Hm	2.55	2.27	2.16	1.42	5.30	11.09	10.05
Il	0.09	0.09	0.15	0.09	0.19	0.50	0.31
Tn	0.00	0.49	0.40	0.23	0.97	1.08	2.15
Ru	0.18	0.00	0.00	0.00	0.23	0.00	0.00
Ap	0.10	0.07	0.07	0.05	0.33	0.17	0.44
			Trace Element Data				
Rb, ppm	6	44	51	8	2	1	6
Sr, ppm	53	70	63	48	176	138	187

Major Element Data

JAMES RUN

Sample #	RL-81-44	RL-81-15	RL-81-16 (Aberdeen)	MJ 8165	MJ 8168	MJ 8171	MJ 8176
Oxide:							
SiO_2	54.14	63.26	47.60	59.76	75.62	76.14	76.86
TiO_2	0.73	1.25	0.28	1.52	0.24	0.25	0.23
Al_2O_3	15.60	14.93	16.17	14.01	12.40	12.50	12.17
Fe_2O_3	11.93	8.66	9.43	9.29	2.30	2.15	1.95
MnO	0.14	0.11	0.14	0.18	0.04	0.09	0.08
MgO	3.95	1.79	8.74	3.34	0.50	0.29	0.90
CaO	6.30	3.45	13.41	3.03	1.31	1.22	1.25
Na_2O	4.26	4.69	0.64	3.84	5.88	5.63	4.49
K_2O	0.15	0.13	0.01	1.69	0.96	0.12	0.86
P_2O_5	0.10	0.37	0.06	0.24	0.05	0.05	0.03
LOI	0.67	0.92	1.18	2.12	1.10	0.85	0.86
Total	97.99	99.56	97.67	99.03	100.39	99.27	99.69
			C.I.P.W. Norms				
Q	11.64	11.64	7.91	20.81	34.92	40.66	44.04
C	0.00	0.00	0.00	0.96	9.99	1.03	1.68
Or	0.91	0.91	0.06	10.31	5.71	0.72	5.14
Ab	37.05	37.05	5.61	33.53	50.11	48.39	38.45
An	23.67	23.64	42.72	13.90	4.64	5.82	6.08
Wo	2.41	2.41	10.60	0.00	0.37	0.00	0.00
En	10.11	10.11	22.56	8.58	1.25	0.73	2.27
Hm	12.26	12.26	9.77	9.58	2.32	2.18	1.97
Il	0.31	0.31	0.31	0.40	0.09	0.20	0.17
Tn	1.44	1.44	0.31	0.00	0.48	0.00	0.00
Ru	0.00	0.00	0.00	1.36	0.00	0.15	0.14
Ap	0.24	0.24	0.15	0.59	0.12	0.12	0.07
			Trace Element Data				
Rb, ppm	1	1	0	38	28	3	22
Sr, ppm	146	144	87	63	44	80	88

Table XII. USGS standards.

	G-2		AGV		BCR-1		GSP	
	Measured	Flanagan	Measured	Flanagan	Measured	Flanagan	Measured	Flanagan
Rb, ppm	175	168	67	67	46	47	254	254
Sr, ppm	485	479	657	657	325	330	233	233

Table XIII. XRF vs ID Rb-Sr concentrations

	Rb		Sr		$^{87}Sr/^{86}Sr$	
	XRF	ID	XRF	ID		
RL-80-33	46	43	111	111	0.71790^{10}	0.71790^{10}
RL-80-40	20		138	135	0.71225^{10}	0.71217^{8}
RL-80-41	76	75	82	81	0.72728^{8}	0.72713^{8}
RL-80-41R				80		
RL-80-53	54	47	111	107	0.71865^{8}	0.71849^{8}
RL-80-62	44	42	70	68	0.71860^{8}	0.71856^{22}
RL-81-21	48	42	122	120	-	-
MJ 8152	56	53	109	109	0.71978^{8}	0.71971^{8}
MJ 8152R		53		106		

Instrumentation modification to the mass spectrometer during Sr-data collection caused a change in the measured values of the Eimer and Amend $SrCO_3$ standard. Prior to modification, the measured values averaged 0.70831 $\pm$ 3 (n = 19). Subsequent to modification, the measured values averaged 0.70861 $\pm$ 3 (n = 21). All standard errors of the mean were calculated by the relation:

Standard Deviation: $$\frac{\sqrt{\Sigma(X_i - \bar{X})^2}}{\sqrt{N - 1}}$$

Standard Error: $$\frac{S_D}{\sqrt{N}}$$

and are quoted at the two sigma confidence level.

The decay constant of ^{87}Rb was taken as $\lambda = 1.42 \times 10^{-11}\ yr^{-1}$ (Steiger and Jager, 1977). Regressions were calculated according to the method of York (1966) as presented by Faure (1977); ages and MSRS values are drawn from regression Model II, and all errors are quoted at the two sigma confidence level. Analytical uncertainties used in the calculation are:

$$^{87}Sr/^{86}Sr = 0.05\%$$
$$^{87}Rb/^{86}Sr = 2.00\%$$

Tables XIV through XVIII are the printouts of the York regression. Calculated correlation coefficients for each data point are included. Regressions were performed for the lithologic units:

Table XIV	Conowingo Diamictite	n = 5
Table XV	Sheared Port Deposit Gneiss	n = 6

Table XVI	Port Deposit Gneiss	n = 18
Table XVII	Port Deposit Gneiss	n = 8
Table XVIII	James Run Formation	n = 9

T A B L E X I V

CONOWINGO DIAMICTITE

YORK LEAST SQUARES REGRESSION - MODEL I

NUMBER OF SAMPLES= 5
ESTIMATED SLOPE= 0.00481
EXPERIMENTAL ERROR IN X = 0.02000
EXPERIMENTAL ERROR IN Y = 0.00050

SLOPE B= 0.006733175 INTERCEPT A= 0.710645318
SE OF B= 0.000537842 SE OF A= 0.000681955
MEAN X = 1.08699512 MEAN Y = 0.717964292

X	PERCENTAGE RESIDUAL X	Y	PERCENTAGE RESIDUAL Y	CORRL COEFF	
0.3250	0.4989	0.713570	-0.1017	0.0	RL-80-3
1.6370	1.1888	0.722150	-0.0487	0.0	RL-80-5
2.3190	0.4913	0.726440	-0.0143	0.0	RL-80-6
0.7830	-1.0428	0.715230	0.0884	0.0	RL-80-11
1.0340	-1.1813	0.716980	0.0760	0.0	RL-80-20

AGE= 472.6 +/- 37.8 M.Y.
INITIAL RATIO= 0.71065 +/- 0.00068

(RB87 DECAY CONSTANT USED 1.4200)
(AGE AND INITIAL RATIO ESTIMATES GIVEN AT ONE SIGMA CONFIDENCE LEVEL)

T A B L E X I V , C o n t i n u e d

C o n o w i n g o D i a m i c t i t e

YORK LEAST SQUARES REGRESSION TREATMENT - MODEL II

NUMBER OF SAMPLES= 5
ESTIMATED SLOPE= 0.00673
EXPERIMENTAL ERROR IN X = 0.02000
EXPERIMENTAL ERROR IN Y = 0.00050

ITER= 1
MINIMIZED WEIGHTED SUM OF RESIDUALS SQUARED (SUMS)= 11.7007322
MEAN SUM OF RESIDUALS SQUARED (SUMS/(N-2))= 3.9002438
SQUARE ROOT OF (SUMS/N-2))= 1.9749031

SLOPE B= 0.006733168 INTERCEPT A= 0.710645199
SE OF B= 0.000264907 SE OF A= 0.000338626
MEAN X = 1.08699512 MEAN Y = 0.717964172

X	PERCENTAGE RESIDUAL X	Y	PERCENTAGE RESIDUAL Y	CORRL COEFF	
0.3250	0.4989	0.713570	-0.1017	0.0	RL-80-3
1.6370	1.1891	0.722150	-0.0487	0.0	RL-80-5
2.3190	0.4916	0.726440	-0.0143	0.0	RL-80-6
0.7830	-1.0426	0.715230	0.0884	0.0	RL-80-11
1.0340	-1.1811	0.716980	0.0760	0.0	RL-80-20

AGE= 470.6 +/- 18.6 M.Y.
INITIAL RATIO= 0.71065 +/- 0.00034

(RB87 DECAY CONSTANT USED 1.4200)
(AGE AND INITIAL RATIO ESTIMATES GIVEN AT ONE SIGMA CONFIDENCE LEVEL)

T A B L E X V

SHEARED PORT DEPOSIT GNEISS

YORK LEAST SQUARES REGRESSION - MODEL I

NUMBER OF SAMPLES= 6
ESTIMATED SLOPE= 0.00074
EXPERIMENTAL ERROR IN X = 0.02000
EXPERIMENTAL ERROR IN Y = 0.00050

SLOPE B= 0.005120646 INTERCEPT A= 0.710831523
SE OF B= 0.000920678 SE OF A= 0.001805922
MEAN X = 1.37794018 MEAN Y = 0.717887521

X	PERCENTAGE RESIDUAL X	Y	PERCENTAGE RESIDUAL Y	CORRL COEFF	
2.3100	0.1518	0.722720	-0.0058	0.0	RL-80-32
0.1550	-0.5477	0.709450	0.3060	0.0	RL-81-27
1.9800	-9.4434	0.717020	0.4174	0.0	RL-81-44
0.0590	0.2745	0.714030	-0.4055	0.0	RL-81-45
5.3210	2.9194	0.739240	-0.0495	0.0	RL-81-45S
1.7710	5.3742	0.722320	-0.2675	0.0	RL-81-46

AGE= 359.7 +/- 64.8 M.Y.
INITIAL RATIO= 0.71083 +/- 0.00181

(RB87 DECAY CONSTANT USED 1.4200)
(AGE AND INITIAL RATIO ESTIMATES GIVEN AT ONE SIGMA CONFIDENCE LEVEL)

TABLE XV, Continued

Sheared Port Deposit Gneiss

YORK LEAST SQUARES REGRESSION TREATMENT - MODEL II

NUMBER OF SAMPLES= 6
ESTIMATED SLOPE= 0.00512
EXPERIMENTAL ERROR IN X = 0.02000
EXPERIMENTAL ERROR IN Y = 0.00050

ITER= 1
MINIMIZED WEIGHTED SUM OF RESIDUALS SQUARED (SUMS)= 234.292419
MEAN SUM OF RESIDUALS SQUARED (SUMS/(N-2))= 58.5731049
SQUARE ROOT OF (SUMS/N-2))= 7.6533070

SLOPE B= 0.005120631 INTERCEPT A= 0.710831285
SE OF B= 0.000116223 SE OF A= 0.000231720
MEAN X = 1.37794018 MEAN Y = 0.717887223

X	PERCENTAGE RESIDUAL X	Y	PERCENTAGE RESIDUAL Y	CORRL COEFF	
2.3100	0.1525	0.722720	-0.0058	0.0	RL-80-32
0.1550	-0.5477	0.709450	0.3060	0.0	RL-81-27
1.9800	-9.4426	0.717020	0.4174	0.0	RL-81-44
0.0590	0.2746	0.714030	-0.4056	0.0	RL-81-45
5.3210	2.9203	0.739240	-0.0495	0.0	RL-81-45
1.7710	5.3747	0.722320	-0.2676	0.0	RL-81-46

AGE= 359.7 +/- 8.1 M.Y.
INITIAL RATIO= 0.71083 +/- 0.00023

(RB87 DECAY CONSTANT USED 1.4200)
(AGE AND INITIAL RATIO ESTIMATES GIVEN AT ONE SIGMA CONFIDENCE LEVEL)

T A B L E X V I

PORT DEPOSIT GNEISS

YORK LEAST SQUARES REGRESSION - MODEL 1

NUMBER OF SAMPLES= 18
ESTIMATED SLOPE= 0.00754
EXPERIMENTAL ERROR IN X = 0.02000
EXPERIMENTAL ERROR IN Y = 0.00050

SLOPE B= 0.006660257 INTERCEPT A= 0.709553480
SE OF B= 0.000134444 SE OF A= 0.000239956
MEAN X = 1.65056419 MEAN Y = 0.720546663

X	PERCENTAGE RESIDUAL X	Y	PERCENTAGE RESIDUAL Y	CORRL COEFF	
1.2000	1.2298	0.718140	-0.0691	0.0	RL-80-33
2.0700	2.2359	0.724180	-0.0734	0.0	RL-80-37
1.8830	-0.7913	0.721790	0.0285	0.0	RL-80-39
0.4200	-0.0868	0.712250	0.0138	0.0	RL-80-40
2.6870	-0.4661	0.727280	0.0118	0.0	RL-80-41
1.4090	-0.6573	0.718650	0.0315	0.0	RL-80-53
2.1350	0.1527	0.723830	-0.0049	0.0	RL-81-13
2.0250	-1.0627	0.722640	0.0356	0.0	RL-81-17
2.0940	-1.3380	0.723000	0.0434	0.0	RL-81-18
1.1390	-0.1591	0.717060	0.0094	0.0	RL-81-21
2.0910	-1.6590	0.722860	0.0538	0.0	RL-81-28
2.7050	-0.6034	0.727350	0.0152	0.0	RL-81-29
2.1810	0.0823	0.724110	-0.0026	0.0	MJ 8143
1.9970	0.8608	0.723180	-0.0293	0.0	MJ 8144
2.1050	0.6868	0.723830	-0.0222	0.0	MJ 8147
2.0740	0.7550	0.723650	-0.0247	0.0	MJ 8151
1.4880	0.7424	0.719780	-0.0337	0.0	MJ 8152
0.3830	-0.0981	0.711980	0.0171	0.0	MJ 8154A

AGE= 467.4 +/- 9.4 M.Y.
INITIAL RATIO= 0.70955 +/- 0.00024

(RB87 DECAY CONSTANT USED 1.4200)
(AGE AND INITIAL RATIO ESTIMATES GIVEN AT ONE SIGMA CONFIDENCE LEVEL)

TABLE XVI, Continued

Port Deposit Gneiss

YORK LEAST SQUARES REGRESSION TREATMENT - MODEL II

NUMBER OF SAMPLES= 18
ESTIMATED SLOPE= 0.00666
EXPERIMENTAL ERROR IN X = 0.02000
EXPERIMENTAL ERROR IN Y = 0.00050

ITER= 1
MINIMIZED WEIGHTED SUM OF RESIDUALS SQUARED (SUMS)= 12.8837795
MEAN SUM OF RESIDUALS SQUARED (SUMS/(N-2))= 0.8052362
SQUARE ROOT OF (SUMS/N-2))= 0.8973495

SLOPE B= 0.006660238 INTERCEPT A= 0.709553301
SE OF B= 0.000151230 SE OF A= 0.000269512
MEAN X = 1.65056419 MEAN Y = 0.720546484

X	PERCENTAGE RESIDUAL X	Y	PERCENTAGE RESIDUAL Y	CORRL COEFF	
1.2000	1.2302	0.718140	-0.0691	0.0	RL-80-33
2.0700	2.2364	0.724180	-0.0734	0.0	RL-80-37
1.8830	-0.7907	0.721790	0.0284	0.0	RL-80-39
0.4200	-0.0866	0.712250	0.0138	0.0	RL-80-40
2.6870	-0.4656	0.727280	0.0118	0.0	RL-80-41
1.4090	-0.6569	0.718650	0.0314	0.0	RL-80-53
2.1350	0.1533	0.723830	-0.0049	0.0	RL-81-13
2.0250	-1.0620	0.722640	0.0356	0.0	RL-81-17
2.0940	-1.3375	0.723000	0.0433	0.0	RL-81-18
1.1390	-0.1587	0.717060	0.0094	0.0	RL-81-21
2.0910	-1.6583	0.722860	0.0538	0.0	RL-81-28
2.7050	-0.6028	0.727350	0.0152	0.0	RL-81-29
2.1810	0.0829	0.724110	-0.0026	0.0	MJ 8143
1.9970	0.8613	0.723180	-0.0293	0.0	MJ 8144
2.1050	0.6873	0.723830	-0.0222	0.0	MJ 8147
2.0740	0.7555	0.723650	-0.0247	0.0	MJ 8151
1.4880	0.7428	0.719780	-0.0337	0.0	MJ 8152
0.3830	-0.0980	0.711980	0.0171	0.0	MJ 8154A

AGE= 467.4 +/- 10.6 M.Y.
INITIAL RATIO= 0.70955 +/- 0.00027

(RB87 DECAY CONSTANT USED 1.4200)
(AGE AND INITIAL RATIO ESTIMATES GIVEN AT ONE SIGMA CONFIDENCE LEVEL)

T A B L E X V I I

PORT DEPOSIT GNEISS/RELICT PLUTONIC AND AMPHIBOLITE TEXTURES

YORK LEAST SQUARES REGRESSION - MODEL I

NUMBER OF SAMPLES= 8
ESTIMATED SLOPE= 0.00763
EXPERIMENTAL ERROR IN X = 0.02000
EXPERIMENTAL ERROR IN Y = 0.00050

SLOPE B= 0.006507792 INTERCEPT A= 0.706790447
SE OF B= 0.000351836 SE OF A= 0.000367407
MEAN X = 0.506546319 MEAN Y = 0.710086942

X	PERCENTAGE RESIDUAL X	Y	PERCENTAGE RESIDUAL Y	CORRL COEFF	
0.9530	1.8886	0.714080	-0.1359	0.0	RL-80-46
0.2630	0.4250	0.709290	-0.1101	0.0	RL-80-48
0.0240	0.0321	0.707590	-0.0909	0.0	RL-80-49
1.1530	-2.0527	0.713270	0.1220	0.0	RL-81-12
0.0160	-0.0209	0.706270	0.0884	0.0	RL-81-24
0.2320	-0.4699	0.707320	0.1376	0.0	RL-81-26
4.8810	0.1060	0.738600	-0.0015	0.0	MJ 8148
0.0490	0.0072	0.707180	-0.0100	0.0	MJ 8156

AGE= 456.7 +/- 24.7 M.Y.
INITIAL RATIO= 0.70679 +/- 0.00037

(RB87 DECAY CONSTANT USED 1.4200)
(AGE AND INITIAL RATIO ESTIMATES GIVEN AT ONE SIGMA CONFIDENCE LEVEL)

T A B L E X V I I , C o n t i n u e d

Port Deposit Gneiss/Relict Plutonic and Amphibolite Textures

YORK LEAST SQUARES REGRESSION TREATMENT - MODEL II

NUMBER OF SAMPLES= 8
ESTIMATED SLOPE= 0.00651
EXPERIMENTAL ERROR IN X = 0.02000
EXPERIMENTAL ERROR IN Y = 0.00050

(ITER= 1
MINIMIZED WEIGHTED SUM OF RESIDUALS SQUARED (SUMS)= 34.2803650
MEAN SUM OF RESIDUALS SQUARED (SUMS/(N-2))= 5.7133942
SQUARE ROOT OF (SUMS/N-2))= 2.3902712

SLOPE B= 0.006507788 INTERCEPT A= 0.706790507
SE OF B= 0.000147383 SE OF A= 0.000153727
MEAN X = 0.506546438 MEAN Y = 0.710087001

X	PERCENTAGE RESIDUAL X	Y	PERCENTAGE RESIDUAL Y	CORRL COEFF	
0.9530	1.8886	0.714080	-0.1359	0.0	RL-80-46
0.2630	0.4250	0.709290	-0.1101	0.0	RL-80-48
0.0240	0.0321	0.707590	-0.0909	0.0	RL-80-49
1.1530	-2.0528	0.713270	0.1220	0.0	RL-81-12
0.0160	-0.0209	0.706270	0.0884	0.0	RL-81-24
0.2320	-0.4699	0.707320	0.1376	0.0	RL-81-26
4.8810	0.1059	0.738600	-0.0015	0.0	MJ 8148
0.0490	0.0072	0.707180	-0.0100	0.0	MJ 8156

AGE= 456.7 +/- 10.3 M.Y.
INITIAL RATIO= 0.70679 +/- 0.00015

(RB87 DECAY CONSTANT USED 1.4200)
(AGE AND INITIAL RATIO ESTIMATES GIVEN AT ONE SIGMA CONFIDENCE LEVEL)

T A B L E X V I I I

JAMES RUN FORMATION

YORK LEAST SQUARES REGRESSION - MODEL I

NUMBER OF SAMPLES= 9
ESTIMATED SLOPE= 0.00505
EXPERIMENTAL ERROR IN X = 0.02000
EXPERIMENTAL ERROR IN Y = 0.00050

SLOPE B= 0.006117981 INTERCEPT A= 0.708163857
SE OF B= 0.000304547 SE OF A= 0.000350945
MEAN X = 0.791506886 MEAN Y = 0.713006318

X	PERCENTAGE RESIDUAL X	Y	PERCENTAGE RESIDUAL Y	CORRL COEFF	
0.3280	0.3699	0.710760	-0.0819	0.0	RL-80-57
1.8210	-1.7569	0.718600	0.0708	0.0	RL-80-62
2.3460	1.9483	0.723240	-0.0614	0.0	RL-80-63
0.4820	0.7315	0.711920	-0.1104	0.0	RL-80-65
0.0330	0.0369	0.708940	-0.0810	0.0	RL-80-66
0.0210	-0.0288	0.707590	0.0993	0.0	RL-80-68
0.0930	-0.1329	0.708000	0.1034	0.0	RL-80-68
1.8220	0.5955	0.719550	-0.0240	0.0	MJ 8169
1.6250	-1.8812	0.717310	0.0848	0.0	MJ 8170

AGE= 429.5 +/- 21.4 M.Y.
INITIAL RATIO= 0.70816 +/- 0.00035

(RB87 DECAY CONSTANT USED 1.4200)
(AGE AND INITIAL RATIO ESTIMATES GIVEN AT ONE SIGMA CONFIDENCE LEVEL)

TABLE XVIII, Continued

James Run Formation

YORK LEAST SQUARES REGRESSION TREATMENT - MODEL II

NUMBER OF SAMPLES= 9
ESTIMATED SLOPE= 0.00612
EXPERIMENTAL ERROR IN X = 0.02000
EXPERIMENTAL ERROR IN Y = 0.00050

ITER= 1
MINIMIZED WEIGHTED SUM OF RESIDUALS SQUARED (SUMS)= 27.8850250
MEAN SUM OF RESIDUALS SQUARED (SUMS/(N-2))= 3.9835749
SQUARE ROOT OF (SUMS/N-6))= 1.9958897

SLOPE B= 0.006117973 INTERCEPT A= 0.708163679
SE OF B= 0.000152174 SE OF A= 0.000175525
MEAN X = 0.791506767 MEAN Y = 0.713006139

X	PERCENTAGE RESIDUAL X	Y	PERCENTAGE RESIDUAL Y	CORRL COEFF	
0.3280	0.3700	0.710760	-0.0819	0.0	RL-80-57
1.8210	-1.7565	0.718600	0.0708	0.0	RL-80-62
2.3460	1.9488	0.723240	-0.0614	0.0	RL-80-63
0.4820	0.7317	0.711920	-0.1104	0.0	RL-80-65
0.0330	0.0369	0.708940	-0.0810	0.0	RL-80-66
0.0210	-0.0288	0.707590	0.0992	0.0	RL-80-68
0.0930	-0.1329	0.708000	0.1034	0.0	RL-80-68
1.8220	0.5959	0.719550	-0.0240	0.0	MJ 8169
1.6250	-1.8808	0.717310	0.0848	0.0	MJ 8170

AGE= 429.5 +/- 10.7 M.Y.
INITIAL RATIO= 0.70816 +/- 0.00018

(RB87 DECAY CONSTANT USED 1.4200)
(AGE AND INITIAL RATIO ESTIMATES GIVEN AT ONE SIGMA CONFIDENCE LEVEL)

AN RB-SR ISOTOPIC STUDY OF THE PORT DEPOSIT/METASEDIMENT CONTACT

Sample RL-80-29C was taken from the Wissahickon/Port Deposit contact and was slabbed in an effort to determine a metamorphic or structural age for this fault contact. The rock (12 cm x 6 cm) was first slabbed perpendicular to the amphibolite/Port Deposit matrix interface (orientation S60°W, 90°) and then slabbed again for thin section chips and chips for analysis. Figure 9 diagrams this dissection. The isotopic data and discussion are presented on pages 68 and 71, and 66 of the text, respectively.

Sample: RL-80-29/Contact

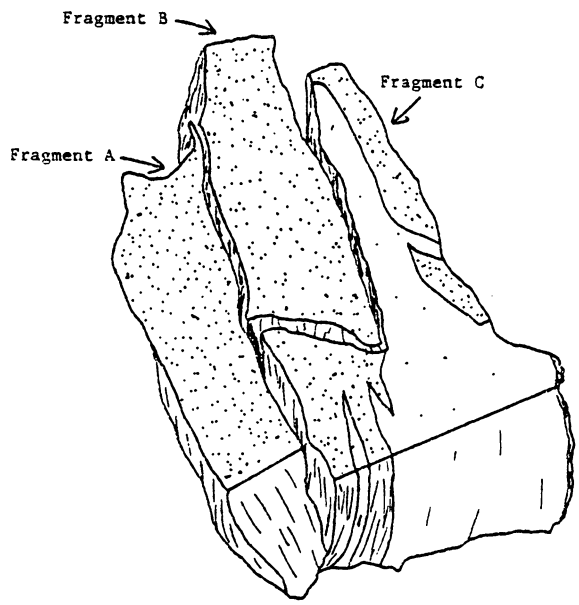

Fractured sample of the Fort Deposit - Wissahickon metagreywacke contact prior to sectioning for isotopic analysis.

Sample: RL-80-29/Contact

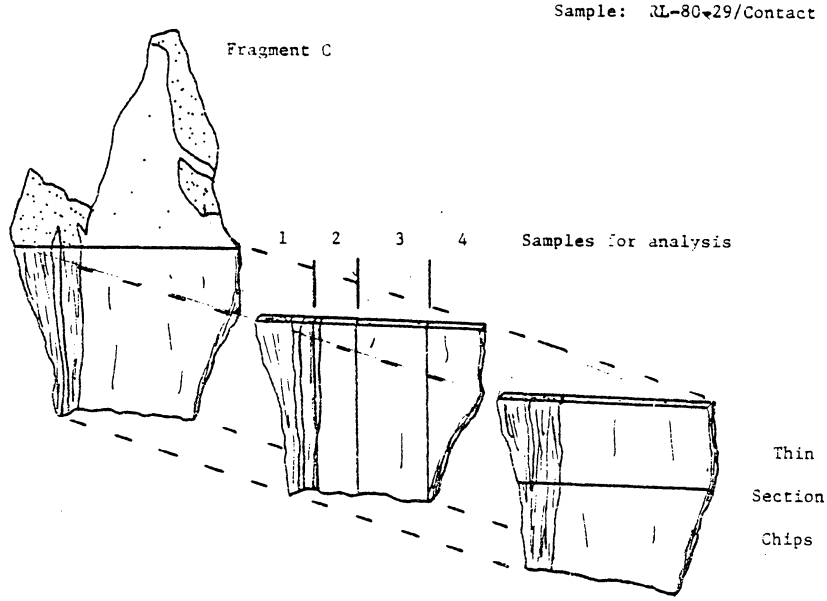

SELECTED BIBLIOGRAPHY, APPENDIX V

Faure, G., 1977. Principles of Isotope Geology. John Wiley and Sons, New York, 464 pp.

Flanagan, F. J., 1976. 1972 compilation of data on USGS standards. In: F. J. Flanagan (ed.), Description and Analyses of Eight New USGS Rock Standards, USGS Prof. Paper 840, 131-184.

Harvey, P. K., Taylor, D. M., Hendry, R. D., and Bancroft, F., 1973. An accurate fusion method for the analysis of rocks and chemically related materials by x-ray fluorescence spectrometry. X-Ray Spectrometry 2, 33-44.

Norrish, K. and Hutton, J. T., 1969. An accurate x-ray spectrographic method for the analysis of a wide range of geological samples. Geochim. Cosmochim. Acta 33, 431-453.

Norrish, K. and Chappell, B. W., 1977. X-ray fluorescence spectrometry. In: J. Zussman (ed.), Physical Methods in Determinative Mineralogy, p. 201-272.

Mattinson, J. M., 1972. Preparation of hydrofluoric, hydrochloric, and nitric acids at ultralow lead levels. Anal. Chem. 44, 1715-1716.

Steiger, R. H. and Jager, E., 1977. Subcommission on geochronology: convention and use of decay constants in geo- and cosmochronology. Earth Planet. Sci. Lett. 35, 359-362.

York, D., 1966. Least-squares fitting of a straight line. Canadian J. Phys. 44, 1079-1086.

The vita has been removed from the scanned document

MAJOR ELEMENT AND ISOTOPIC STUDIES ON THE JAMES RUN/PORT DEPOSIT ASSOCIATION, MARYLAND: TECTONIC ANALOGUES AND TACONIC DEFORMATION

by

Richard Peter Lesser

(ABSTRACT)

The gneissic Port Deposit pluton and associated James Run metavolcanics bear a fault relation with the Wissahickon metasediments of the Glenarm terrane of the northeastern Maryland Piedmont, USA. Bulk chemical and mineralogical data classify the meta-igneous rocks as a bimodal tholeiite-dacite/tonalite suite with trondhjemitic affinities and indicate that subsolidus alteration during dynamic metamorphism was minor. Comparison of these data with other tectonic environments suggests their generation by partial fusion of amphibolitic basement.

Previous studies have dated magmatic events in the Maryland Piedmont at 520 Ma, 420 Ma, and 300 Ma (Sinha et al., 1980). The U-Pb zircon upper intercept age for the Port Deposit is 525 $\pm$ 10 Ma, the Rb-Sr whole rock isochron age is 467 $\pm$ 21 Ma, and Rb-Sr model biotite ages are 400 and 300 Ma. Regional and theoretical considerations indicate the 525 zircon age may represent the time of igneous consolidation. Detailed petrographic observations in the Port Deposit indicate the Rb-Sr whole rock age represents the time of deformation and development of gneissic textures. The 467 Middle Ordovician age of deformation for the Port Deposit is interpreted as representative of the Taconic orogeny for the central Appalachian Piedmont; Rb-Sr whole rock systematics were

upset, but concurrent anatexis of felsic basement is not locally evident. The fault contact between the Port Deposit and easternmost facies of the Wissahickon places an upper age limit of 467 Ma for that particular facies. Rb-Sr model biotite ages are interpreted as metamorphic cooling phenomenon and reflect the 420 and 300 Ma thermal highs.